IDENTIFICATION AND ANALYSIS OF E3 LIGASES AND HELPER NLRS IN PLANT IMMUNITY

by

Meixuezi Tong

B. Sc., Northwest A&F University, 2011

A THESIS SUBMITTED IN PARTIAL FULFILLMENT OF THE

REQUIREMENTS FOR THE DEGREE OF

DOCTOR OF PHILOSOPHY

in

The Faculty of Graduate and Postdoctoral Studies

(Botany)

THE UNIVERSITY OF BRITISH COLUMBIA

(Vancouver)

April 2016

Abstract

Plant immunity is usually initiated with two types of immune receptors: 1) pattern recognition receptors (PRRs) recognize the conserved molecular features of pathogens (pathogen-associated molecular patterns, PAMPs) and trigger PTI (PAMP-triggered immunity) and; 2) nucleotide-binding/leucine-rich repeats (NLRs) serve as intracellular immune receptors with the ability to recognize the presence of relatively diverse pathogen effectors and trigger ETI (effector-triggered immunity). The *Arabidopsis thaliana* mutant *snc1* contains a gain-of-function mutation in a *Toll/interleukin-1* (*TIR*)-type *NLR* (*TNL*) gene and displays a dwarf morphology. Here, I report on the results of a *snc1*-influencing plant E3 ligase reverse genetic (SNIPER) screen that looked for *snc1* plants with altered dwarfism in the presence of overexpressed E3 ligases. Six *SNIPER* genes were identified with four *snc1*-suppressors and two *snc1*-enhancers. *SNIPER1/2/3* were selected for further characterization. The analysis of *SNIPER1/2* is incomplete, thus is not included in this thesis.

Chapter 3 describes *SNIPER3,* previously known as *SAUL1* (*Senescence-Associated E3 Ubiquitin Ligase 1)* or *PUB44* (*Plant U-box 44),* which encodes a U-box-type E3 ligase. Our data suggests that SAUL1 plays a dual role in plant immunity: on one hand, SAUL1 positively regulates basal resistance; on the other hand, SAUL1 suppresses a typical TNL immune receptor SUSA1 (Suppressor of *saul1*) to prevent its autoimmunity.

ADR1, ADR1-L1 and ADR1-L2 are three homologous coiled-coil (CC)-type NLRs (CNLs), which were previously shown to work as helper NLRs. Chapter 4 further explores the specificity of the genetic requirement of ADR1s for typical TNLs, SNC1 and CHS2 (CHILLING SENSITIVE 2). Among the three ADR1 members, ADR1 is the leading contributor while ADR1-L1 is the least. Moreover, loss-of-function mutation of *ADR1-L1* leads to over compensation of the transcript expression level of *ADR1* and *ADR1-L2* and results in the enhancement of *snc1*-mediated immunity.

Overall, the studies I completed as part of my Ph.D. thesis expand our knowledge of the roles of E3 ligases and ADR1s in plant defense and help us to better understand the sophisticated regulatory mechanisms of plant innate immunity.

Preface

The chapters reported in this Ph.D. thesis describe the research results collected from January 2012 through January 2016. Below is a list of manuscripts (published or in revision) and the author contributions that comprise this thesis.

Chapter 2 - A reverse genetic screen looking for key E3 ubiquitin ligases involved in plant immunity

- The candidate performed most of the experiments under the supervision of Li X. Zhang Y. analyzed microarray data and selected the list of E3 ligase genes for the SNIPER screen. Zhu C. generated *35S::SNIPER2* transgenic lines in *snc1* background. Kapos P. provided pathogen infection data of *35S::SNIPER4/5* plants.

Chapter 3 - E3 ligase SAUL1 serves as a positive immune regulator guarded by a TNL receptor SUSA1 was modified from the manuscript:
Tong, M. *; Koturc, T. *; Li, Y.; Vogelmann, K.; Kleine, T.; Leister, D.; Zhang, Y.; Hoth, S.; Li, X. E3 ligase SAUL1 serves as a positive immune regulator guarded by a TNL receptor SUSA1.

- The candidate performed most of the experiments and wrote the manuscript under the supervision of Li X. The *saul1* suppressor screens were performed in two independent labs: one by the candidate under the supervision of Li X., the other by Koturc T., Vogelmann K., Kleine T., Leister D. under the supervision of Hoth S. Li Y. analyzed the whole genome sequencing data of *saul1 susa1* mutants. Koturc T., Vogelmann K., Kleine T., Leister D. contributed the subcellular localization figure of SUSA1. Zhang Y. selected the list of E3 ligase genes for the SNIPER screen.

Chapter 4 - ADR1 family is required for the signalling of typical TNL-mediated immunity in *Arabidopsis* was modified from the manuscript:

Dong, O. *; Tong, M. *; Bonardi, V.; Kasmi, F.; Woloshen, V.; Wünsch, L.; Dangl, J.; Li, X. TNL-mediated immunity in *Arabidopsis* requires complex transcriptional regulation of the redundant ADR1 gene family. (* Co-first authors) New Phytologist. 2016; doi:10.1111/nph.13821.

- The candidate generated and phenotypically assayed the collection of all combinatorial double, triple and quadruple adr1 snc1 mutants. The candidate generated Figure 2d and Figure 6 under the supervision of Li X. Bonardi V., Kasmi F. and Wünsch L. generated the Figure 4.4 and 4.5 under the supervision of Dangl. J. Dong O. and Li X. wrote the manuscript. All the other co-authors edited the manuscript.

Table of contents

List of tables

List of figures

List of abbreviations

35S	a very strong constitutive promoter found in Cauliflower mosaic virus (CaMV); the coefficient of sedimentation of viral transcript whose expression is naturally driven by this promoter is 35S
ABRC	Arabidopsis Biological Resource Center
ACT	Actin
ADP	Adenosine Di-Phosphate
ADR	Activated Disease Resistance
AFP	Anti Fungal Protein
ANOVA	Analysis of Variance
APC	Anaphase-Promoting Complex
ARF	Auxin Responsive Transcription Factor
ARM	Armadillo
ATP	Adenosine Tri-Phosphate
ATXR7	Arabidopsis Trithorax-related 7
Avr	Avirulent or Avirulence
AvrB	Avirulence protein B; an avirulence effector from *Pseudomonas syringae* pv. *glycinea*
Avr-Pita	Avirulence protein Pita; an avirulence effector from *Magnaporthe grisea*
AvrPto	Avirulence protein Pto; an avirulence protein from *Pseudomonas syringae*
AvrRpm1	Avirulence protein Rpm1; an avirulence protein isolated from *Pseudomonas syringae* pv. *maculicola* strain M2
AvrRps4	Avirulence protein Rps4; an avirulence protein isolated from *Pseudomonas syringae* pv. *pisi*
AvrRpt2	Avirulence protein Rpt2; an avirulence protein isolated from *Pseudomonas syringae* pv. *tomato*
Ax21	Activator of *Xa21*-mediated immunity
BAK1	Brassinosteroid Associated Kinase 1
BAT2	HLA-B ASSOCIATED TRANSCRIPT 2
Bgh	*Blumeria graminis* f. sp. *hordei*
bHLH	basic Helix-Loop-Helix
BIK1	Botrytis-Induced Kinase 1
BLAST	Basic Local Alignment Search Tool
BTB	Bric à Brac, Tramtrack, and Broad Complex
CaMV	Cauliflower Mosaic Virus
Cas9	CRISPR-associated
CC	Coiled-coil

CDPK	Calcium-Dependent Protein Kinase
CERK1	Chitin Elicitor Receptor Kinase 1
CEBiP	Chitin Elicitor Binding Protein
CFU	Colony Forming Unit
ChIP	Chromatin immunoprecipitation
CHS	Chilling-Sensitive
COI1	Coronatine-Insensitive 1
Col	Columbia-0, an Arabidopsis ecotype; it is also referred as wild type in this thesis work
CPR1/CPR30	Constitutive Expresser of PR Genes 1; also known as Constitutive Expresser of PR Genes 30
CRISPR	Clustered Regularly Interspaced Short Palindromic Repeats
CSA	Constitutive Shade-Avoidance 1
C terminal	Carboxyl terminal
Cul1	Cullin 1
Dex	Dexamethasone
DND1	Defense No Death 1
DND2	Defense No Death 2
E1	Ubiquitin-activating enzyme
E2	Ubiquitin-conjugating enzyme
E3	Ubiquitin ligase
EDS1	Enhanced Disease Susceptibility 1
EFR	EF-Tu receptor
EF-Tu	Bacterial Elongation Factor Tu
elf18/26	An N-acetylated peptide comprising the first 18/26 amino acids of bacterial elongation factor Tu
EMS	Ethyl methanesulfonate; a chemical mutagen
ETI	Effector-Triggered Immunity
Exo70	Exocyst subunit 70
FLAG	An epitope protein tag compose of a single or repeated DYKDDDDK sequence
flg22	Flagellin conserved domain 22
FLS2	FLAGELLIN-SENSITIVE 2
GFP	Green Fluorescent Protein
GR	Glucocorticoid Receptor
GSL	Glucosinolate
H3K4	Lysine 4 of Histone 3
H.a.	*Hyaloperonospora arabidopsidis*
HA	Hemagglutinin; an epitope protein tag compose of a single or repeated YPYDVPDYA sequence
HR	Hypersensitive Response

HSP90	Heat Shock Protein 90
IAA	Indole-3-Acetic Acid
IP	Immunoprecipitation
IP-MS	Immunoprecitpation-mass Spectrometry
JA	Jasmonic Acid
JAZ	JA-ZIM domain
Ler	*Landsberg erecta*; an Arabidopsis ecotype
L	Flax NBS-LRR protein with specific recognition of AvrL from the flax rust fungus *Melampsora lini*
LORE	Lipooligosaccharide-specific reduced elicitation
LPS	Lipopolysaccharide
LRR	Leucine-rich Repeat
MAP	Mitogen-activated Protein
MG132	A proteasome inhibitor
MKP1	MAP Kinase Phosphatase 1
MLA	Mildew A
MOS	Modifier of *snc1*
MOS1	Modifier of *snc1*, 1; a BAT2 domain containing protein
MOS2	Modifier of *snc1*, 2; a G-patch and KOW domains containing protein
MOS3	Modifier of *snc1*, 3; also known as AtNup96 or SAR3
MOS4	Modifier of *snc1*, 4; a nuclear protein homologous to human Breast Cancer-Amplified Sequence (BCAS2)
MOS5	Modifier of *snc1*, 5; also known as UBIQUITIN-ACTIVATING ENZYME 1 (UBA1), one of the two Arabidopsis Ubiquitin-activating enzymes
MOS6	Modifier of *snc1*, 6; also known as IMPORTIN ALPHA 3 (IMPA-3)
MOS7	Modifier of *snc1*, 7; homologous to human and Drosophila Nup88
MOS8	Modifier of *snc1*, 8; also known as ENHANCED RESPONSE TO ABA 1 (ERA1)
MOS9	Modifier of *snc1*, 9
MOS10	Modifier of *snc1*, 10; also known as Topless-Related 1 (TPR1)
MOS11	Modifier of *snc1*, 11; homologous to the human RNA binding protein CIP29
MOS12	Modifier of *snc1*, 12; an Arabidopsis cyclin L homolog
MOS14	Modifier of *snc1*, 14; a nuclear importer of serine-arginine rich (SR) proteins
MKS1	MAP kinase 4 substrate 1
MUSE	Mutant, *snc1*-enhancing Screen
MS medium	Murashige and Skoog medium; a plant growth medium

N	*Nicotiana*
NADPH	Nicotinamide adenine dinucleotide phosphate
NAIP	Neuronal Apotopsis Inhibitory Protein
Nat	N-terminal Acetyltransferase
NB-LRR	Nucleotide Binding-Leucine Rich Repeat
NDR1	Non-race Specific Disease Resistance 1
NLR	Nod-Like Receptor or nucleotide binding and leucine-rich repeat-containing R protein
NLRC4	Nod-Like receptor 4
NLS	Nuclear Localization Signal or Sequence
NOD	Nucleotide Oligomerization Domain
NPC	Nuclear Pore Complex
NPR1	NONEXPRESSER OF PR GENES 1
NRG	N-Required Gene
N terminal	Amino Terminal
Nup88	Nucleoporin 88kDa that functions in CRM1-Dependent Nuclear Protein Export
OD	Optical Density
ORF	Open Reading Frame
PAD	Phytoalexin Deficient
PDR	Pleiotropic Drug Resistance
SDS-PAGE	Sodium Dodecyl Sulfate Polyacrylamide Gel Electrophoresis
PAMP	Pathogen-Associated Molecular Pattern
PBS1	AvrPphB Susceptible 1
PBL	PBS1-like
PEN	Penetration
Pita	Rice NBS-LRR protein confers resistance to *Magnaporthe grisea* that express Ave-Pita
PM	Plasma Membrane
PopP2	An avirulence effector from *Ralstonia solanacearum*
PP5	Protein Phosphatase 5
PR	Pathogenesis-related
PRR	Pattern Recognition Receptor
Psm	*Pseudomonas syringae* pv. *maculicola*
Pst	*Pseudomonas syringae* pv. *tomato*
PTI	PAMP-Triggered Immunity
Pto	Tomato R protein confers resistance to races of *Pseudomonas syringae* pv. *tomato* that carry the AvrPto
PUB	Plant U-box
pv	Pathovar
qRT-PCR	Quantitative Reverse Transcriptase PCR

R	Resistance
RAR1	Required for MLA12 Resistance 1
Rax	Required for Activation of XA21
RBOHD	Respiratory Burst Oxidase Homolog D
RIN4	RPM1-Interacting Protein 4
RING	Really Interesting New Gene
RLK	Receptor-Like Kinase
RLU	Relative Light Units
ROS	Reactive Oxygen Species
RPM1	Resistant to *P. syringae* pv *maculicola 1*
RPP4	Recognition of *Peronospora parasitica* 4
RPS2	Resistant to *P. syringae* 2
RPS4	Resistant to *P. syringae* 4
RPS5	Resistant to *P. syringae* 5
RRS1	Resistant to *Ralstonia solanacearum* 1; also known as AtWRKY52 or Sensitive to Low Humidity 1 (SLH1)
RT-PCR	Reverse Transcriptase PCR
RPW8	Resistance to Powdery Mildew 8
SA	Salicylic Acid
SAUL1	Senescence-Associated Ubiquitin Ligase 1
SERK	Somatic Embryogenesis Receptor-like Kinase
SCF	Skp1-Cullin-F-box
SD	S-domain
SGT1	Suppressor of G2 Allele of SKP1
SID2	SA Induction Deficient 2
SKP1	Suppressor of Kinetochore Protein 1
SNC1	Suppressor of *npr1*, Constitutive, 1
snc1-r1	the revertant mutant of *snc1* that has 10 nucleotides deleted in the first exon of *SNC1*
SNIPER	*snc1*-influencing plant E3 ligase reverse genetic
SR	Serine-arginine Rich proteins
SRFR1	Suppressor of *rps4-RLD* 1
SUMM	Suppressor of *mkk1 mkk2*
SUSA	Suppressor of *saul1*
SYP	Syntaxin of Plants
T3SS	Type III secretion system
TALEN	Transcription Activator-Like Effector Nuclease
T-DNA	Transfer DNA
TIR	Toll/interleukin-1 Receptor or Transport Inhibitor Response
TMV	Tobacco Mosaic Virus
TN	TIR-NB

TNL	Toll/interleukin-1/nucleotide-binding/leucine-rich repeat
TPL	TOPLESS
TPR1	TOPLESS-RELATED 1
Ub	Ubiquitin
UPS	Ubiquitin-26S Proteasome System
WT	Wild-type
Xa21	A rice resistance locus that confers disease resistance to *Xanthomonas oryzae* pv. *oryzae*
Xoo	*Xanthomonas oryzae* pv. *oryzae*

Acknowledgements

First and foremost, I would like to thank my supervisor Dr. Xin Li. Her dedication to science, kindness to people and efficiency at work has influenced me positively. Most importantly, she can always see the bright side of situations no matter how dire they are. It is her optimism that helped me navigate through all the difficulties in Science during my Ph.D. career. Moreover, her availability in the lab allowed me to discuss questions or to explore new puzzles efficiently with her whenever they arose. My projects would not have gone so smoothly without her supervision. I would also like to thank my committee members Dr. Lacey Samuels, Dr. Carl Douglas and Dr. Jim Kronstad for their advice and guidance during the course of my degree.

Special thanks also goes to past and current lab members. A big thank-you goes to Fang Xu, who taught me almost all the experimental techniques I needed when I first got started. I am also grateful for her companionship through all the ups and downs during the first three years of my graduate studies. Thanks to Yu Ti Cheng for being a reliable leader in the lab; I really miss the hiking trips and hotpot parties she organized and hosted. Thanks to Oliver Dong for always being delightful and responsible and for the tremendous efforts he put into the maintenance of the lab as a lab manager. Thanks to Kaeli Johnson, Kevin Ao, Charles Copeland and Paul Kapos for helping me edit my proposals, manuscripts and thesis. Thanks to Shuai Huang for helpful discussions on my experiments. Thanks to Jianhua Huang, a reliable friend who never said “no” when I asked for help. Thanks to Kevin Ao, Wanwan Liang and Zhongshou Wu, the three new graduate students in the lab, for taking over my projects and developing them further. Last but not least, I would also like to thank all the Zhang Lab members who provided me with lots of support and help that allowed me to finish my degree successfully.

I would like to express my appreciation for the financial support from Chinese Scholarship Council (CSC), Natural Sciences and Engineering Research Council of Canada

(NSERC), and the William Cooper Endowment Fund. I would also like to thank the UBC Botany Department for providing a teaching assistantship opportunity, from which I sincerely learned a lot.

Finally, I would like to give my sincerest thanks to my incredibly supportive family and friends, who always believe in me and have my back. My thesis could not have been completed without you by my side. It is your love and support that drove me through my Ph.D. years.

1 Introduction

1.1 Host and non-host resistance

Plants are constantly confronted with pathogen attacks in nature. However, plant diseases are rare; most plants are healthy the majority of time. This is because plants have evolved complicated mechanisms that form an immune system mainly composed of host and non-host disease resistance, in order to combat pathogens.

Non-host resistance defines the non-specific, broad-spectrum resistance to almost all the microbial pathogens in plants; whereas host resistance describes the defense responses triggered by adapted pathogens, which are able to colonize the host plants. Host resistance often consists of two layers of immunity mediated by two different types of immune receptors: PAMP (pathogen-associated molecular pattern)-triggered immunity (PTI) mediated by membrane-localized PRRs (pattern recognition receptors) and effector triggered immunity (ETI) mediated by intracellular effector receptors NLRs (nucleotide-binding, leucine-rich repeats domains) (Jones and Dangl, 2006).

1.2 Non-host resistance

The preformed structures present on plant surfaces, such as rigid cell walls, play a role in preventing the initial establishment of pathogen invasion (Heath, 2000). Additionally, components present in the apoplast: antimicrobial chemicals (reactive oxygen species, phytoalexins, etc.), proteins (defensins, PR-1, etc.), and enzymes (chitinase, beta-glucanases, etc.), compose a second chemical barrier to limit pathogen invasion (Heath, 2000). For example, the phytoalexin-deficient (pad) mutant *pad3*, which fails to produce the phytoalexin camalexin, was shown to display enhanced susceptibility to a necrotrophic fungal pathogen *Alternaria brassicicola* (Thomma et al., 1999). Moreover, overexpression of a radish defensin encoding gene *Raphanus sativus-antifungal protein 2* (*RsAFP2*) in tobacco leads to

increased resistance upon infection with the fungal pathogen *Alternaria longipes* (Broekaert et al., 1995). These examples suggest that antimicrobial molecules are crucial to inhibit pathogen growth.

More mutant studies in the genetic dissection of non-host immunity using nonhost interaction between *Arabidopsis* and the grass powdery mildew fungus, *Blumeria graminis* f. sp. *hordei* (*Bgh*) uncovered three *PENETRATION* (*PEN*) genes: *PEN1* (Collins et al., 2003), *PEN2* (Lipka et al., 2005) and *PEN3* (Stein et al., 2006). These studies further highlighted the importance of vesicle trafficking and the secretion of antimicrobial components in non-host resistance (Clay et al., 2009; Lu et al., 2015; Karnik et al., 2015). *PEN1/AtSYP121* encodes a syntaxin protein that is involved in SNARE (soluble NSF attachment protein receptor)-mediated membrane fusion events (Collins et al., 2003). *PEN2* encodes an atypical beta-thioglucoside glucohydrolase that metabolizes indole glucosinolates (GSLs) to produce antimicrobials following pathogen attack (Clay et al., 2009; Bednarek et al., 2009). PEN3 is a pleiotropic drug resistance (PDR)-type ATP-binding cassette transporter to efflux molecules during defense responses (Collins et al., 2003; Lu et al., 2015). Although the precise role of each *PEN* gene in penetration resistance is unclear, it is hypothesized that PEN2 is involved in the production of antimicrobials like GSL, and PEN1 and PEN3 participate in exporting the antimicrobials extracellularly to inhibit pathogen infection (Stein et al., 2006; Lu et al., 2015).

1.3 Two forms of innate immunity mediated by two types of immune receptors

Plants employ a two-layered immunity, mediated by two different types of immune receptors, against pathogen infection. Plasma membrane localized PRRs (Pattern Recognition Receptors) initiate the first layer of immunity by perception of conserved features of pathogens (known as Pathogen-Associated Molecular Patterns, PAMPs) called PAMP-triggered immunity (PTI). Pathogens, in order to overcome these primary lines of

defense, evolved a repertoire of effector molecules to dampen PTI and to promote their own growth. Through the pathogen-host co-evolution process, plants developed a family of nucleotide-binding/leucine-rich-repeat (NLR) receptors that allows them to detect the presence of pathogen effectors and to trigger a more robust and sustained immune response, known as effector-triggered immunity (ETI) (Jones and Dangl, 2006).

1.3.1 Perception of pathogen presence by PRRs

The entry of pathogens first triggers PTI responses through the recognition of PAMPs by PRRs. All PRRs are membrane-localized receptor-like kinases (RLKs) or Receptor-like Proteins (RLPs) depending on whether they have a C-terminal kinase domain. A typical RLK usually consists of an extracellular LRR domain, a transmembrane domain and an intracellular kinase domain. The well-known PRR examples are bacterial flagellin receptor FLS2 (Zipfel et al., 2004), bacterial Elongation Factor-Tu receptor EFR (Zipfel et al., 2006), and chitin receptor CERK1 (*Arabidopsis*) and CEBiP (rice) (Miya et al., 2007; Kaku et al., 2006).

Over 20 years ago, Ronald's group first identified XA21, a RLK that confers resistance to *Xanthomonas oryzae* pv. *oryzae* (*Xoo*) (Song et al., 1995), but identification of the real corresponding ligand turned out to be a long journey. The previously published report of the type I-secreted sulphated protein Ax21 as the XA21 ligand in 2009 was retracted because of mislabelled *Xoo* strains (Lee et al., 2009). Six years later, the same group corrected their mistakes and identified the sulphated RaxX (required for activation of XA21, X), rather than Ax21, which is required for activation of XA21-mediated immunity (Pruitt et al., 2015).

1.3.2 PRR signalling events

After elicitation by PAMPs, the plant cells undergo a series of rapid responses including

bursts of calcium and reactive oxygen species (ROS), as well as activation of mitogen-associated kinases (MAPKs) and calcium-dependent protein kinases (CDPKs), leading to massive transcriptional programming (Nühse et al., 2000; Blume et al., 2000).

The activation of PRRs FLS2 and EFR requires a family of small LRR-RLK SERK (SOMATIC EMBRYOGENESIS RECEPTOR-LIKE KINASE) proteins: BAK1/SERK3 and BKK1/SERK4 (Roux et al., 2011). Upon ligand perception, the SERKs rapidly form complexes with FLS2 and EFR, then trans-phosphorylate cytoplasmic kinase BIK1 (BOTRYTIS-INDUCED KINASE1) and its paralogous protein PBS1 (AvrPphB susceptible 1), PBL (PBS1-like)1 and PBL2 (Lu et al., 2010; Zhang et al., 2010). BIK1 and its paralogs subsequently transduce signals through phosphorylating their downstream targets.

The ROS burst is an important immunity signalling output shared by different kingdoms and species. Extracellular ROS is proposed to act as a cross-linker of plant cell wall components, a direct anti-microbial agent, as well as a secondary messenger to trigger downstream immune responses (Lamb and Dixon, 1997). Generation of ROS bursts upon PAMP perception is through plasma-membrane localized NADPH oxidase respiratory burst oxidase homolog D (RBOHD) (Torres et al., 2005). Recent studies from Zipfel's and Zhou's groups have revealed that activation of ROBHD requires phosphorylation events by BIK1 upon elicitation by the PAMPs flg22 and elf18 (Kadota et al., 2014; Li et al., 2014).

MAPK cascades act as conserved signalling modules downstream of PAMP elicitation. The *Arabidopsis* genome encodes approximately 60 MAP3Ks/MEKKs, 10 MAP2Ks/MKKs and 20 MAPKs (Ichimura et al., 2002). Genetic studies have proposed two MAPK cascades in PAMP-triggered immunity (PTI): MEKK1-MKK1/2-MPK4 and MEKK1-MKK4/5-MPK3/6 (Ichimura et al., 1998; Kiegerl, 2000; Yang et al., 2001). MPK3/6/4 are rapidly phosphorylated upon PAMP stimulation (Cardinale et al., 2000), but the molecular linkages between PRR receptors and MAPK cascades remain obscure. Yeast-two-hybrid screens have identified MAP kinase 4 substrate 1 (MKS1) and WRKY transcription factors WRKY25/WRKY33 as MPK4's direct substrates (Andreasson et al.,

2005). It was proposed that MPK4 may complex with MKS1 to phosphorylate and activate transcription factors WRKY25 and WRKY33 to regulate transcription of defense related genes (Andreasson et al., 2005).

Loss of function mutants of *MEKK1*, *MKK1 MKK2* double mutant, or *MPK4* all exhibit similar dwarf phenotypes with enhanced defense responses, suggesting that the MEKK1-MKK1/2-MPK4 cascade negatively regulates plant immune responses (Petersen et al., 2000; Gao et al., 2008). A suppressor screen of *mkk1 mkk2* double mutants revealed that the autoimmunity of the MPK cascade is inhibited by a signalling pathway which requires a MAP kinase kinase kinase MEKK2/SUMM1 (SUPPRESSOR OF *mkk1 mkk2* 1) and a nucleotide-binding/leucine-rich-repeat (NLR) protein SUMM2 (Kong et al., 2012; Zhang et al., 2012). It was hypothesized that MEKK2 monitors the intactness of MEKK1-MKK1/2-MPK4 cascade. The perturbation of MEKK1-MKK1/2-MPK4 cascade presumably by pathogen effectors can be sensed by MEKK2, which subsequently activates SUMM2-mediated defense responses (Kong et al., 2012; Zhang et al., 2012).

The perception of PAMPs also triggers an influx of calcium ions, leading to an increase of intracellular calcium concentration. Even though the exact identity of the calcium channel in plants is not clear, it has been shown that plant calcium-dependent protein kinases (CDPKs, abbreviated as CPKs in *Arabidopsis*) are responsible for sensing intracellular calcium concentration changes and conducting signal transmissions by phosphorylation of their downstream substrates (Harmon et al., 2000; Kudla et al., 2010). In particular, *Arabidopsis* CPK5 was shown to directly phosphorylate NADPH oxidase RHOBD in a ligand-dependent manner, and thereby positive regulate the production of ROS upon pathogen infection (Dubiella et al., 2013). Moreover, CPK28 was identified as a negative regulator in PTI by directly binding and phosphorylating BIK1. The phosphorylation of BIK1 by CPK28 subsequently contribute to BIK1's turnover (Monaghan et al., 2014).

1.3.3 Pathogen effectors perturbing plant immunity

The inhibition of pathogen growth by PTI imposes selective pressure on pathogens to overcome this layer of immunity. One successful strategy that adapted pathogens have employed is to use a large repertoire of effector molecules to suppress PAMP-triggered defenses. For example, *Pseudomonas syringae* effector AvrPto directly targets and inhibits the kinase activities of PRRs, including FLS2 and EFR, thus blocking PAMP-induced immunity in *Arabidopsis* (Xiang et al., 2008). Another well-known effector example is HopAI1. Previous studies have shown that plants expressing transgenic HopAI1 are able to inactivate MPK3 and MPK6 to promote virulence (Zhang et al., 2007). Moreover, MPK4 was shown to be an additional virulence target of HopAI1 in a more recent study (Zhang et al., 2012). A third effector example includes AvrPphB, a cysteine protease that cleaves the BIK1' paralogous protein PBS1 to inhibit immune signal transduction (Shao et al., 2003).

1.3.4 Gene-for-gene concept

In the 1940's, H. H. Flor's studies on the inheritance of pathogenicity of flax rust fungus yielded a gene-for-gene hypothesis which proposed that the resistant variant of the plant has a gene for resistance in correspondence to the avirulence gene of pathogens (Flor, 1971). Together, both the plant resistance (R) gene and pathogen avirulence (Avr) or effector gene determine the disease resistance specificity (Flor, 1971). Over the last century, numerous *R* genes have been cloned. Most of *R* genes were found to encode nucleotide-binding/leucine-rich-repeat (NLR) proteins. Genome-wide analysis has revealed that there are around 150 NLR coding genes in *Arabidopsis*, which mainly fall into two distinct groups: TIR-NB-LRR (TNL) group with an N-terminal Toll and interleukin-1 (TIR)-like domain, and CC-NB-LRR (CNL) group with an N-terminal coiled-coil domain (Meyers, 2003).

1.3.5 NLR structure

NLR proteins usually have a tri-domain structure, consisting of a nucleotide-binding (NB) domain, a C-terminal leucine-rich repeat (LRR) domain, and either a coiled-coil or a TIR-like domain at the N-terminus (Meyers, 2003). The presence of either a CC or TIR domain typically determines whether the NLR-mediated defense response requires NDR1 (Non-race-specific Disease Resistance) or the EDS1 (Enhanced Disease Susceptibility 1) / PAD4 (Phytoalexin Deficient 4) / SAG101 (Senescence Associated Gene 101) complex, respectively (Aarts et al., 1998). However, the detailed molecular linkages between these pathways remain elusive.

As NLR proteins are modular with multi-domains, it is important to know how individual sub-domains contribute to the functional roles of NLR proteins as pathogen sensors. Mutational analyses and domain-swap experiments revealed that the recognition of pathogen effectors is mainly determined by the LRR domain (Ravensdale et al., 2012; Krasileva et al., 2010). In the absence of the effectors, the NB domain interacts with the LRR domain, keeping the protein in an inactive conformation. Upon effector recognition, the NLR's conformation undergoes a conformation change that allows the NB domain to exchange ADP with ATP, thereby activating nucleotide hydrolysis and triggering downstream signalling (Takken and Tameling, 2009). Besides the structural constraints that maintain the R protein conformation (Takken and Goverse, 2012), the chaperone SGT1/HSP90 (Heat Shock Protein 90) / RAR1 (Required for MLA12 Resistance 1) / PP5 (Protein Phosphatase 5) complex is required for the proper folding of R proteins. Reduced expression or activity of HSP90, RAR1 or PP5 compromises steady-state protein levels of many NLR proteins and results in enhanced disease susceptibility (Azevedo et al., 2002; Mauch et al., 2004; Holt III et al., 2005).

1.3.6 Perception of pathogen's presence by NLRs

Plant NLRs act as intracellular immune receptors that recognize cytoplasmic effectors delivered by pathogens. The recognition could be direct or indirect depending on different effectors. As an example of direct recognition cases, rice NLR protein Pi-ta detects Avr-Pita effector of rice blast fungus, *Magnaporthe grisea* by direct protein-protein interaction revealed from a yeast-two-hybrid system and an *in vitro* binding assay (Jia et al., 2000). Flax TNL L5 and L6 recognize rust effector Avr567 by direct protein interaction (Dodds et al., 2006).

However, more and more cases suggest that NLRs act by monitoring/guarding the target of pathogen effectors (guardees), rather than recognition through direct physical interaction. One well-studied guardee, RIN4 (RPM1-INTERACTING 4), is targeted by two unrelated *P. syringae* effectors AvrB and AvrRpm1, leading to phosphorylation of RIN4 which triggers the activation of NLR RPM1 (RESISTANCE TO *P. SYRINGAE* PV *MACULICOLA* 1) (Chung et al., 2011; Liu et al., 2011). Another *P.* syringe effector AvrRpt2 cleaves RIN4, activating RPS2 (RESISTANT TO *P. SYRINGAE* 2)-mediated immunity (Axtell and Staskawicz, 2003; Chung et al., 2011; Mackey et al., 2003).

Recognition of pathogen effectors by monitoring the effects of effectors (indirect recognition) rather than physical shapes of effectors (direct recognition) allows the plants to detect a wide variety of pathogen effectors with a limited number of NLR proteins. Thus, compared with direct recognition, indirect recognition could be a more efficient strategy employed by plants to combat pathogens through the arms race between them during the evolutionary time.

1.3.7 NLR homo- and hetero-dimerization

NLRs were found to self-associate as oligomers after activation (Xu et al., 2014a; Maekawa

et al., 2011; Ntoukakis et al., 2014). Disruption of self-association by site-directed mutations abolished the cell death mediated by NLRs (Maekawa et al., 2011), suggesting that self-association is critical for NLR signalling.

RRS1 is a TNL protein integrated with a WRKY domain as its recognition domain to detect bacterial effectors AvrRps4 and PopP2 (Sarris et al., 2015; Le Roux et al., 2015). Evidence has shown that RRS1 complexes with another TNL RPS4 through their TIR domain. The TIR domain heterodimerization is required for the recognition of the effectors AvrRps4 and PopP2 (Williams et al., 2014).

In mammalian immunity, NLRC4 (Nod-like receptor 4) associates with two independent immune receptors NAIP2 (neuronal apotopsis inhibitory protein 2) and NAIP5 upon PAMP perception (Kofoed and Vance, 2011). The heteromers then organize into the inflammasome to initiate innate immune responses by activating the caspase 1 protease (Schroder and Tschopp, 2010). This corroborating evidence from both plant and mammalian systems highlighted the importance of assembling heteromeric NLR complexes in innate immunity.

1.3.8 Nuclear translocation of some NLRs

Recent studies have highlighted the significance of nuclear accumulation of various NLRs in immunity. For example, barley CNL mildew A (MLA1) and *Arabidopsis* TNL-WRKY RRS1 showed an increased nuclear accumulation upon pathogen perception (Shen et al., 2007; Tasset et al., 2010). Additionally, *Arabidopsis* TNL SNC1 was shown to only activate immunity after shuttling into the nucleus (Xu et al., 2014a). Conditionally retaining snc1 in the cytosol by fusion to a glucocorticoid receptor (GR) fully suppresses *snc1* dwarfism (Xu et al., 2014a). In the absence of dexamethasone (DEX), the SNC1–GR fusion protein was expected to be sequestered by cytoplasmic HSP90/HSP70 chaperones (Pratt et al., 2001) and therefore inactive. Whereas DEX treatment releases snc1 to the nucleus, resulting in

dwarfism and enhanced disease resistance (Xu et al., 2014a).

Further evidence implies that translocation of NLR proteins to the nucleus requires the nuclear pore complex (NPC). One of the core component of NPC: MOS7 (Modifier of *snc1* 7), which is homologous with Drosophila and human nucleoporin protein Nup88, plays a critical role in maintaining the nuclear pool of SNC1 (Cheng et al., 2009). Additionally, MOS6, which was identified from the same *snc1* suppressor screen as MOS7, works as an importin alpha protein that could be involved in the recognition of nuclear-localization signal (NLS) peptides of SNC1 to translocate SNC1 to the nucleus (Palma et al., 2005).

1.3.9 Transcriptional controls by NLRs

From the significance of nuclear localization of NLRs, it is speculated that these NLRs shuttling into the nucleus would function to regulate the expression of defense-related genes. Barley *MLA* gene encodes a barley CNL protein that confers resistance to barley powdery mildew pathogen *Erysiphe graminis* f. sp. *hordei* (Wei et al., 1999). It was found that MLA directly interacts with transcription repressors WRKY1 and WRKY2 to release their inhibition of defense transcriptional reprogramming (Shen et al., 2007). Moreover, one additional transcription factor MYB6 was identified from a yeast-two hybrid screen to be MLA's direct interactor (Chang et al., 2013). MYB6 was shown to positively regulate basal defense and MLA-mediated immunity (Chang et al., 2013). After activation, MLA relocates to nucleus and releases WRKY1 repression of MYB6, thus initiating defense transcription (Chang et al., 2013).

More recent genetic and biochemical evidences have revealed several transcriptional regulators as nuclear targets of SNC1, which encodes a typical TNL in *Arabidopsis*. *MOS10/TPR1* (*Topless-related1*) (Zhu et al., 2010) encodes a transcriptional co-repressor with high homology to *TPR4* and *TPL*. The single mutant *tpr1* partially suppresses the *snc1* phenotype, and the combination of *tpr1 tpr4* and *tpl* mutations completely suppresses the

snc1 dwarfism and enhanced disease resistance, suggesting redundancy in the *TPR* family. Biochemical data revealed a physical association between TPR1 and SNC1, suggesting that SNC1 may activate defense response by regulating the transcriptional repression activity of TPR1 which suppresses the expression of negative regulators of immune responses (Zhu et al., 2010). Moreover, a reverse genetic screen has identified a bHLH (basic Helix-Loop-Helix) type transcription factor bHLH84 capable of physically associating with SNC1 (Xu et al., 2014b). *bHLH84* triggers significantly enhanced immunity when it is overexpressed. The constitutive defense response conferred by ectopic expression of *bHLH84* is partially lost when *SNC1* is knocked-out (Xu et al., 2014b).

Collectively, this evidence suggested that some NLRs likely activate defense responses by translocating into the nucleus to modulate transcriptional regulators to confer immune responses.

1.3.10 Plasma membrane localized CNLs

A number of *Arabidopsis* CNL proteins, such as RPM1, RPS2 and RPS5, were found to associate with the plasma membrane. So far, there is no evidence that these membrane-localized CNLs translocate to the nucleus. It is therefore an open question of how those CLRs transmit the signals into the nucleus. It is possible that the membrane localized CLRs may share common downstream pathways with PRRs to transduce signals. For example, RPS2 has been shown to activate MPK3/6 upon pathogen perception in a more sustained manner (Tsuda et al., 2013). MPK3/6 could further go to the nucleus to activate defense related transcription factors, such as WRKY33 to initiate defense transcription programming (Mao et al., 2011).

1.4 Regulation of SNC1 by MOSes and MUSEs

SNC1 encodes a typical TNL that was identified through a suppressor screen of *npr1*

(nonexpresser of PR gene 1) (Zhang et al., 2003b; Xu et al., 2014a). The mutant *snc1* carries a glutamic acid to lysine gain-of-function mutation in the linker region between the NB and LRR domains (Zhang et al., 2003b). Recent evidence has shown that the point mutation stabilizes snc1 protein, increasing its steady state level (Cheng et al., 2011a). The subsequent over-accumulation of snc1 protein consequently results in constitutive activation of defense signal transduction with increased levels of SA, constitutive expression of *PR* genes, and increased resistance against virulent pathogens such as the bacterium *Pseudomonas syringae* pv. *maculicola* (*P.s.m*) ES4326 and the oomycete *Hyaloperonospora arabidopsidis* (*H.a.*) Noco2 (Zhang et al., 2003b). Furthermore, *snc1* plants exhibit dwarf morphology without producing HR lesions, making this autoimmune mutant a powerful tool for genetic analysis without the interference of cell death.

Multiple forward genetics strategies have been employed in *snc1* genetic screens in order to find both positive and negative regulators of SNC1-mediated immunity, allowing for the identification of a number of *modifier of snc1* (*mos*) mutants (reviewed in Johnson et al., 2012) and *mutant*, *snc1-enhancing* (*muse*) mutants (Huang et al., 2013; Li et al., 2015), respectively. Characterization of these *MOS* and *MUSE* genes revealed a series of molecular events that are important for the regulation of SNC1-mediated immunity, most of which are involved in transcriptional regulations, mRNA processing and SNC1's protein stability control (*MOS6*, *MOS7* and *MOS10* mentioned above, are involved in protein nucleocytoplasmic transport and downstream gene transcription regulation of SNC1, respectively).

1.4.1 Transcriptional regulation of SNC1

MOS1 encodes a protein containing an HLA-B ASSOCIATED TRANSCRIPT 2 (BAT2) domain (Li et al., 2010). Methylation levels of the DNA upstream of coding region of *SNC1* was largely reduced in the *mos1* loss-of-function background (Li et al., 2010), suggesting

that MOS1 regulates the expression of *SNC1* at the chromatin level.

An additional *MOS* gene, *MOS9* encodes a plant-specific gene with an unknown function (Xia et al., 2013). In an effort to identify MOS9-associated proteins, an immunoprecipitation-mass spectroscopy experiment (IP-MS) was performed on *MOS9-GFP* transgenic plants, resulting in the identification of the Set1 class lysine 4 of histone 3 (H3K4) methyltransferase ATXR7 (ARABIDOPSIS TRITHORAX-RELATED 7) as a MOS9 direct interactor. Chromatin immunoprecipitation (ChIP) assays revealed a decrease in trimethylated H3K4 marks on the promoters of *SNC1* and its homologous *TNL* gene *RESISTANCE TO PERONOSPORA PARASITICA4* (*RPP4*), associated with a reduced expression of *SNC1* and *RPP4* transcripts in *mos9* plants (Xia et al., 2013). Taken together, these data suggested that chromatin regulators including MOS1, ATXR7 and MOS9 alter methylation of histone codes to regulate *SNC1* gene transcription.

1.4.2 *SNC1* mRNA splicing and export

Following transcription, MOS2, MOS4 and associated complex proteins (MAC), MOS12, MOS14 are all required for proper splicing of the transcripts of *SNC1* (Zhang et al., 2005; Palma et al., 2007; Xu et al., 2012, 2011). After splicing, 5' capping and addition of 3' polyA tail, mature mRNAs are exported from the nucleus to the cytosol to be translated. This export step involves an RNA cochaperone, MOS11, as well as the Nup 107-160 nuclear pore complex which includes MOS3 (Germain et al., 2010; Zhang and Li, 2005). Collectively, these pre-translational regulatory steps of *SNC1* suggest that the up-regulation of *SNC1* expression is important during defense response. The increased amount of an NLR protein would likely enhance pathogen detection capabilities and amplify immune response signalling.

1.4.3 Post-translational regulation: NLR's protein stability is control by N-terminal acetylation and ubiquitination

The protein levels of NLR immune receptors must be tightly controlled to avoid autoimmunity. The functional identification of *CPR1/CPR30* (*Constitutive Expressor of PR genes*), which encodes the F-box protein of a Cullin-based E3 ligase complex, revealed that it controls the protein stability of TNL SNC1 and CNL RPS2 (Cheng et al., 2011b). The SNC1 and RPS2 proteins accumulated in the *cpr1* mutant, and were rapidly degraded when CPR1 was overexpressed. Additionally, the constitutive defense responses in *cpr1* can be largely suppressed by the loss-of-function mutation of *SNC1*. (Cheng et al., 2011b).

Moreover, the *MUSE* screen identified a novel gene *MUSE3* that facilitates the ubiquitination process of SNC1 and RPS2 (Huang et al., 2014b). *MUSE3* encodes an E4 ubiquitin ligase, a highly conserved gene in eukaryotes that promotes ubiquitin chain elongation during the ubiquitination process (Huang et al., 2014b). Mutation in *MUSE3* leads to the enhancement of *snc1*-mediated immunity and accumulation of SNC1 and RPS2 protein levels (Huang et al., 2014b). The SNC1 or RPS2 protein levels were reduced when *MUSE3* was transiently co-expressed with *CPR1* and *SNC1* or *RPS2* compared with co-expressing *CRP1* and *SNC1* or *RPS2* alone in *Nicotiana benthamiana*. Interestingly, the SNC1 protein level was not altered when *MUSE3* and *SNC1* were co-expressed, suggesting that MUSE3 only facilitates to degrade SNC1 and RPS2 in the presence of the proper E3 ligase (Huang et al., 2014b).

Furthermore, mutations in two additional *MUSE*s, *MUSE10* and *MUSE12,* also result in accumulation of the protein levels of the NLRs including SNC1, RPS2 and RPS4 (Huang et al., 2014a). *MUSE10* and *MUSE12* encode two isoforms of *HSP90*, *HSP90.3* and *HSP90.2*, respectively. Co-immunoprecipitation analysis revealed that HSP90.3 and HSP90.2 directly interact with SNC1 to facilitate its degradation, possibly through the assistance of SCF E3 ubiquitin ligase complex assembly with SGT1 (Huang et al., 2014a).

In addition to ubiquitination, N-terminal acetylation was found to be another important mechanism to regulate SNC1 turnover (Xu et al., 2015a). It has been shown that SNC1 protein undergoes N-terminal translation initiation at two independent codons and acetylation that leads to opposite consequences for protein stability (Xu et al., 2015a). Initiation of SNC1 from the first Met results in being acetylated by N-terminal acetyltransferase (Nat) A, causing a more unstable SNC1 protein. Whereas acetylation of the second Met mediated by Nat B results in a more stable SNC1 protein (Xu et al., 2015a). *MUSE6* encodes a subunit of the Nat A complex. Loss-of-function of *MUSE6* leads to the abolishment of the first Met acetylation and consequently, a heightened protein level of SNC1 (Xu et al., 2015a).

Collectively, the identification of the negative regulators of SNC1's turnover, including CPR1, MUSE3, MUSE6, MUSE10 and MUSE12, uncovered the significance of maintaining NLR's homeostasis in plant cells, as over-accumulation of NLR proteins could lead to autoimmunity and be detrimental to plant growth and propagation.

1.5 Thesis objectives

1.5.1 Identification and characterization of E3 ubiquitin ligases involved in plant immunity

The identification of negative regulators of SNC1 turnover highlighted the importance of homeostatic control of immune regulators in plants. One of the most common homeostasis regulatory mechanisms is by ubiquitination. By labeling a protein with a ubiquitin chain (at least four moieties) linked via the Lys48 residue, the protein is targeted for degradation by the ubiquitin-26S proteasome (Smalle and Vierstra, 2004). The ubiquitin-26S proteasome system (UPS) involves the sequential steps of three enzymes, a ubiquitin activating enzyme (E1), a ubiquitin conjugating enzyme (E2), and a ubiquitin ligase enzyme (E3). Among the three enzymes, E3 ubiquitin ligases are key factors in determining substrate specificity

(Smalle and Vierstra, 2004). There are over 1500 E3 ubiquitin ligase encoding genes in the *Arabidopsis* genome (Vierstra, 2003). However, so far only a small number of them have been well characterized. In order to uncover important E3 ubiquitin ligases involved in plant immunity, I aimed to use a reverse overexpression genetic screen to identify key immune-related E3 ubiquitin ligases and to investigate how they are involved in plant immunity. This was the first objective of my thesis.

1.5.2 Studying the role and specificity of ADR1s in NLR signalling

The *Arabidopsis* ADR1 (Activated Disease Resistance) is a small family of CNLs consisting of three members (ADR1, ADR1-L1, ADR1-L2) (Chini and Loake, 2005). ADR1s function as "helper NB-LRRs" to transduce signals after activation of specific NLR proteins and are essential for basal defense against virulent pathogens (Bonardi et al., 2011). Auto-activation of *ADR1* or *ADR1-L2* results in the constitutive activation of defense responses (Grant et al., 2003; Chini et al., 2004; Chini and Loake, 2005; Bonardi et al., 2011). Loss-of-function of *adr triple* (i.e. the *adr1 adr1-l1 adr1-l2* triple mutant) leads to compromised basal defense and significant suppression of ETI mediated defence by specific NLRs such as RPP4 and RPP2 (Bonardi et al., 2011). However, the role of ADRs in NLR signalling and the specificity of ADRs required by different NLRs are unknown. Thus, the second objective of my thesis was to specifically investigate the involvement of ADRs in SNC1-mediated immunity using molecular genetic approaches.

2 A reverse genetic screen looking for key E3 ubiquitin ligases involved in plant immunity

2.1 Summary

As a common post-translational modification, ubiquitination is used for regulating protein function, notably in terms of stability. In recent years, ubiquitination has emerged as a major player in plant immunity regulation; however, not many E3 ligases have been identified in this biological process, likely due to the high redundancy or knock-out lethality of E3 ubiquitin ligase families in plants. In an effort to identify E3 ubiquitin ligases involved in plant defense, I conducted a *snc1*-influencing plant E3 ligase reverse genetic (SNIPER) screen. I first selected candidate E3 ligase-encoding genes whose transcripts are up-regulated upon plant defense, according to TAIR Microarray Expression databases. The chosen candidates were then overexpressed in the autoimmune mutant *snc1* background, and screened for transgenic enhancers or suppressors that altered *snc1*-mediated autoimmunity. From the screen, six *SNIPER* genes were identified. When overexpressed, four of them suppress *snc1* phenotype to different degrees and two of them enhance it.

2.2 Introduction

A three-step enzyme catalytic reaction (E1 activation, E2 conjugation, E3 ligation) that covalently attaches ubiquitin polymers at lysine 48 on targeted substrates, subjects them to degradation by the 26S proteasome (Smalle and Vierstra, 2004). Among these three ubiquitin catalytic enzymes, E3 ligases are the key factors determining the specificities for substrates. There are more than 1500 E3 ubiquitin ligase-coding genes in *Arabidopsis* genome, accounting for over 5% the *Arabidopsis* proteome (Vierstra, 2003), suggesting that they have significant roles in plant physiological regulation.

The plant E3 ubiquitin ligases can be grouped into two classes, each including three

types, depending on their different conserved domains and mechanisms of action: 1) simple E3s including HECT (Homology to E6AP C Terminus)-type, RING (Real Interesting New Gene)-type and U-box-type; and 2) complex E3s including Cullin 1-based SCF complex, Cullin 3-based BTB (Bric à Brac, Tramtrack, and Broad Complex)-type and APC (Anaphase-Promoting Complex)-type (Cheng and Li, 2012). HECT E3 ligases contain unique HECT domains that enable them to form ubiquintin-E3 thiol-ester intermediates prior to the ubiquitin-substrate product (Downes et al., 2003). RING/U-box E3 ligases, on the other hand, bear either RING domains or RING derivative domains called U-box domains that allow the E3 ligases to bind E2 conjugating enzymes. The RING domain contains eight highly conserved cysteines (Cs) and histidines (Hs), which bind two zinc ions in one of two formats: C3H2C3 or C3H1C4 (Deshaies and Joazeiro, 2009). The U-box domain is structurally similar to the RING domain (Ohi et al., 2003). However, instead of using zinc ion chelation, the U-box domain exploits electrostatic interactions to stabilize its structure (Ohi et al., 2003).

SCF is an E3 complex consisting of three subunits: S phase kinase-associated protein 1 (SKP1), Cullin1 and an F-box protein. Similar to RING/U-box E3s, SCF complexes serve as scaffolds that bring together an E2 enzyme and a specific substrate, allowing the transfer of ubiquitin molecules from the E2 to the substrate. Among the three subunits of the SCF complex, the F-box protein is the substrate-determining factor. F-box genes compose the biggest E3 ubiquitin ligase group in plants, accounting for over 700 in the *Arabidopsis* genome (Gagne et al., 2002).

It has been shown that E3 ligases are at the core of almost all aspects of plant development and physiology (Dreher and Callis, 2007). The most representative examples are the roles of E3 ligases in hormone signalling in response to auxin, jasmonic acid (JA), gibberellins, etc. Auxin is a plant developmental hormone that directly regulates plant growth through a family of auxin responsive transcription factors (ARFs) (Okushima et al., 2005). These ARFs are strongly repressed by AUXIN (AUX) or INDOLE-3-ACETIC ACID (IAA)

proteins. The presence of auxin induces the degradation of AUX/IAA proteins; F-box E3 ubiquitin ligases in the TRANSPORT INHIBITOR RESPONSE 1 (TIR1) family target AUX/IAA proteins in the presence of auxin, resulting in the de-repression of ARF transcription factors that activate auxin responses (Dharmasiri et al., 2005).

A similar mechanism of de-repression by the ubiquitin proteasome system (UPS) also applies to JA signalling. Normally, the family of JA responsive transcription factors MYB DOMAIN PROTEINs (MYBs) is inhibited by a family of JA-ZIM domain (JAZ) repressors (Thines et al., 2007; Chini et al., 2007). The presence of a biological active form of JA, JA-Ile, serves as a molecular glue to significantly enhance the interaction of an F-box protein, CORONATINE-INSENSITIVE 1 (COI1), with JAZs for their efficiently degradation (Katsir et al., 2008). The degradation of the JAZ repressors consequently reverses the repression of the transcription of the MYB family, thus triggering the activation of JA responses (Katsir et al., 2008).

In addition to plant hormone signalling, there is emerging evidence showing that many E3 ubiquitin ligases are involved in plant immunity. For example, a trio of Plant U-box (PUB) E3 ubiquitin ligases PUB22/PUB23/PUB24 has been shown to negatively regulate PTI (Trujillo et al., 2008). The *pub22 pub23 pub24* triple mutant displayed elevated oxidative burst, enhanced MPK3/MPK6 activity, and increased transcriptional activation of PTI marker genes (Trujillo et al., 2008). Yeast-two hybrid screens identified Exo70B2, a subunit of the exocyst complex that mediates vesicle tethering during exocytosis, as the substrate of PUB22, PUB23 and PUB24 (Stegmann et al., 2012). Moreover, two homologous E3 ligases PUB12 and PUB13 were identified to specifically regulate the turnover of flagellin receptor FLS2. Upon flg22 treatment, PUB12 and PUB13 are phosphorylated by BAK1, which primes them to subsequently ubiquitinate and degrade FLS2 through 26S proteasome (Lu et al., 2011).

In order to identify additional important E3 ligases involved in plant immunity, I

conducted a *snc1*-influencing plant E3 ubiquitin ligase reverse genetic (SNIPER) screen. I selected candidate E3 ligase-encoding genes whose transcripts are up-regulated upon plant defense, according to TAIR Microarray Expression databases. Next, these E3 ligase genes were overexpressed in *snc1* background to look for *snc1*-enhancers or suppressors. Here we described the SNIPER screen and the six *SNIPER* mutants identified through the screen.

2.3 Results

2.3.1 Primary screen

2.3.1.1 Compilation of the candidate list of putative E3 ligases based on microarray data

In order to investigate the E3 ligases involved in plant innate immunity, we selected 50 putative E3 ligase-encoding genes whose transcripts are up-regulated upon PAMP treatment based on TAIR Microarray Expression databases (1.7-fold induction was used as the cut off threshold), and aimed to overexpress them in the *snc1* background searching for either suppressors or enhancers.

2.3.1.2 Overexpression of E3 ligase genes in *snc1* background

To accelerate cloning, we ordered available U-clones from ABRC (Arabidopsis Biological Resource Center). U-clones are PCR-amplified, sequence verified ORF (Open Reading Frame) clones in the pUNI vector. These U-clones were subcloned into a modified pGreen0229 binary vector driven by the CaMV *35S* promoter with an N-terminus HA tag. These binary vectors containing E3 ligase genes were then transformed into *Agrobacterium tumefaciens* and then agro-transformed into *snc1* plants using a floral dipping method (Clough and Bent, 1998) (Figure 2.1). For each E3 ligase transgene, an average number of 24

transformants were obtained.

The *snc1* mutant displays typical autoimmune phenotypes with stunted growth, dark green curly leaves and siliques organized in bushy clusters (Li et al., 2001a). These *snc1*-related morphological phenotypes usually correlate with defense outputs, and were used as criteria to select *snc1*-suppressing and enhancing mutants. The detailed morphological phenotypes of E3 ligase transformants were collected and summarized in Table 2.1. The morphology photographs of a representative suppressor and enhancer are shown in Figure 2.1.

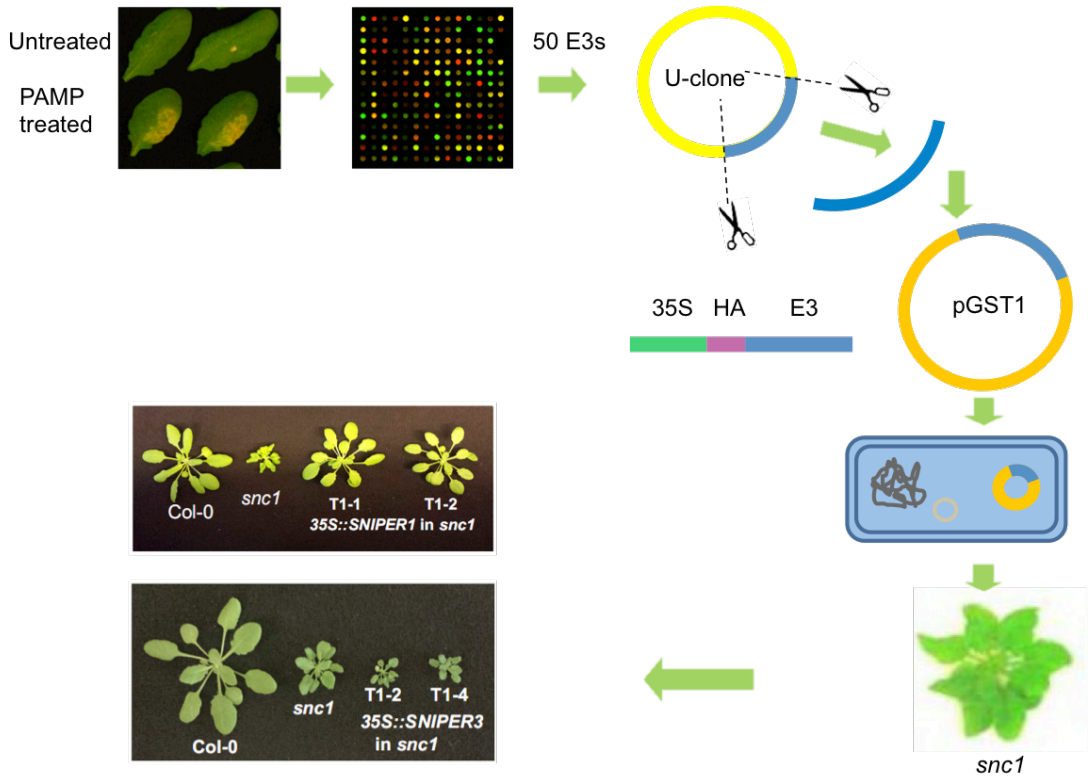

Figure 2.1 SNIPER screen strategy and two representative SNIPERs.

A diagram of SNIPER screen workflow: 50 E3 coding genes with upregulated expression upon PAMP treatment were selected through the microarray data. U-clones of 33 of these E3 genes were obtained from ABRC and were subsequently subcloned into pGST1 vector. Once transformed into *Agrobacterium*, the E3-containing pGST vectors were transformed into the *snc1* background by *Agrobacterium*-mediated floral dip method (Clough and Bent, 1998). Pictures of the morphology of one representative *snc1*-suppressor and one representative *snc1*-enhancer are shown on the bottom left.

Table 2.1 A summary of SNIPER screen and their overexpression phenotypes in *snc1*.

No.	E3 type	Phenotype	Gene ID/lab code
1	RING	---	SNIPER2/U4H
2	RING	+/-	U1
3	U-box	++	SNIPER3/U3
4	RING	---	SNIPER1/U4
5	F-box	++	U5
6	RING	-	U6
7	U-box	++	CMPG1/U7
8	F-box	+/-	U8
9	F-box	-	U9
10	F-box	+/-	U10
11	F-box	+	U11
12	BTB/POZ	--	SNIPER4/U12
13	ASK3	+/-	U13
14	RING	+/-	U15
15	F-box	+/-	U17
16	RING	+/-	U18
17	RING	+	U19
18	RING	-	U20
19	RING	+	U21
20	U-box	+	U22
21	F-box	+++	SNIPER5/U23
22	RING	++	U25
23	BTB/POZ	+/-	U26
24	RING	+++	U27
25	U-box	+/-	U28
26	F-box	+/-	U30
27	RING	--	SNIPER6/U31
28	F-box	+/-	U32
29	RING	+	U33
30	F-box	+/-	U35
31	U-box	+/-	U36
32	RING	+	U37
33	RING	+/-	U38

Note: "+" enhancing, "-" suppressing, "+/-" no changes

2.3.1.3 Selection of candidate E3 genes

Phenotypic observations of the *snc1* plants containing E3 ligase transgenes indicated that 19 out of 33 overexpressed E3 ligases altered *snc1* dwarfism to varying degrees, six of which displayed dramatic *snc1* phenotypic alterations. When overexpressed, two E3 ligases fully suppress *snc1*, two partially suppress *snc1*, and two enhance *snc1* (Table 2.1). These six E3 ligases were then named *SNIPER1* to *SNIPER6* (Table 2.1).

2.3.2 Secondary screen: phenotypic and functional characterization of candidate SNIPERs

In order to confirm that the phenotypes of the E3 transformants resulted from over expression of the E3 ligase genes rather than silencing, the transcript levels of transgenes were examined by Reverse Transcriptase-mediated (RT)-PCR and the protein expression levels were analyzed by Western blot. The enhanced transcript and/or protein levels of the transgenes were correlated with the altered *snc1* phenotypes, suggesting that the phenotypes are not the consequences of gene silencing (data not shown).

To rule out possible interference of the epitope HA tag with the function of the E3 ligase, untagged E3 ligase driven by CaMV *35S* promoter transgenic plants were generated and phenotypically assayed. Consistent morphological phenotypes of the untagged E3 ligase transgenic plants with that observed in the tagged E3 transgenic plants were observed (data not shown), suggesting that the HA epitope tag did not interfere with the E3 ligase overexpression phenotypes.

2.3.2.1 Phenotypic characterizations of *35S::SNIPER* lines

To confirm that the *35S::SNIPER* mutants isolated from the primary screen are indeed involved in immunity, defense-related phenotypes including resistance to virulent pathogens

were assessed in each *35S::SNIPER* mutant.

For *SNIPER* suppressors and *SNIPER* enhancers, enhanced susceptibility and enhanced resistance were confirmed with pathogen infections with *Hyaloperonospora arabidopsidis* (*H.a.*) Noco2 (Figure 2.2). For *H.a.* Noco2 infections, the plant seedlings (~14 days old, grown on soil) were sprayed with a solution of Noco2 conidiospores and were maintained under high humidity. Scoring was performed after incubation for a week by assessing the appearance of conidiospores on the leaves of the seedlings following a protocol described in Li *et al.* (2001).

To test whether the suppressing or enhancing phenotypes of *35S::SNIPER* lines in *snc1* are dependent on *snc1*, *35S::SNIPER* lines in the Col-0 background were generated. (As SNIPER2 has 37% amino acid identities with SNIPER1 and overexpression of *SNIPER2* displayed *snc1*-suppressing phenotypes as overexpression of *SNIPER1*, we concluded that *SNIPER1* and *SNIPER2* are homologous to each other, thus only the data of *35S::SNIPER1* in Col-0 was shown here. Data of *35S::SNIPER5* not shown here.) Each *35S::SNIPER* line was phenotypically characterized with the infections of *H.a.* Noco2 and/or *Pseudomonas syringae* pv. *Maculicola* (*P.s.m.*) ES4326. For *P.s.m.* infection, four-week-old adult plant leaves were infiltrated with a bacterial solution (OD_{600} = 0.0001). Infected leaves were harvested, ground and serial diluted to a countable colony-forming unit (cfu) number at 0 and 3 days after inoculation. The results showed that the overexpression *SNIPER* *snc1*-suppressors (*SNIPER1* and *4*) /enhancers (*SNIPER3* and *6*) also showed enhanced disease susceptibility and resistance, respectively, in the Col-0 background (Figure 2.3), suggesting that the overexpression phenotypes of *SNIPERs* are not *snc1*-dependent.

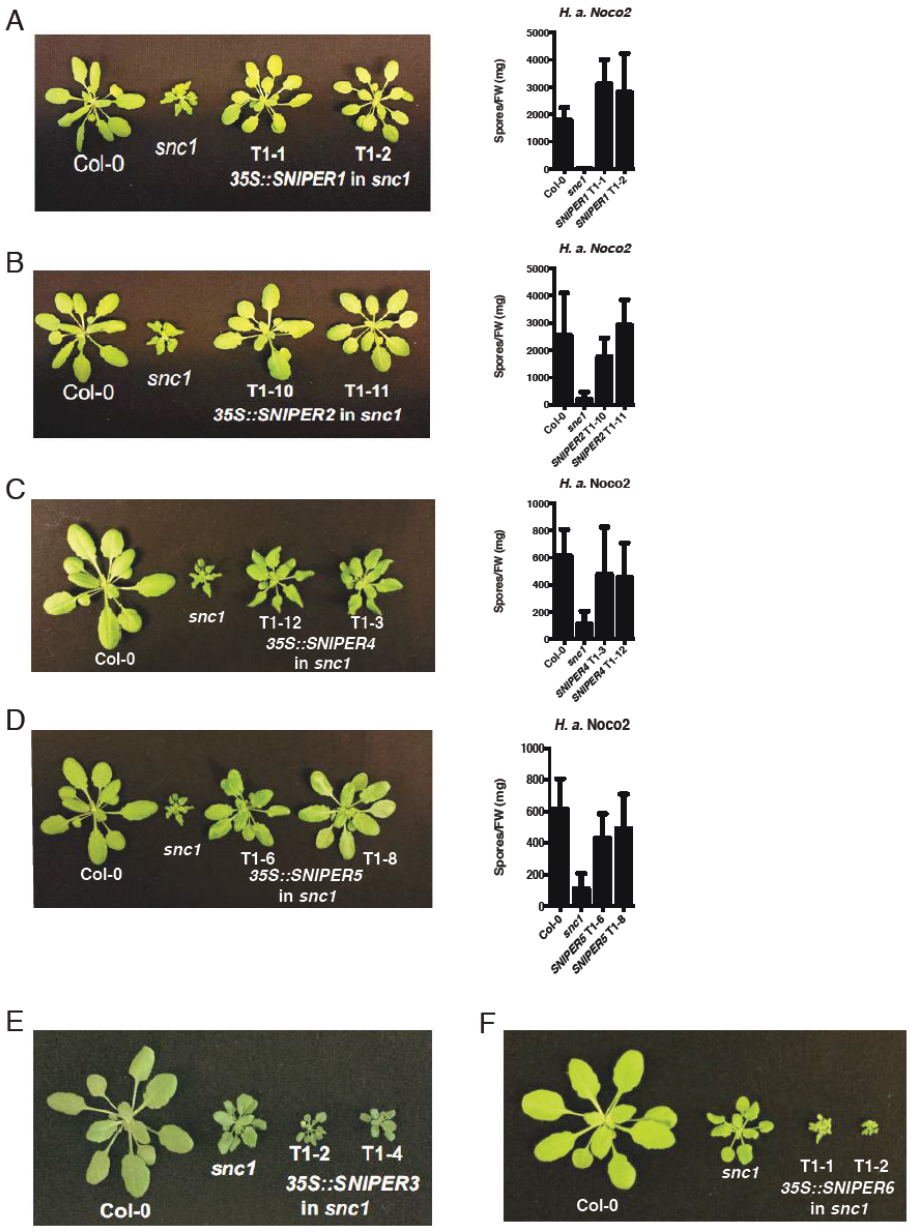

Figure 2.2 Phenotypic characterization of representative transgenic lines of *35S::SNIPER1-6* in *snc1* plants.

(A to D) Morphology of four-week-old plants and the growth of *H.a.* Noco2 on two-week old Col-0, *snc1*, and two representative transgenic lines of *snc1*-suppressing *SNIPER* plants. (E to F) Morphology of four-week-old Col-0, *snc1*, and two representative transgenic lines of *snc1*-enhancing *SNIPER* plants.

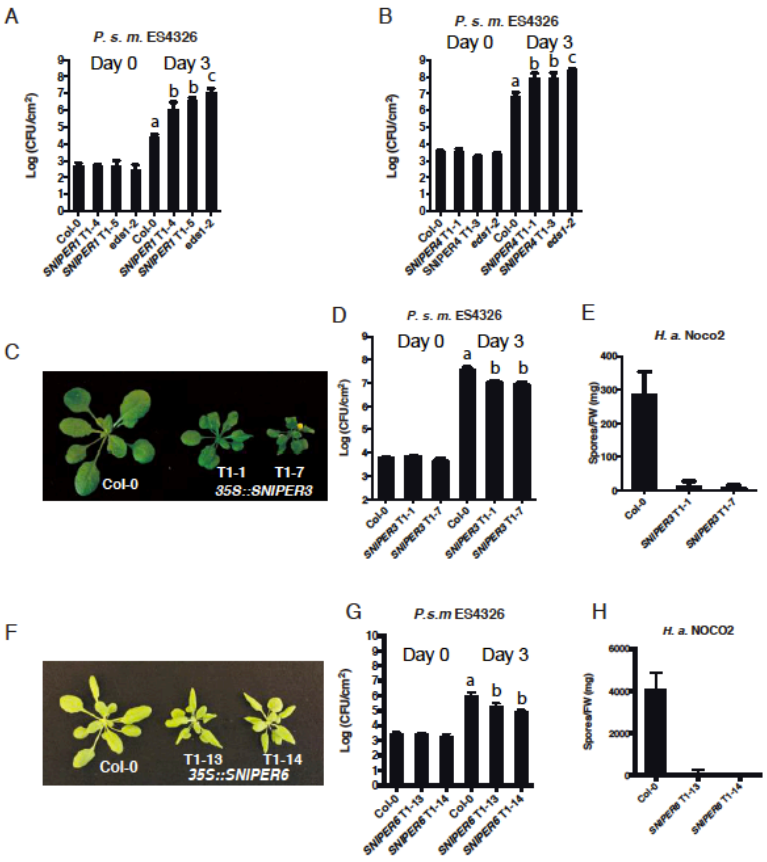

Figure 2.3 Phenotypic characterization of representative transgenic lines of *35S::SNIPER1, 3-6* in Col-0 background.

(A to B) Bacterial growth of *P.s.m.* ES4326 on four-week old Col-0, *snc1*, and two representative transgenic lines of *snc1*-suppressing *SNIPER1* and *4* plants.

(C to E) Morphology, pathogen growth of *P.s.m.* ES4326 and *H.a.* Noco2 of four-week-old Col-0, *snc1*, and two representative transgenic lines of *snc1*-enhancing *SNIPER3* plants.

(F to H) Morphology, pathogen growth of *P.s.m.* ES4326 and *H.a.* Noco2 of four-week-old Col-0, *snc1*, and two representative transgenic lines of *snc1*-enhancing *SNIPER6* plants.

(A, B, D, E, G and H) Data represent means of five replicates. Error bars are standard deviations. Different superscripts indicate significant differences between groups, whereas identical superscripts denote no significant differences (One-way ANOVA, GraphPad Prism 6).

2.4 Discussion

Here we report the SNIPER screen to identify E3 ligases whose overexpression resulted in altered *snc1*-mediated immunity. From the screen, we identified six *SNIPER* genes as well as CMPG1 (Table 2.1), which was previously found as a positive regulator required for ETI responses in tobacco and tomato (González-Lamothe et al., 2006). *SNIPER1* and *SNIPER2* encode two homologous RING-type E3 ligases. Overexpression of *SNIPER1* completely suppressed *snc1*-related phenotypes in *snc1* background and enhanced disease susceptibility to virulent pathogens in wild-type background. *SNIPER4* and *SNIPER5*, encoding a BTB- and a U-box-type E3 ligase, respectively, are two partial *snc1*-suppressors when overexpressed. In contrast, overexpression of *SNIPER3* and *SNIPER6,* which encode a U-box-type and an F-box E3 ligase showed enhanced disease resistance phenotypes in both *snc1* and Col-0 background. Overall, 6 out of 33 E3 ligases (encompassing a range of different E3-types) tested from the screen have varying degrees of alteration in defense responses in both *snc1* and Col-0. Among the 6 *SNIPER*s, I selected the *SNIPER1/2* gene pair and *SNIPER3* for further analysis. The analysis of *SNIPER1/2* is incomplete, and thus is not included in this thesis. Chapter 3 will describe *SNIPER3* in more detail.

The analysis of *SNIPER* loss-of-function mutants could confirm the functions of these SNIPERs. The *SNIPER*s loss-of-function mutants are expected to show the opposite defense phenotypes of the *SNIPER* overexpression lines. Due to genetic redundancy, double or higher order mutants can be generated in order to observe the phenotypes. As the *SNIPERs* encode E3 ligases, identification of their ubiquitination substrates is fundamental to understand how these SNIPERs regulate plant immunity. This could be done using Yeast-2-Hybrid screens and/or immunoprecipitation-mass spectrometry (IP-MS) approaches. Targets could also be speculated from known regulators of SNC1-mediated immunity based on the phenotypes. For example, for *snc1*-suppressing E3s, the targets could be positive regulators such as EDS1, PAD4; transcriptional regulators MOS10, bHLH84; or SNC1 itself.

For *snc1*-enhancing E3s, the targets could be negative regulators such as CPR1 or MUSE proteins. To test these possibilities, protein levels of these potential targets can be examined in both E3 knock-out mutants and E3-overexpressing transgenic plants.

3. E3 ligase SAUL1 serves as a positive immune regulator guarded by a TNL receptor SUSA1

3.1 Summary

Ubiquitination is a common post-translational modification for regulating protein functions, notably in terms of stability. Although E3 ligase-encoding gene families are highly expanded in higher plants, not very many have been functionally characterized. To search for E3s functioning in plant immunity, we designed a *snc1*-influencing plant E3 ligase reverse genetic screen (SNIPER), where candidate E3s were overexpressed in the sensitized autoimmune *snc1* background to search for E3s that can alter the phenotypes of *snc1* upon overexpression. Here we describe *SNIPER3/SAUL1/PUB44* as a *snc1* enhancer, as its overexpression leads to enhanced resistance responses in both *snc1* and wild-type backgrounds. Since loss-of-function *saul1-1* plants exhibit seedling lethality, suppressor screens were conducted with *saul1-1* to search for its E3 ligase substrate. From the screens, we identified a novel Toll Interleukin 1 Receptor (TIR)-type nucleotide-binding leucine-rich repeat (TNL) immune receptor-encoding gene *Suppressor of saul1 1* (*SUSA1*). Knocking out *SUSA1* completely suppresses *saul1*-related autoimmune phenotypes. In addition, SAUL1 associates with SUSA1 *in planta*. However, SUSA1 does not seem to be the ubiquitination substrate of SAUL1. Interestingly, the SAUL1 overexpression autoimmune phenotypes also require SUSA1, suggesting a role of SUSA1 in sensing SAUL1's homeostasis. Although *SUSA1* is genomically in tandem with *CHS1* and *TN2*, which encode truncated TNLs without LRR domains, *saul1-1* does not seem to rely on *CHS1* or *TN2*. Moreover, triple mutant analysis of *saul1-1 susa1 pub43* revealed that SAUL1 works redundantly with it closest homolog PUB43 in positively regulating pathogen-associated molecular patter (PAMP)-triggered immunity. In summary, the E3 ligase SAUL1 serves as a positive regulator of immunity and its homeostasis is monitored by TNL SUSA1.

3.2 Introduction

Plant immune responses against microbial pathogen infections can be initiated by two types of immune receptors (Jones and Dangl, 2006; Dodds and Rathjen, 2010). Plasma membrane-localized pattern recognition receptors (PRRs) recognize pathogen-associated molecular patterns (PAMPs), such as bacterial flagellin and fungal chitin to activate PAMP triggered immunity (PTI) (Boller and Felix, 2009; Monaghan and Zipfel, 2012). In contrast, intracellular nucleotide-binding leucine-rich repeats proteins (NLR; or Nod-like receptor) confer disease resistance by monitoring the presence or activity of pathogen effectors to initiate effector-triggered immunity (ETI). In Arabidopsis, there are two typical classes of NLR proteins depending on their N-terminal structure, one with a coiled-coil (CC) domain, and the other with a Toll and interleukin-1 receptor (TIR) domain (Li et al., 2015). *Suppressor of NPR1, Constitutive 1* (*SNC1*) encodes a TIR-type NLR (TNL). Mutant *snc1* carries a gain-of-function mutation resulting in the constitutive activation of immune responses, with constitutive expression of defense marker *Pathogenesis Related* (*PR*) genes, and enhanced resistance against virulent pathogens such as bacteria *Pseudomonas syringae* pv. *maculicola* (*P.s.m.*) ES4326 and oomycete *Hyaloperonospora arabidopsidis* (*H.a.*) Noco2 (Li et al., 2001a; Zhang et al., 2003a). Furthermore, unlike many other autoimmune mutants, *snc1* plants exhibit a dwarf morphology without cell death lesions, making it a useful sensitized background for genetic screening (Johnson et al., 2012).

Ubiquitination is a common post-translational modification in eukaryotes, which is most often utilized to regulate its substrate protein's stability (Vierstra, 2009). By covalently attaching ubiquitin linked via the Lys48 residue to its substrate, the protein is marked and subsequently targeted for degradation by the 26S proteasome. The ubiquitination reaction involves three sequential steps catalyzed by three enzymes, a ubiquitin activating enzyme (E1), a ubiquitin conjugating enzyme (E2), and a ubiquitin ligase (E3). Among these proteins, E3 ligases are key factors in determining substrate specificity (Hershko and Ciechanover, 1998). Compared to less than 700 E3-encoding genes in the human genome, higher plants

have largely expanded E3 gene families. For example, the Arabidopsis genome contains over 1400 E3-encoding genes (Cheng and Li, 2012). Such expansion suggests their likely roles in plant-specific processes and/or the potential existence of genetic redundancy.

Recent studies revealed that E3 ligases play important roles in immune signaling in both PTI and ETI. For example, the Arabidopsis Plant U-box (PUB) protein PUB12 and PUB13 were identified to negatively regulate flagella-induced PTI responses through the degradation of flagellin receptor FLS2 (Flagellin-Sensitive 2) (Lu et al., 2011). A triplet of U-box protein paralogs PUB22, PUB23 and PUB24 redundantly target exocyst complex component EXO70B2 (Exocyst subunit EXO70 B2) for degradation, required for PTI responses (Stegmann et al., 2012). In addition, the F-box protein CPR1 (Constitutive Expressor of *PR* genes) was found to control the stability of NLRs including SNC1 and RPS2 (Cheng et al., 2011a). The process of the polyubiquitination and degradation of SNC1 and RPS2 was facilitated by the E4 ubiquitin ligase MUSE3 (Mutant, *snc1*-enhancing 3) (Huang et al., 2014b). Furthermore, the mutant of E3 ligase *saul1-1* (Senescence-Associated E3 Ubiquitin Ligase 1; also named PUB44) was identified as an autoimmune mutant whose autoimmunity can be suppressed by environment factors such as high temperature and high light conditions(Disch et al., 2015; Vogelmann et al., 2012) Interestingly, the leaf necrosis/seedling lethality phenotype of *saul1-1* fully depends on *PAD4* and *EDS1* (Disch et al., 2015), suggesting that knocking out *SAUL1* promotes PAD4- and EDS1-dependent immune responses.

To search for novel E3s involved in plant immunity regulation, we conducted a *snc1*-influencing plant E3 ligase reverse genetic screen (SNIPER), which identified *SAUL1*/*SNIPER3/PUB44*. When overexpressed, *SAUL1* enhances *snc1* phenotypes and also results in autoimmunity in wild-type background, suggesting that *SAUL1* positively regulates immune responses. Suppressor screens of *saul1-1* mutant reveal that loss of *SAUL1* leads to the activation of a typical TNL protein SUSA1 (Suppressor of *saul1* 1). SUSA1 can associate with SAUL1 *in planta*. Interestingly, the autoimmunity of *SAUL1* overexpressing plants also

relies on SUSA1. Triple mutant *saul1-1 susa1 pub43* exhibit susceptibility to *P.s.t.* hrcC-, suggesting that SAUL1 and PUB43 function redundantly in PTI. These results indicate that SAUL1 is a positive immune regulator, whose homeostasis is monitored by a TNL protein.

3.3 Results

3.3.1 Overexpression of *SAUL1* enhances *snc1* and leads to autoimmunity in wild-type Col-0

In an effort to search for E3 ligases involved in plant immunity, a *snc1*-influencing plant E3 ligase reverse genetic screen (SNIPER) was conducted. We selected 50 candidate E3-encoding genes whose transcripts are up-regulated upon plant defense, according to TAIR Microarray Expression databases. The chosen candidates were overexpressed in the autoimmune mutant *snc1* background. In the primary screen, we searched for transgenic enhancers and suppressors that altered *snc1*-mediated dwarfism.

From the SNIPER screen, we identified *SNIPER3/SAUL1* (also named *PUB44/AT1G20780*, hereafter *SAUL1*) as a *snc1* enhancer. When overexpressed in *snc1,* it enhanced *snc1* dwarfism (Figure 3.1A and 3.1B). To examine its overexpression phenotypes in wild-type background, independent transgenic plants carrying *SAUL1* driven by Cauliflower Mosaic Virus (CaMV) 35S promoter were obtained. The majority of the transformants exhibited stunted growth and necrosis (Figure 3.1C), indicative of autoimmunity. In the *35S::SAUL1* transgenic plants, the expression of *PR1* was up-regulated significantly compared with Col-0 (Figure 3.1D). Consistent with the constitutive *PR1* expression, the growth of virulent pathogens oomycete *Hyaloperonospora arabidopsidis* (*H.a.*) Noco2 (Figure 3.1E) and bacteria *Pseudomonas syringae* pv. *maculicola* (*P.s.m.*) ES4326 (Figure 3.1F) was also reduced. Taken together, these data suggest that *SAUL1* plays a positive role in promoting immune responses. When overexpressed, the plants exhibit autoimmunity.

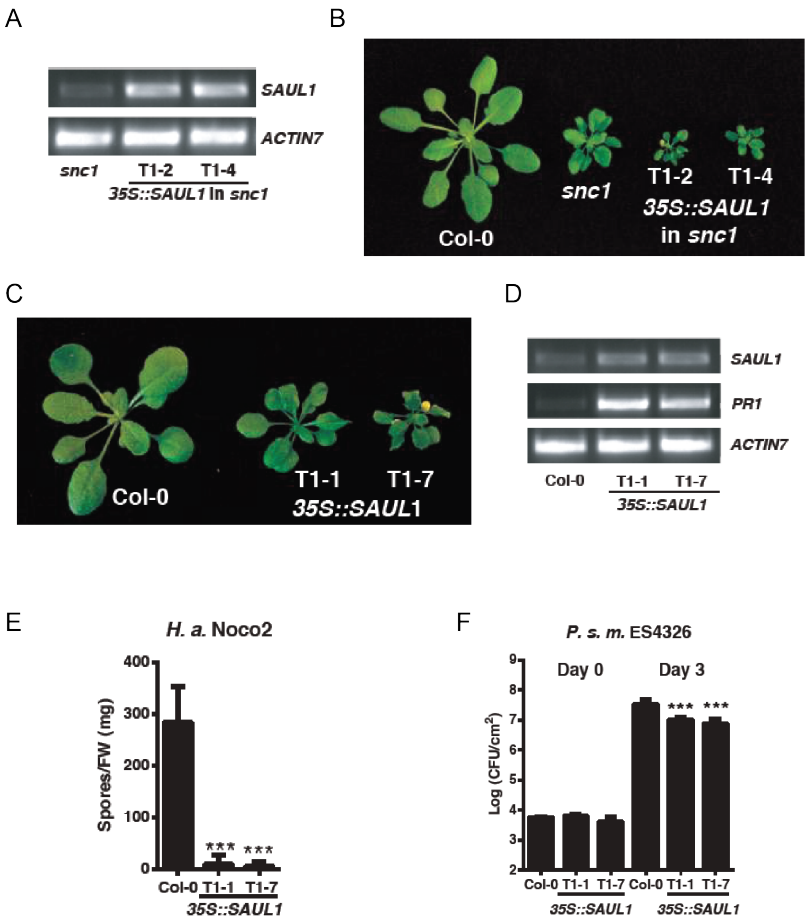

Figure 3.1 Overexpression of SAUL1 enhances *snc1* and confers autoimmunity in wild-type Col-0 background.

(A) *SAUL1* expression in the indicated genotypes as determined by RT-PCR. *ACTIN7* serves as loading control. The fragments of *SAUL1* and *ACTIN1* were amplified from cDNA templates by 31 cycles of PCR. The PCR products were then analyzed by agarose gel electrophoresis.

(B) Morphology of four-week-old Col-0, *snc1* and two independent *35S::SAUL1* transgenic lines in the *snc1* background.

(C) Morphology of four-week-old Col-0 and two independent *35S::SAUL1* transgenic lines in Col-0 background.

(D) *SAUL1* and *PR1* genes expression in the indicated genotypes as determined by RT-PCR. *ACTIN7* serves as loading control. The fragments of *SAUL1* and *PR1* were amplified from cDNA templates by 31 and 26 cycles of PCR, respectively. The PCR products were then analyzed by agarose gel electrophoresis.

(E) Quantification of *H.a.* Noco2 sporulation on the indicated genotypes. Three-week-old plants were spay-inoculated with *H.a.* Noco2 conidia spores at a concentration of 100,000 conidia spores per ml water. Quantification of conidia growth on leaf surface was determined 7 days post inoculation (dpi). Data represent means of four replicates. Error bars are standard deviations. ***$p< 0.001$. (Student's *t* test, GraphPad Prism 6)

(F) Bacterial growth of *P.s.m.* ES4326 in the indicated genotypes. Leaves of four-week-old plants were infiltrated with *P.s.m.* ES4326 at OD_{600} = 0.001. Quantification of colony-forming-units (cfu) in the infected area was examined at 0 and 3 dpi, respectively. Data represent means of five replicates. Error bars are standard deviations. ***$p< 0.001$. (Student's *t* test, GraphPad Prism 6)

3.3.2 Identification and molecular cloning of *SUPPRESSOR OF SAUL1 1 (SUSA1)*

saul1-1 knockout mutants exhibit autoimmunity that is dependent on *PAD4* and *EDS1* (Vogelmann et al., 2012; Disch et al., 2015). Because E3 ligases mostly target proteins for degradation, loss-of-function of an E3 would likely result in higher accumulation of its target protein. The E3 substrate can therefore be identified by screening for genetic suppressors using the E3 mutant. Additionally, such suppressor screen may also identify component(s) downstream of or in parallel with SAUL1 to reveal its signaling mechanism. Two independent genetic suppressor screens were carried out with *saul1-1*, one in Germany (Hoth Lab), and the other in Canada (Li Lab). As shown in Figure 3.2A, these *saul1-1 susa1* suppressor mutants completely or partially reverted *saul1-1* to wild-type size and abolished its necrosis phenotype. They were named *suppressor of saul1 1* (*susa1*) mutants.

In order to map *susa1*, *saul1-1 susa1-2* mutant in Columbia (Col-0) background was crossed with Landsberg *erecta* (Ler) to generate an F2 segregating population. However, among 288 F2 plants, none exhibited *saul1*-like phenotypes, indicating a tight genetic linkage between *saul1* and *susa1*. This was further confirmed with crosses between *saul1-1 susa1-2*, *saul1-1 susa1-7*, *saul1-1 susa1-8*, or *saul1-1 susa1-10* and Col-0. Among 100 to 400 F2 plants from each cross, no *saul1*-like progeny was identified. In addition, when *saul1-1 susa1-2* was crossed with *saul1-1 susa1-5*, failed complementation was observed in F1 progeny, suggesting that these two *susa1* mutants carry mutations in the same gene. Pair-wise allelism tests among *saul1-1 susa1-7*, *saul1-1 susa1-8*, *saul1-1 susa1-9*, *saul1-1 susa1-10*, *saul1-1 susa1-12*, and *saul1-1 susa1-13* further confirmed that the *susa1* mutants identified in the Hoth Lab were allelic to each other.

In order to identify the molecular lesions in *susa1* mutants, whole genome re-sequencing was carried out on *saul1-1 susa1-2* and *saul1-1 susa1-5* identified in the Li Lab and on *saul1-1 susa1-7*, *saul1-1 susa1-12*, and *saul1-1 susa1-13* from the Hoth Lab. Close examination of mutations in the genomic region close to *saul1* in all mutants identified only one common candidate, *AT1G17600*, where independent mutations were found in all the *susa1* mutants. In *susa1-2*, a C to T mutation caused a Leucine to Phenylalanine change at amino acid position 455. In *susa1-5*, a C to T mutation resulted in a Leucine to Phenylalanine change at amino acid position 922. In *susa1-7*, a G to A mutation resulted in a change from Glycine to Arginine at amino acid position 212. In *susa1-12*, a C to T mutation resulted in a change from Serine to Phenylalanine at amino acid position 960. In *susa1-13*, a G to A mutation resulted in a change from Valine to Methionine at amino acid position 712. Eight more alleles of *susa1* were further identified by Sanger sequencing of *AT1G17600* with genomic DNAs from other *saul1-1 susa1* alleles (Figure 3.2B). Collectively, these data indicate that *SUSA1* is most likely *AT1G17600*.

Sequence analysis revealed that *SUSA1* encodes a typical TNL immune receptor protein.

Among the 13 *susa1* alleles isolated from the screens, one missense mutation was found in the TIR domain, five in the NB domain, six in the LRR domain, and one at the C-terminus (Figure 3.2C), suggesting that each domain of the TNL is important for its function. A canonical NLR protein requires an intact P-loop motif that facilitates ATP binding and hydrolysis (Takken and Tameling, 2009). From the screen, we obtained two P-loop mutant alleles, *susa1-7* (G212R) and *susa1-8* (G214R) (Figure 3.3A), suggesting that the P-loop motif is indispensible for the proper function of SUSA1.

To further confirm the proper cloning of *SUSA1*, we obtained two exonic T-DNA knock out alleles of *susa1*, SALK_200339 designated as *susa1-14*, and SALK_069931 designated as *susa1-15* (Figure 3.2B and 3.2C). The *saul1-1 susa1-14* double mutant completely reverted *saul1* to WT morphology (Figure 3.2D). Additionally, the higher expression level of *PR1* in *saul1* was completely suppressed in the *saul1-1 susa1-14* double mutant (Figure 3.2E). Taken together, these data indicate that *SUSA1* is *AT1G17600,* which encodes a P-loop dependent putative TNL immune receptor.

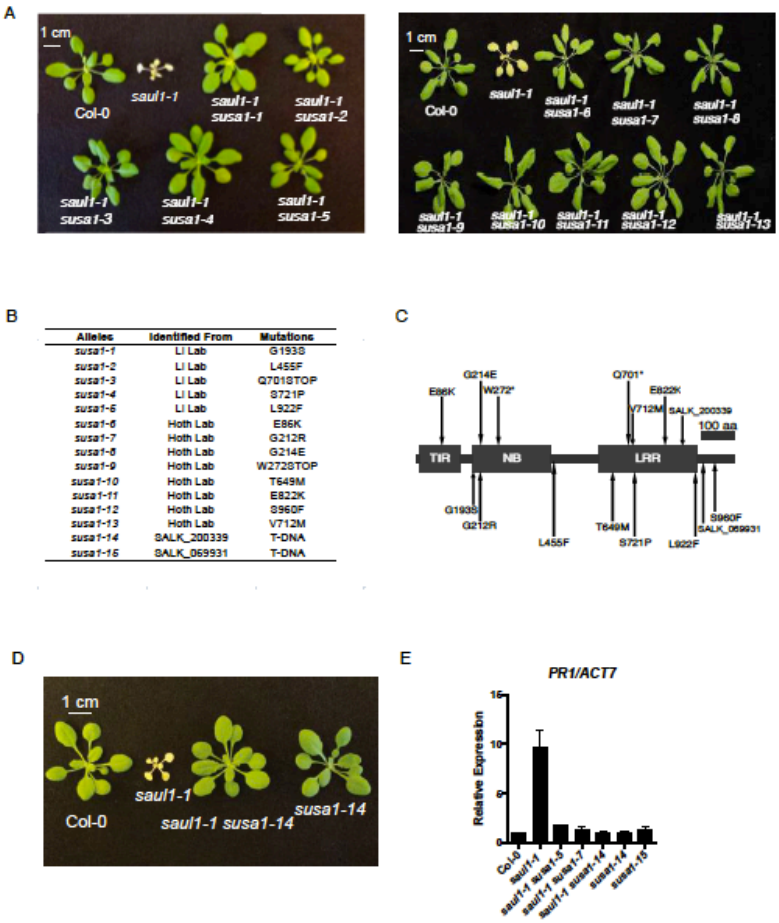

Alleles	Identified From	Mutations
susa1-1	LI Lab	G1938
susa1-2	LI Lab	L455F
susa1-3	LI Lab	Q701STOP
susa1-4	LI Lab	S721P
susa1-5	LI Lab	L922F
susa1-6	Hoth Lab	E86K
susa1-7	Hoth Lab	G212R
susa1-8	Hoth Lab	G214E
susa1-9	Hoth Lab	W272STOP
susa1-10	Hoth Lab	T649M
susa1-11	Hoth Lab	E822K
susa1-12	Hoth Lab	S960F
susa1-13	Hoth Lab	V712M
susa1-14	SALK_200339	T-DNA
susa1-15	SALK_069931	T-DNA

Figure 3.2 Characterization of *saul1* suppressors.

(A) Morphology of four-week-old Col-0, *saul1-1* and *saul1 susa1* mutants.

(B) List of *susa1* alleles identified from independent screens carried out in Canada or Germany. The consequences of the mutations at the protein level are annotated.

(C) Predicted protein structure of SUSA1 with amino acid changes in each *susa1* alleles indicated as arrows. *SUSA1* encodes a typical TNL.

(D) Morphology of four-week-old Col-0, *saul1-1, saul1-1 susa1-14* and *susa1-14* plants.

(E) Relative transcript levels of *PR1* in the indicated genotypes as determined by RT-PCR. Total RNA was extracted from four-week-old plants grown at 22°C under long day conditions (16hr light/8hr dark). *ACT7* was used to normalize the transcript levels. Data

represent means of three replicates. Error bars are standard deviations. *saul1-1* plants were grown at 28°C for three weeks before moving to 22°C to rescue the seedling lethal phenotypes.

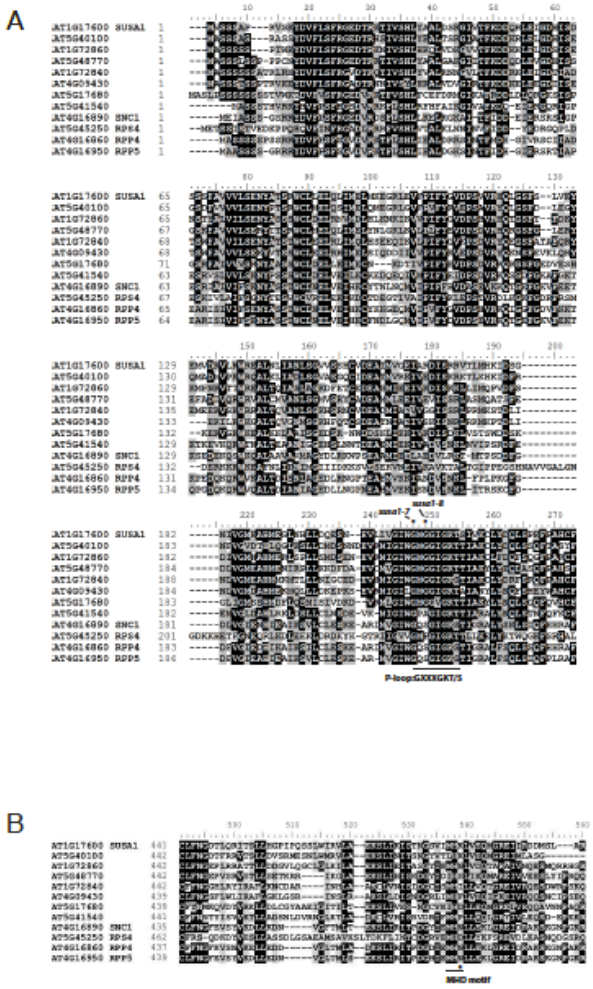

Figure 3.3 Amino acid sequence alignments of SUSA1 with SUSA1-like proteins and selected TNLs from Arabidopsis.

Amino acid sequence alignment of 1-273 aa (A) and 441-560 aa (B) of SUSA1 with SUSA1-like proteins and selected TNLs. was carried out with ClustalW (BioEdit Sequence Alignment Editor). The positions of the P-loop and MHD motif are indicated with black lines. The mutation sites of *susa1-7* and *susa1-8* in the P-loop region are labeled.

3.3.3 PAMP-triggered responses are impaired in *saul1-1 susa1 pub43* triple mutant

As SAUL1 serves a positive role in immune regulation (Figure 4.1), loss of SAUL1 function should yield an enhanced susceptibility phenotype. As the autoimmunity of *saul1-1* is mediated by SUSA1, the real phenotype of *saul1-1* is likely masked by the activation of SUSA1. To investigate the exact biological function of SAUL1 in basal defense, we challenged *saul1-1 susa1* double mutants with virulent pathogen *P.s.m.* ES4326 (Figure 4.3A) and *P.s.t.* DC3000 (Figure 4.3B). We consistently observed a slight, but not always significant increase in bacterial growth in *saul1-1 susa1* double and *susa1* single mutants. This suggests that SUSA1 might be recognizing an effector in *P.s.m.* ES4326 or *P.s.t.* DC3000. Loss of SUSA1 leads to enhanced susceptibility to these two bacterial strains. However, *saul1-1 susa1* double mutants and *susa1* single mutants showed wild-type level of susceptibility against virulent oomycete pathogen *H.a.* Noco2 (Figure 4.3C), suggesting that SAUL1 and SUSA1 are not required for the immunity to *H.a.* Noco2.

To further determine whether SAUL1 is required for immune responses by known NLR proteins, we conducted pathogen growth assays on *saul1-1 susa1* double mutants with avirulent bacteria *P.s.t.* DC3000 expressing AvrRps4 or AvrRpt2 effectors. These pathogen effectors are recognized by TNL protein RPS4 (Resistance to *Pseudomonas syringae* 4) (Axtell and Staskawicz, 2003) or CNL protein RPS2 (Mackey et al., 2003), respectively. The growth of either *P.s.t.* DC3000 AvrRps4 or AvrRpt2 were not significantly affected in *saul1 susa1* double mutant (Figure 4.3D and 4.3E), suggesting that SAUL1 is not required for RPS4- and RPS2-mediated immunity.

In order to investigate the role of SAUL1 in PAMP-triggered immunity, we challenged *saul1-1 susa1* double mutant with the Type III Secretion System (T3SS) deficient bacterial strain *P.s.t* DC3000 hrcC-. No alteration of the growth of hrcC- was observed in *saul1 susa1* plants (Figure 4.3F). Since SAUL1 shares 73% amino acid identities with its closest homolog PUB43 (Figure 5), we speculated a possible functional redundancy between SAUL1 and

PUB43. Thus, we generated *saul1-1 susa1-5 pub43* triple mutant for hrcC- growth assays. As shown in Figure 4.3F, the day 3 bacterial growth was significantly increased in *saul1-1 susa1-5 pub43* triple mutants compared to *saul1 susa1* double mutants and wild type plants, suggesting that *SAUL1* and *PUB43* work redundantly in positive regulation of PTI. To examine whether *SAUL1* and *PUB43* are required for ROS production, we conducted a time-course ROS assay on *saul1-1 susa1* and *saul1-1 susa1-5 pub43* plants in response to flg22. As shown in Figure 4.3G, the ROS production in *saul1-1 susa1* and *saul1-1 susa1-5 pub43* accumulated to a similar level as wild type, suggesting that *SAUL1* and *PUB43* are not required for ROS production triggered by flg22. Taken together, these data indicate that *SAUL1* and *PUB43* are redundantly required for PTI responses, but are not required for ROS production.

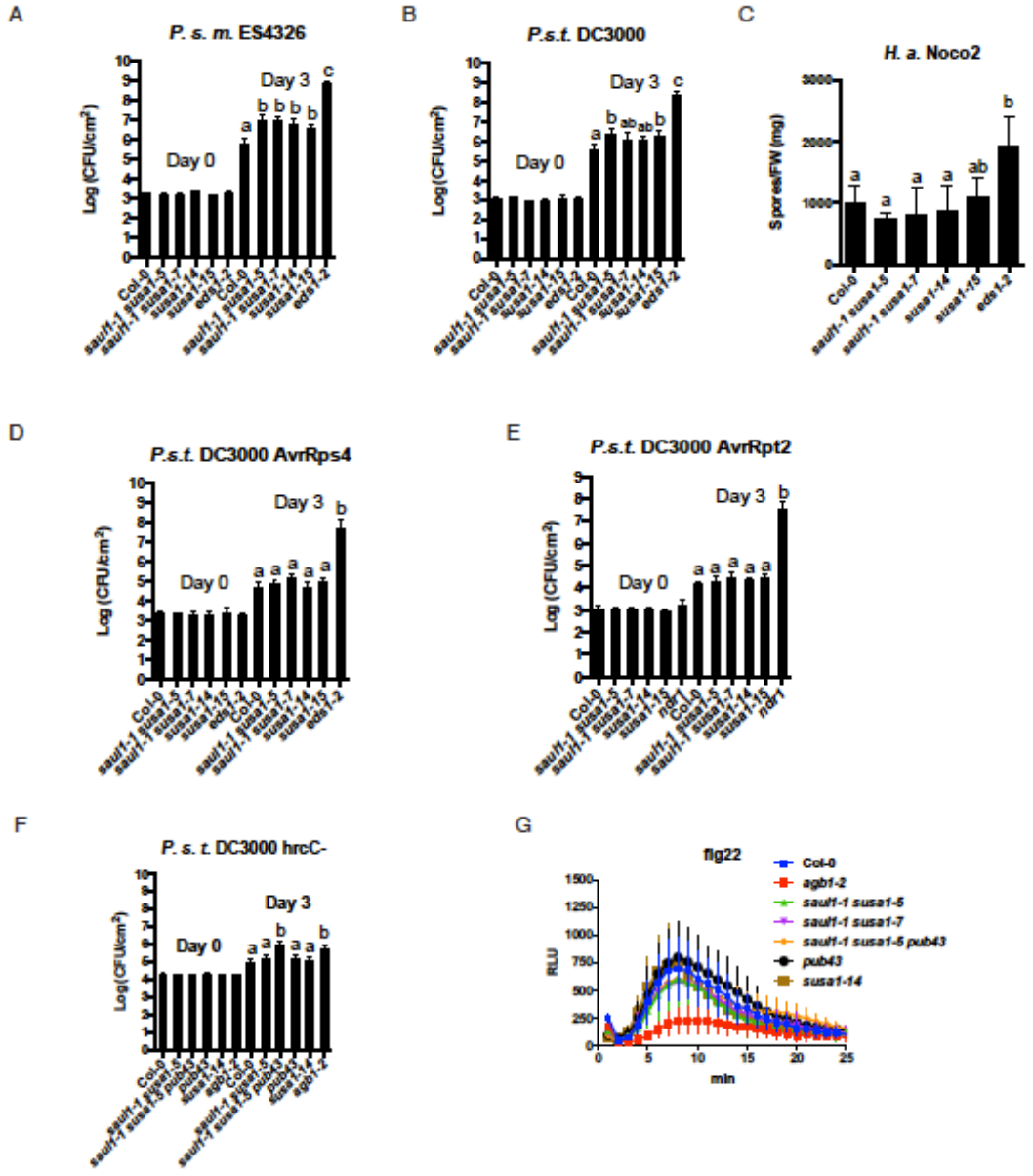

Figure 3.4 Characterization of *saul1-1 susa1* double and *saul1-1 susa1-5 pub43* triple mutants.

(A,B,D,E) Bacterial growth of *P.s.m.* ES4326 (A), *P.s.t.* DC3000 (B), *P.s.t.* DC3000 AvrRps4 (D), and *P.s.t.* DC3000 AvrRpt2 (E) in the leaves of the indicated genotypes. Leaves of four-week-old plants were infiltrated with bacterial culture of *P.s.m.* ES4326, *P.s.t.* DC3000, *P.s.t.* DC3000 AvrRps4 and *P.s.t.* DC3000 AvrRpt2 at a dosage of OD_{600} = 0.0001,

0.0001, 0.002 and 0.002, respectively. Quantification of cfu was carried out at 0 and 3 dpi. Data represent means of five replicates. Error bars are standard deviations. Different superscripts indicate significant differences between groups, whereas identical superscripts denote no significant differences (One-way ANOVA, GraphPad Prism 6, $p<0.05$).

(C) Quantification of *H.a.* Noco2 sporulation on the indicated genotypes. Two-week-old plants were spray-inoculated with *H.a.* Noco2 conidia at a concentration of 100,000 conidia per ml water. Quantification of conidia growth on leaf surface was determined 7 days post inoculation (dpi). Data represent means of four replicates. Error bars are standard deviations. Different superscripts indicate significant differences between groups, whereas identical superscripts denote no significant differences (One-way ANOVA, GraphPad Prism 6, $p<0.05$).

(F) Bacterial growth of *P.s.t.* DC3000 hrcC$^-$ in the indicated genotypes. Leaves of four-week-old plants were infiltrated with *P.s.t.* DC3000 hrcC$^-$ at OD_{600}=0.001. Quantification of cfu was examined at 0 and 3 dpi. Data represent means of five replicates. Error bars are standard deviations. Different superscripts indicate significant differences between groups, whereas identical superscripts denote no significant differences (One-way ANOVA, GraphPad Prism 6, $p<0.05$). The mutant *agb1-2* (*Arabidopsis G-protein ß-subunit 1*) was previously shown to have PTI defects [64], and it served as a positive control in *hrcC*- growth and ROS assays.

(G) Time course of ROS production in response to flg22 in the indicated genotypes. Excised leaves of four-week-old plants were treated with 100 nM flg22. RLU (Relative Light Units) were quantified using a luminometer.

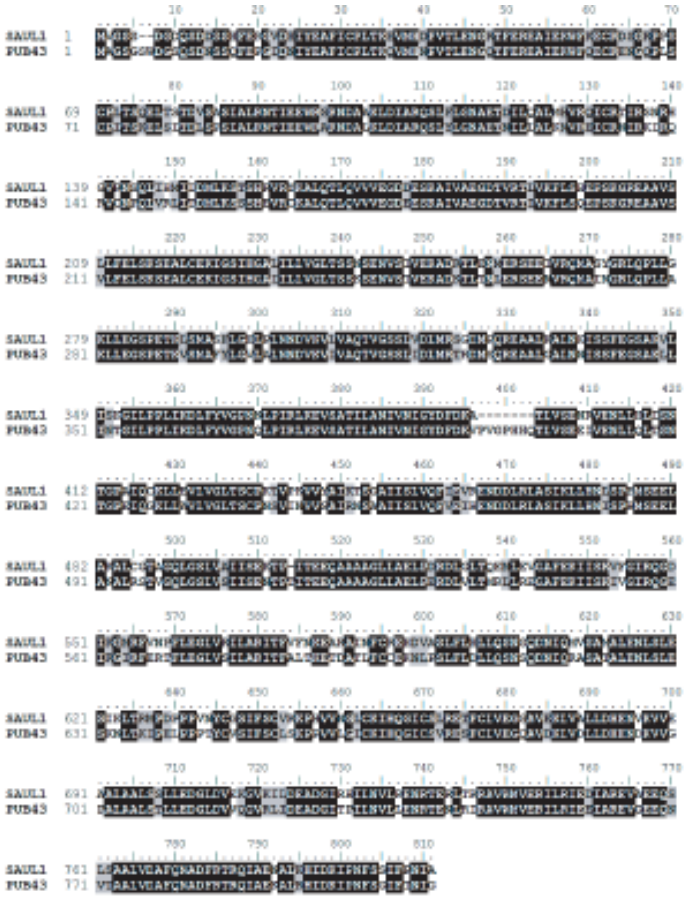

Figure 3.5. Amino acid alignment of full length SAUL1 and PUB43.

Amino acid sequence alignment was carried out with ClustalW (BioEdit Sequence Alignment Editor).

3.3.4 The autoimmune *SAUL1* overexpression phenotypes are dependent on *SUSA1.*

As *saul1-1* knockout phenotypes are fully dependent on SUSA1, we asked whether *SAUL1* overexpression autoimmune phenotypes are also dependent on SUSA1. To test this, we crossed *35S::SAUL1* T1-7 with *susa1-14*. Intriguingly, *susa1-14* completely suppressed the dwarf phenotype of the *SAUL1* overexpression line (Figure 3.6A). In addition, the enhanced immunity of *SAUL1* transgenic line *35S::SAUL1* T1-7 against *H.a.* Noco2 was reverted to WT level by *susa1-14* (Figure 3.6B). Moreover, the decreased bacterial growth in *SAUL1* overexpression line in response to *Pst* DC3000, *Psm* ES4326, *Pst* DC3000 (AvrRps4 and AvrRpt2) was also fully suppressed in *35S::SAUL1* T1-7 *susa1-14* double mutants (Figure 3.6C-3.6F). Overall, these data suggest that the autoimmune *SAUL1* overexpression phenotypes are dependent on *SUSA1*. In addition, when *35S::SAUL1* was transformed in *susa1-14* and Col-0 backgrounds, among the T1 plants obtained, 67% (14/21) T1 in Col-0 showed dwarfism, whereas all (35/35) of the T1 progeny in *susa1-14* background showed a WT morphology, confirming that the SAUL1 overexpression phenotypes require SUSA1.

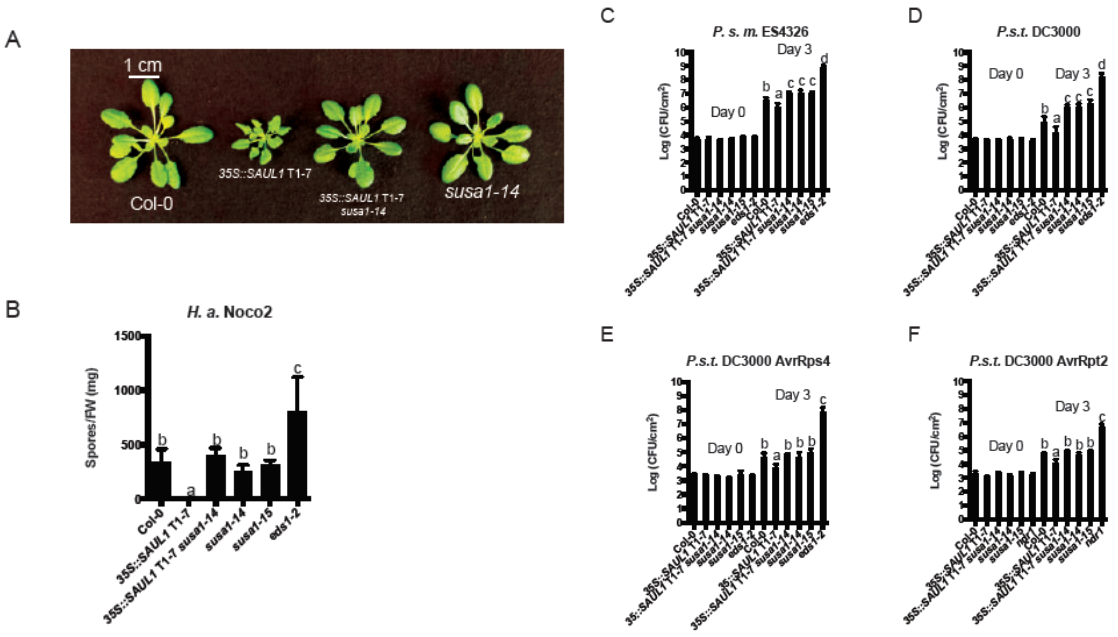

Figure 3.6. The autoimmune *SAUL1* overexpression phenotypes are dependent on *SUSA1*.

(A) Morphology of four-week-old Col-0, *35S::SAUL1 T1-7*, *35S::SAUL1 T1-7 susa1-14* and *susa1-14* plants.

(B) Quantification of *H.a.* Noco2 sporulation on the indicated genotypes. Three-week-old plants were spay-inoculated with *H.a.* Noco2 conidia spores at a concentration of 100,000 conidia spores per ml water. Quantification of conidia growth on leaf surface was determined 7 days post inoculation (dpi). Data represent means of four replicates. Error bars are standard deviations. (One-way ANOVA, GraphPad Prism 6, $p<0.05$).

(C to F) Bacterial growth of *P.s.m.* ES4326 (C), *P.s.t.* DC3000 (D), *P.s.t.* DC3000 AvrRps4 (E), and *P.s.t.* DC3000 AvrRpt2 (F) in the leaves of the indicated genotypes. Leaves of four-week-old plants were infiltrated with bacterial culture of *P.s.m.* ES4326, *P.s.t.* DC3000, *P.s.t.* DC3000 AvrRps4 or *P.s.t.* DC3000 AvrRpt2 at a dosage of OD_{600} = 0.0001, 0.0001,

0.002 and 0.002, respectively. Quantification of cfu was carried out at 0 and 3 dpi. Data represent means of five replicates. Error bars are standard deviations. Different superscripts indicate significant differences between groups, whereas identical superscripts denote no significant differences (One-way ANOVA, GraphPad Prism 6, $p<0.05$).

3.3.5 Subcellular localization of SUSA1

As SAUL1 associates with the plasma membrane (Vogelmann et al., 2014), we examined the subcellular localization of SUSA1. Full-length genomic *AT1G17600* was cloned in-frame with an N-terminal GFP tag driven by CaMV 35S promoter. When transformed into *saul1-1 susa1-5* double mutant, the T1 *GFP-SAUL1* transformants were able to fully complement the phenotypes of *susa1-5* (Figure 3.7A). Therefore GFP-SUSA1 should localize to its correct subcellular compartments. From western blot experiments, the full-length GFP-SUSA1 was properly expressed (Figure 3.8). When *GFP-SUSA1* was expressed in Arabidopsis leaf protoplasts, GFP fluorescence was observed in the cytosol in some protoplasts, but to the endoplasmic reticulum (ER) in others (Figure 3.7B). When *GFP-SUSA1* was co-expressed with red-fluorescent cytosol/nucleus or ER markers, respectively, merging green and red fluorescence indicated that in both cases the signals largely overlapped (Figure 3.7B). We did not observe overlap of GFP-SUSA1 with the cytosol/nucleus marker in the nucleus of protoplasts. However, when transiently expressing GFP-SUSA1 in *Nicotiana benthamiana* leaf epidermal cells, GFP fluorescence indicated the presence of the fusion protein in some nuclei, whereas other nuclei were only surrounded by the GFP fluorescence signal. This was different from the GFP control that showed GFP fluorescence in all nuclei as expected (Figure 3.7C). Collectively, these data suggest that SUSA1 localizes to cytosol, ER, and nucleus. When *GFP-SUSA1* and *SAUL1-RFP* were transiently co-expressed in *N. benthamiana* to check for co-localizaton, partial co-localization of SUSA1 and SAUL1 on the plasma membrane was observed (Figure 3.8), suggesting a potential interaction of

SAUL1 and SUSA1 in the co-localized area.

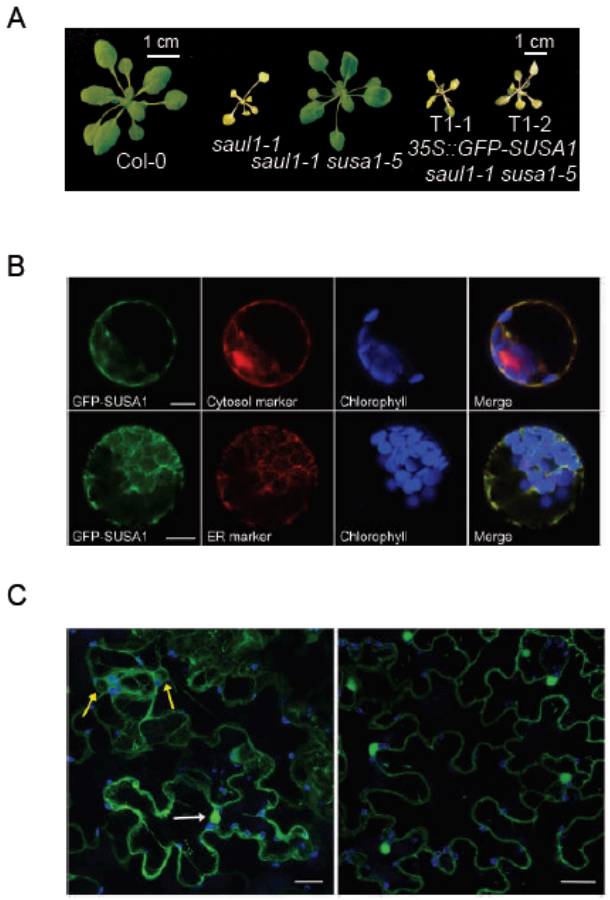

Figure 3.7. Subcellular localization of GFP-SUSA1.

(A) Morphology of four-week-old Col-0, *saul1-1*, *saul1-1 susa1-5*, and two independent complementing *35S::GFP-SUSA1* transgenic T1 plants in *saul1-1 susa1-5* background.

(B) Co-localization of GFP-SUSA1 with the cytosol marker Wave1R*mCherry*pNIGEL (top row) and the ER marker ER-rk CD3-959 (bottom row) in Arabidopsis leaf protoplasts. From left to right, images show GFP fluorescence in green, the respective marker fluorescence in red, chlorophyll fluorescence in blue, and the merged picture. Scale bars represent 10 µm.

(C) Localization of GFP-SUSA1 following transient expression in *Nicotiana benthamiana* leaf epidermal cells, represented in a maximum projection (left). White and yellow

arrows indicate the localization of GFP-SUSA1 in the nucleus or only around the nucleus. The GFP control is represented in a single section (right). Scale bars represent 25 µm.

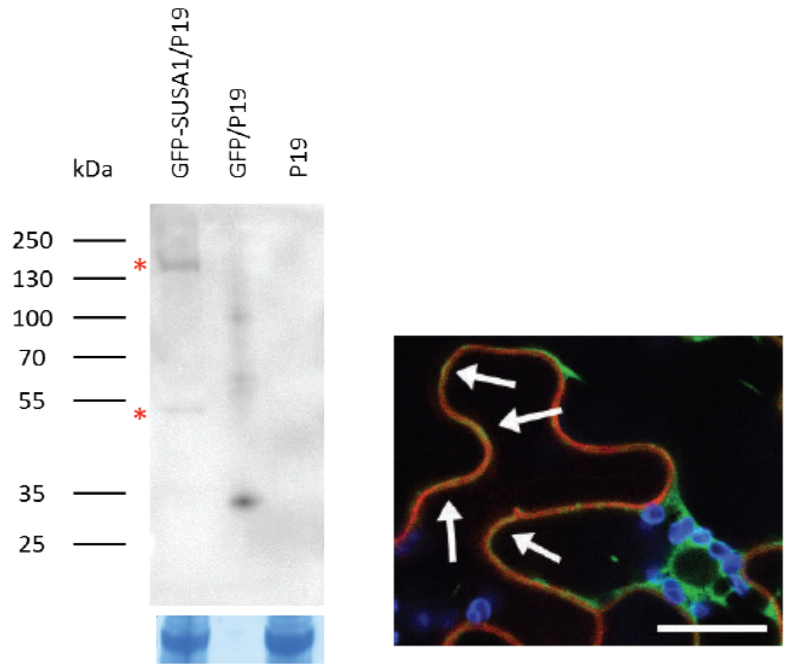

Figure 3.8. The protein expression from full-length *GFP-SUSA1* fusion gene and Colocalization of *SAUL1* and *SUSA1* in *N. benthamiana.*

(Left) Western blot showed the expression of full-length GFP-SUSA1 protein at the predicted size. *N. benthamiana* leaves were infiltrated with GFP-SUSA1/P19, GFP/P19 or P19, respectively. Total protein was extracted from infiltrated *N. benthamiana* leaves 72h after infiltration and was used for western blot analysis. No band was visible in the P19 negative control. GFP alone from the GFP/P19 positive control was visualized at 26.9 kDa. The GFP-SUSA1 full-length protein was detected at the predicted size of about 147 kDa (red asterisk). An additional weak signal, likely a SUSA1 degradation product, was observed at approximately 50 kDa (red asterisk). Coomassie Brilliant Blue Staining of Rubisco served as loading control. **(Right)** *N. benthamiana* leaves were co-infiltrated with Agrobacterium carrying constructs with *GFP-SUSA1* and *SAUL1-RFP*. Co-localization was analyzed by confocal laser scanning microscopy 72h after infiltration. The merge of GFP fluorescence

(green), RFP fluorescence (red), and chlorophyll fluorescence (blue) indicated some partial overlap of GFP-SUSA1 and SAUL1-RFP (arrows). The scale bar represents 25 μm.

3.3.6 SAUL1 associates with SUSA1 in *Nicotiana benthamiana*

To test the interaction between SAUL1 and SUSA1, we transiently expressed *35S::HA-SAUL1* and *Super::SUSA1-HA-FLAG* in *N. benthamiana*. Co-immunoprecipitation by FLAG agarose beads pulled down HA-SAUL1 protein (Figure 3.9A), suggesting that SAUL1 and SUSA1 associate with each other *in planta*. However, in a reverse co-IP experiment, we were not able to pull down HA-SUSA1 using SAUL1-FLAG. This is probably because of the much lower expression level of SUSA1 compared with that of SAUL1 (Figure 3.14). The amount of SAUL1 associated SUSA1 protein may be too low to be detected in the reverse IP (Figure 3.9B). Or, in the reverse IP, the FLAG epitope is masked in the SAUL1-SUSA1 complex, and only free SAUL1 is being pulled down.

We also conducted a split-luciferase assay in *N. benthamiana* and a yeast two-hybrid assay to examine the interaction between SAUL1 and SUSA1 (Figure 3.9C and 3.9D). For split-luciferase assay, SUSA1 was fused with the C-terminal Luciferase (*CLuc-SUSA1*) and SAUL1 was fused with the N-terminal Luciferase (*SAUL1-NLuc*), both driven by the CaMV 35S promoters and transiently co-expressed in *N. benthamiana* leaves. Luciferase activity was detected only in the positive control, but not in the cells carrying *SAUL1-NLuc* and *CLuc-SUSA1* (Figure 3.9C), an indication that SAUL1 and SUSA1 may not interact directly. In the yeast two-hybrid assay, SAUL1ΔNΔC was fused to the binding domain (BD) of the GAL4 transcription factor, and the SUSA1 full-length and the TIR domain of SUSA1 were fused to the GAL4 activation domain (AD), respectively. Co-transformed yeast cells with BD-SAUL1ΔNΔC and SUSA1-AD or SUSA1-TIR-AD were not able to grow on selection agar plates containing 3-AT (Figure 3.9D). Collectively, these data suggest that the interaction between SAUL1 and SUSA1 may be indirect.

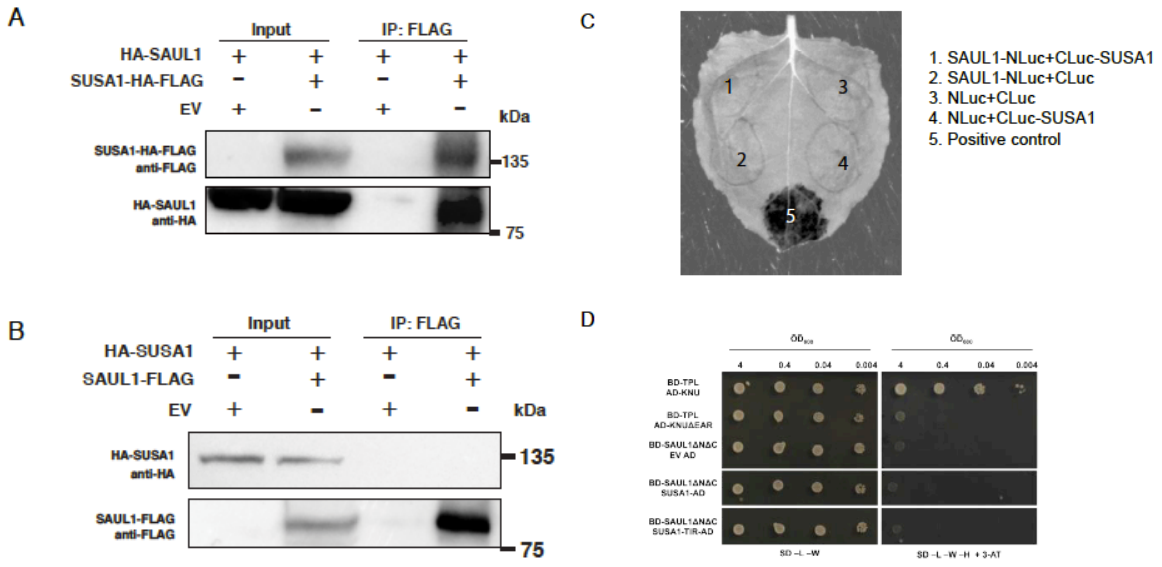

Figure 3.9. SUSA1 associates with SAUL1 in *Nicotiana benthamiana*.

(A and B) Co-immunoprecipitation of HA-SAUL1 by HA-FLAG-SUSA1 (A) and co-IP of HA-SUSA1 by SAUL1-FLAG (B). The leaves of five-week-old *Nicotiana benthamiana* were infiltrated with *Agrobacterium* carrying the constructs expressing the indicated proteins. Total protein was harvested 48 h after infiltration. Total protein extracts were immunoprecipitated with anti-FLAG beads and subjected to western blot analysis.

(D) Split-luciferase assay. Luciferase activity, as revealed by dark spots at the infiltration site in *N. benthamiana* leaves, after co-infiltration of *Agrobacteria* strains containing the indicated constructs. NLuc, N-terminal Luciferase; CLuc, C-terminal Luciferase.

(E) Yeast two-hybrid assay showed negative interactions between BD-SAUL1ΔNΔC and SUSA1-AD or SUSA1-TIR-AD. AD, GAL4 activation domain fusions; BD, GAL4 DNA binding domain fusions; -L-T-H, medium without leucine, tryptophan and histidine.

3.3.7 The ubiquitination activity of SAUL1 is required for the *saul1* phenotype and TN2 is not needed for the autoimmunity of *saul1*

SAUL1 has been shown to exhibit E3 ligase activity, but it remains unclear whether its ubiquitination activity is required for the activation of SUSA1-dependent immunity when it is knocked out or overexpressed. To test this, we made an E3 deficient mutant of *SAUL1* by deleting the *U-box* domain (*SAUL1*Δ*U-box*) and transformed the construct *35S::SAUL1*Δ*U-box* in *saul1-1,* Col-0 or *susa1-14* background, respectively. The results showed that：1）*SAUL1*Δ*U-box* cannot complement *saul1-1*. All of the 22 T1 transgenic plants obtained in *saul1* background resembled *saul1-1* (Figure 3.10A), suggesting that the ubiquitination activity of SAUL1 is required for *saul1*-mediated autoimmunity. Without the U-box domain, *SAUL1*Δ*U-box* cannot complement the *saul1-1* defects. 2) None of the *35S::SAUL1*Δ*U-box* T1 transgenic lines exhibited the dwarf, curly leaf phenotypes of *SAUL1* overexpression plants, indicating that the E3 activity is also needed for the SAUL1 overexpression phenotype. 3) Among 36 T1 transgenic plants of *35S::SAUL1*Δ*U-box* in Col-0 background, 20 plants were WT like and 16 plants exhibited a seedling lethality phenotype resembling *saul1* plants (Figure 3.10B), suggesting that deletion of the U-box domain likely causes a dominant-negative effect. Agreeing with this notion, all of the 36 transformants of *35S::SAUL1*Δ*U-box* in *susa1-14* background exhibited wild-type morphology (Figure 3.10B), suggesting that the dominant-negative phenotypes of *35S::SAUL1*Δ*U-box* are dependent on SUSA1, like with *saul1* mutants.

SUSA1 resides in an *NLR* gene cluster with two *TIR-NB* genes: *CHS1* (*CHILING SENSITIVE 1*, *AT1G17610*) and *TN2* (*AT1G17615*) (Figure 3.11). To test whether *TN2* is required for *saul1*-mediated autoimmunity, we generated the *saul1-1 tn2* double mutant. As shown in Figure 3.10C, the double mutant is *saul1*-like, suggesting that TN2 does not contribute to *saul1* phenotypes.

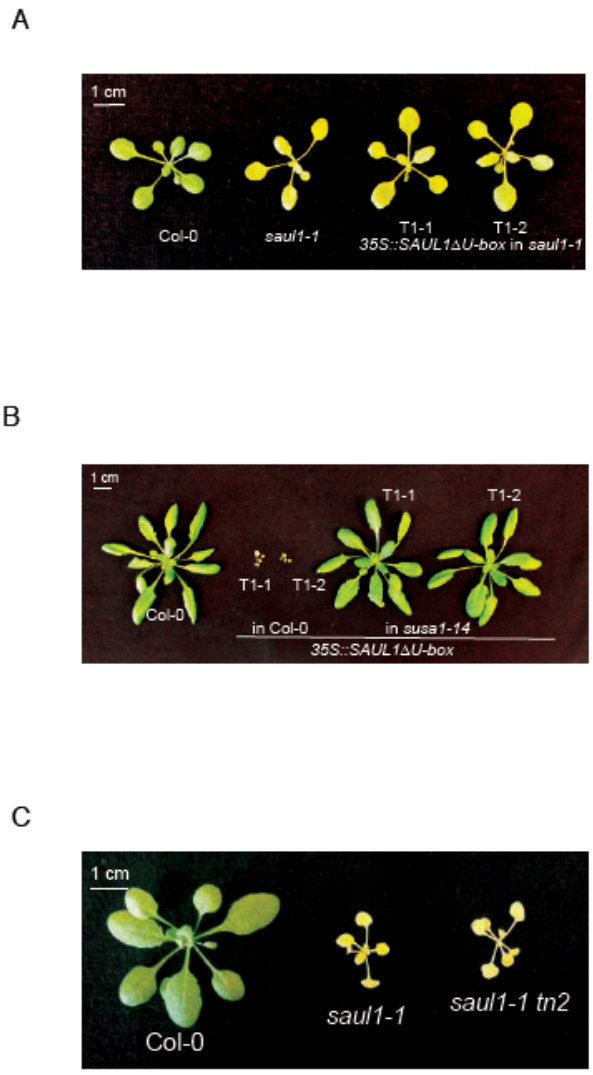

Figure 3.10. The E3 ligase activity is required for the autoimmunity of both the *saul1-1* knockout and *SAUL1* overexpression phenotypes; and *TN2* is not required for *saul1*-mediated autoimmunity.

(A) Morphology of three-week-old Col-0, *saul1* and two representative transgenic plants of *35S:: SAUL1* Δ*U-box* in *saul1-1*.

(B) Morphology of four-week-old Col-0 and two representative transgenic plants of *35S:: SAUL1* Δ*U-box* in Col-0 or *susa1-14* background, respectively.

Morphology of four-week old Col-0, *saul1-1* and *saul1-1 tn2* plants. Plants were grown at 28°C for two weeks and at 22°C for one week to reveal the yellowing *saul1* phenotypes.

Figure 3.11 Genomic arrangements of *SUSA1*, *CHS1* and *TN2*.

Boxes denote exons; lines denote introns; arrows indicate transcription directions.

The regions of encoded protein domains are indicated below the corresponding genomic regions.

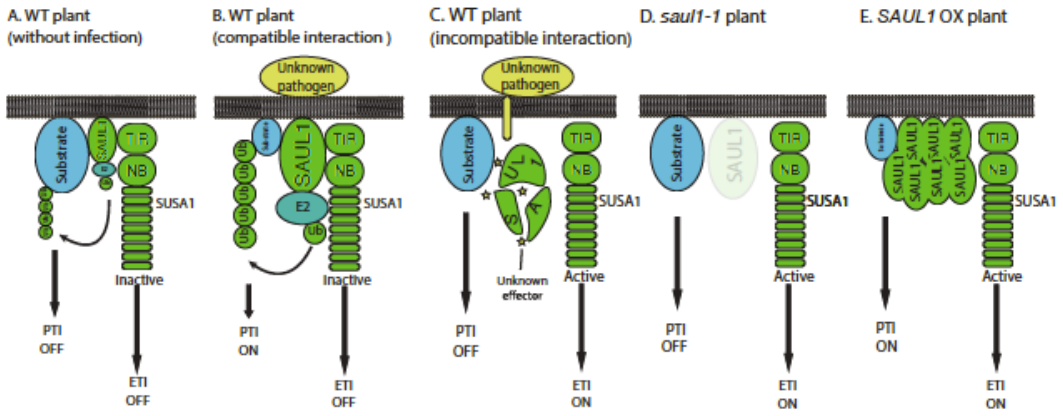

Figure 3.12. A working model for SAUL1 and SUSA1 function.

Substrate = SAUL1 E3 ligase substrate; predicted to be a negative regulator of PTI (see Discussion).

(A) In wild-type plants without infection, *SAUL1* is expressed at a low level. The SAUL1 substrate accumulates and negative regulates PTI, hence basal resistance is off. On the other hand, SAUL1 associates with SUSA1 and SUSA1-mediated ETI is off.

(B) In wild-type plants challenged with a compatible pathogen, *SAUL1* gene expression is induced (from TAIR microarray data analysis). This causes enhanced ubiquitination and a further substrate decrease, releasing the negative regulation of PTI. PTI is enhanced

under this scenario. On the other hand, SAUL1 associates with SUSA1 and SUSA1-mediated ETI is off.

(C) In wild-type plants challenged with an incompatible pathogen carrying an unknown effector that specifically targets SAUL1, SAUL1 is inactivated, leading to accumulation of the substrate to repress PTI. Meanwhile, loss of SAUL1 results in the constitutive activation of SUSA1, triggering strong ETI.

(D) In *saul1-1* plants, loss of SAUL1 results in high accumulation of the substrates to repress PTI and also constitutive activation of TNL SUSA1-mediated ETI. As a consequence, *saul1* plants exhibit strong autoimmunity, which is dependent on PAD4 and EDS1, general TNL regulators.

(E) In *SAUL1* overexpression plants, overexpression of *SAUL1* leads to the reduction of its substrate protein level to activate PTI. On the other hand, *SAUL* overexpression can also lead to the activation of SUSA1-mediated ETI.

3.4 Discussion

From our SNIPER overexpression reverse genetics screen, we identified *SAUL1/SNIPER3* as a *snc1* enhancer when overexpressed (Figure 3.1A and 3.1B). *SAUL1* encodes a U-box type E3 ubiquitin ligase with 12 ARM repeats at its C-terminus (Mudgil et al., 2004). *SAUL1* overexpression also leads to enhanced resistance to pathogens in wild-type background (Figure 3.1C to 3.1F), indicating that SAUL1 is a positive regulator of immunity. However, loss-of-function of *SAUL1* results in *EDS1*-/*PAD4*-dependent seedling lethality in Arabidopsis (Disch et al., 2015; Vogelmann et al., 2012), suggesting that *SAUL1* is a negative regulator of immunity that represses *EDS1*-/*PAD4*-mediated defense. How to explain these seemingly opposite conclusions on SAUL1 function? From two independent *saul1* suppressor screens conducted in Canada and Germany, we identified many alleles of *saul1* suppressor *susa1*. Interestingly, *SUSA1* encodes a TNL protein that is able to interact with SAUL1 *in vivo*. Since SAUL1 has a close homolog PUB43, further phenotypic immune analysis of the *saul1 susa1 pub43* triple mutant revealed that the E3 ligase SAUL1 functions redundantly with PUB43 in positive regulation of PTI. SUSA1 seems to act as a TNL immune sensor to monitor SAUL1's homeostasis (Figure 3.12). Either loss or overexpression of *SAUL1* activates *SUSA1*-mediated immunity.

Positive PTI immune regulators can be guarded by NLR immune receptors. As a consequence, loss-of-function of these regulators would trigger autoimmunity through the activation of NLRs, masking the true susceptibility phenotypes of their knockout mutants. For example, the *mekk1* and *mpk4* single mutants and *mkk1 mkk2* double mutant exhibit lesion mimic phenotypes with enhanced resistance to virulent pathogens (Qiu et al., 2008; Gao et al., 2008). These phenotypes are dependent on the CNL SUPPRESSOR OF MKK1 MKK2, 2 (SUMM2), suggesting that the MEKK1-MKK1/MKK2-MPK4 kinase cascade is guarded by SUMM2 (Zhang et al., 2012). *mkk1 mkk2 summ2* triple mutant plants exhibit enhanced susceptibility to pathogens, revealing the true function of MKK1/MKK2 as positive regulators of PTI. Another well-studied guardee is RIN4 (RPM1-INTERACTING 4).

RIN4 is targeted by two unrelated *P. syringae* effectors AvrB and AvrRpm1, leading to phosphorylation of RIN4 which triggers the activation of CNL RPM1 (RESISTANCE TO *P. SYRINGAE* PV *MACULICOLA* 1) (Chung et al., 2011; Liu et al., 2011). In addition, *P.* syringe effector AvrRpt2 cleaves RIN4, activating CNL RPS2 (RESISTANT TO *P. SYRINGAE* 2)-mediated immunity (Axtell and Staskawicz, 2003; Chung et al., 2011; Mackey et al., 2003). Knockout *rin4* is lethal due to extreme autoimmunity caused by activation of RPS2 and RPM1, however, recent studies on *rpm1 rps2 rin4* plants revealed that RIN4 functions to promote stomata opening through activation of the plasma membrane H^+-ATPase AHA1 (Lee et al., 2015; Zhou et al., 2015). Bacterial effectors manipulate RIN4 to facilitate entry into plants (Lee et al., 2015; Zhou et al., 2015).

From our current study, loss of *SAUL1* results in the activation of TNL SUSA1, leading to a seedling lethality phenotype. Therefore, the real biological function of *SAUL1* is masked by the autoimmunity mediated by SUSA1 (Figure 3.12). Although SAUL1 shares 73% amino acid identities with its closest homolog PUB43 (Figure 3.3), PUB43 does not seem to be guarded by NLRs as *pub43* single mutant plants do not exhibit any abnormal immune phenotypes. Moreover, *PUB43* cannot rescue the *saul1* defects (Figure 3.13), suggesting that PUB43 is not monitored by SUSA1. The *saul1-1 susa1-5 pub43* triple mutant exhibits more *P.s.t.* DC3000 hrcC- growth, revealing that *SAUL1* and *PUB43* work redundantly as positive regulators of PTI. However, how SUSA1 monitors SAUL1 homeostasis is unclear. The slight enhanced susceptibility of *susa1* single mutants is also intriguing (Figure 3.4A and 3.4B). It is possible that *P.s.t.* DC3000 and *P.s.m.* ES4326 may contain SUSA1-targeting effectors.

Figure 3.13. *PUB43* cannot complement *saul1-1*.

Morphology of three-week-old Col-0, *saul1-1* and two representative transgenic plants of *35S::PUB43* in *saul1-1*. Plants were grown at 28°C for two weeks and 22°C for one week to reveal the yellowing *saul1* phenotypes of *saul1-1*.

Positive regulators of PTI can often be targeted by pathogen effectors to suppress basal immunity. For example, *Phytophthora infestans* AVR3a and *Xanthomonasoryzae pv. oryzae* $XopP_{Xoo}$ target positive defense regulators U-box E3 ubiquitin ligases CMPG1 and OsPUB44 respectively to promote virulence (Bos et al., 2010; Ishikawa et al., 2014). AVR3a directly binds CMPG1 to inhibit its E3 ligase activity, whereas $XopP_{Xoo}$ specifically binds to the U-box domain of OsPUB44 to interfere with its activity (Bos et al., 2010; Ishikawa et al., 2014). The positive regulator SAUL1 of PTI can also likely be an effector target. This yet-to-be identified effector can then be indirectly recognized by the TNL immune receptor SUSA1 to trigger ETI (Figure 3.12). Under this guarding scenario, SAUL1 serves as the guardee of SUSA1 that is an intermediate protein between the effector and the NLR receptor.

One major question to be answered is what the protein substrate of SAUL1 is? SAUL1 is a membrane-associated PUB-ARM E3 ligase (Vogelmann et al., 2014). Although SUSA1 was identified as a genetic suppressor of *saul1*, it is unlikely to be a ubiquitination substrate of SAUL1 to be targeted for degradation, since when *SAUL1* and *SUSA1* were co-expressed

in *N. benthamiana*, the SUSA1 protein level was not reduced significantly in the presence of SAUL1 (Figure 3.14). We also did not observe ubiquitinated SUSA1 forms (Figure 3.14). Based on the phenotypes of *saul1 pub43 susa1* triple mutant plants, SAUL1 likely regulates PTI through ubiquitinating one or more membrane associated PTI negative regulator(s), leading to their further degradation by the proteasome (Figure 3.12). Hence, future identification of the ubiquitination substrate(s) of SAUL1 would be a critical step to understand how exactly SAUL1 regulates PTI. Identified from the CCSB interactome database (Dreze et al., 2011), one of SAUL1's alleged interactors is LORE1/SD1.29. *LORE1* encodes a bulb-type lectin S-domain-1 receptor-like kinase, which was shown to confer the recognition of lipopolysaccharide (LPS) from Gram-negative bacteria (Ranf et al., 2015). It can therefore be speculated that SAUL1 may act downstream of LORE1 upon LPS elicitation to trigger PTI.

SUSA1 encodes a typical TNL. The two motifs essential for proper NLR activity are the P-loop (phosphate-binding loop) motif and the MHD motif. The P-loop presumably coordinates with ATP binding and works as a molecular switch to turn on (ATP-bound) or off (ADP-bound) NLR (Hanson and Whiteheart, 2005). Mutations in the P-loop often result in loss of NLR function (Tameling et al., 2006; Xu et al., 2014a). From the current study, two P-loop mutants, *susa1-7* and *susa1-8*, have been identified through the *saul1-1* suppressor screens (Figure 3.3), suggesting that SUSA1 is a typical TNL protein that requires an intact P-loop. On the other hand, MHD motif is a conserved plant-specific motif that locates in the ARC2 sub-domain of the extended NB-ARC domain. In contrast with the effects of P-loop mutations, mutation of the Aspartic acid (D) in the MHD motif often results in auto-activated NLR proteins that induce pathogen-independent, constitutively activated defense responses in plants (van Ooijen et al., 2008; Williams et al., 2011; Zhang et al., 2012). Interestingly, SUSA1 protein contains K residue rather than D in MHD motif (Figure 3.3B), presumably conferring auto-activation. In support of this notion, expression of SUSA1 in *N.benthamiana* alone indeed triggers HR (Figure 3.15). Thus, it is possible that SUSA1 is an autoactive NLR

in Arabidopsis, whose activity must be repressed by one or more negative regulator(s).

SUSA1 forms a head-to-head triplet cluster with two *TIR-NB* (TN) genes: *CHS1* (*CHILING SENSITIVE 1*, *AT1G17610*) and *TN2* (*AT1G17615*) (Figure 3.11). The head-to-head arrangement indicates a possible co-regulation between these genes as suggested by recent studies (Deslandes et al., 2003; Gassmann et al., 1999; Narusaka et al., 2009; Williams et al., 2014; Sarris et al., 2015; Jander et al., 2002; van der Biezen et al., 2002; Le Roux et al., 2015; Xu et al., 2015b; Bi et al., 2011). For example, *TNL RPS4* (*Resistance to Pseudomonas syringae 4*) is genomically head-to-head with *RRS1* (*Resistance to Ralstonia solanacearum 1*). RPS4 pairs with RRS1 to confer resistance to the bacterial effectors AvrRps4 or PopP2 (Deslandes et al., 2003; Gassmann et al., 1999; Narusaka et al., 2009; Williams et al., 2014; Sarris et al., 2015; Jander et al., 2002; van der Biezen et al., 2002; Le Roux et al., 2015). Similarly, *CHS3* (*CHILLING SENSITIVE 3*), which encodes an atypical *TNL* with an additional *LIM* (*Lin-11*, *Isl-1* and *Mec-3*) domain, requires its adjacent head-to-head *TNL* gene *CSA1* (*CONSTITUTIVE SHADE-AVOIDANCE 1*) (Xu et al., 2015b; Bi et al., 2011). However, as we did not isolate any alleles of *chs1* or *tn2* from the exhaustive *saul1* suppressor screens, and knocking out *TN2* does not suppress the autoimmunity of *saul1-1* (Figure 3.10C), *saul1* phenotypes do not seem to require the functionality of either *CHS1* or *TN2*. However, we cannot rule out the possibility that *TN2* and *CHS1* might be functionally redundant to pair with SUSA1. The exact relationship between CHS1/TN2 and SAUL1 will be an interesting question to be addressed in the future.

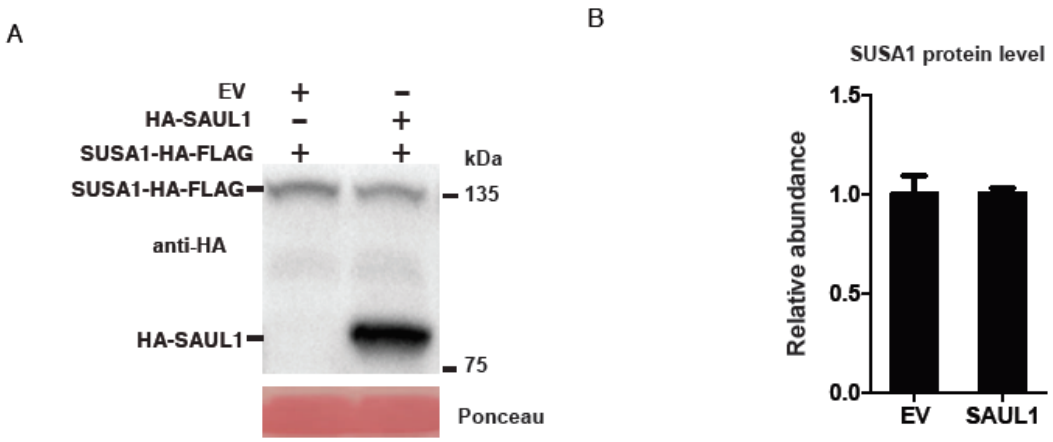

Figure 3.14. SAUL1 does not target SUSA1 for degradation.

(A) *HA-SAUL1* or an *EV* (empty vector) was co-expressed with *SUSA1-HA-FLAG* in *N. benthamiana* leaves. Leaf tissue was harvested 48 hours after infiltration. Total protein extracts were subjected to western blot analysis. Ponceau staining served as loading control.

(B) Quantification of protein levels of SUSA1-HA-FLAG in the presence of HA-SAUL1 or EV in *N. benthamiana*. The band intensity was determined by ImageJ and was normalized to the Ponceau loading control. Data represent means of three replicates. Error bars are standard deviations.

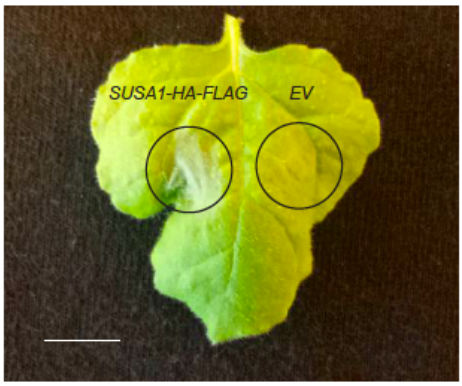

Figure 3.15. SUSA1 causes cell death when expressed in *N. benthamiana.*

Transiently expressing *SUSA1-HA-FLAG* in *N. benthamiana* leaves caused hypersensitive responses in *N. benthamiana*. The picture was taken 48 hours after infiltration. Scale bar represents 1 cm.

3.5 Materials and methods

3.5.1 Plant materials and growth conditions

All plants for assays were grown at 22°C growth chambers under long day conditions (16h light/ 8h dark). As *saul1* phenotypes are temperature sensitive(Disch et al., 2015), they were grown at 28°C under long day conditions for seeds. The suppressor lines were grown at 25°C under long day conditions for 14 days in a growth cabinet and then transferred to 22°C. For protoplast isolation, *Arabidopsis thaliana* Col-0 plants were grown at 22°C under short day conditions (8h light/16h dark).

3.5.2 Plant materials and growth conditions

All plants for assays were grown at 22℃ growth chambers under long day conditions (16h light/ 8h dark). As *saul1* phenotypes are temperature sensitive(Disch et al., 2015), they were grown at 28℃ under long day conditions for seeds. The suppressor lines were grown at 25°C under long day conditions for 14 days in a growth cabinet and then transferred to 22°C. For protoplast isolation, *Arabidopsis thaliana* Col-0 plants were grown at 22°C under short day conditions (8h light/16h dark).

3.5.3 Ethyl methanesulfonate (EMS) mutagenesis, *saul1* suppressor screen and next generation sequencing (Li Lab)

100 mg (~5000) *saul1-1* seeds were soaked in a solution of 0.1 M sodium phosphate (pH 5), 5% dimethyl sulphoxide, and 0.25% EMS for 16 hours with constant shaking. After incubation, the seeds were washed twice in 100 mM sodium thiosulphate for 15 min and three times in distilled water for 15 min.

The mutagenized *saul1* seeds were planted on half strength Murashige and Skoog (MS) plate for 10 days. Then ~4000 seedlings were transplanted on soil and grown at 28°C for seeds. M2 seeds from 25 M1 plants were harvested in each pool. For screening, ~500 M2 seeds from each pool were planted. Seeds from putative mutants reverting partially or completely to wild-type were kept.

The genomic DNA from the candidate suppressors was extracted using CTAB method (Li et al., 2001b) followed by the purification using Qiagen plant DNA extraction kit (Qiagen, Germany). The library preparation and Illumina sequencing were carried by BGI (Beijing Genomic Institute, China).

3.5.4 EMS mutagenesis, suppressor screen, next generation sequencing (Hoth Lab)

For EMS mutagenesis, 500 mg seeds of *saul1-1* mutants were incubated in 0.3% EMS for 15 hours with gentle agitation. After incubation, the seeds were washed in ddH_2O 10 times.

The M2 plants rescuing the *saul1-1* phenotype were backcrossed into *saul1-1* mutants two times. The genotype of the suppressor lines was confirmed for the T-DNA insertion using the *SAUL1* specific primers 5'-TGAGGCCAATCAAATGATTTC-3' and 5'-TTTCCCCATTCATGAGTGAAG-3' as well as the T-DNA insertion (SALK) specific primer LBa1 (5'-TGGTTCACGTAGTGGGCCATCG-3'), respectively.

For next generation sequencing total genomic DNA was extracted from 24-day-old mutant plants. 200 plants were pooled and pestled in liquid nitrogen in aliquots of 10 plants each pool. To each sample 800 µl extraction buffer (1% N-Laurylsarcosine, 100 mM Tris-HCl (pH 8.0), 10 mM EDTA (pH 8.0), 100 mM NaCl) and 800 µl phenol/chloroform/isoamyl alcohol (25:24:1) were added and mixed. The samples were centrifuged for 10 minutes at 13500 x g and room temperature. The supernatant was precipitated with 80 µl 3M sodium acetate (pH 5.2) and 800 µl isopropanol for 30 minutes at -20 °C. After centrifugation for 10 min at 13500 x g and 4 °C the pellet was washed with

1 ml 80 % ethanol twice. The genomic DNA was incubated with 50 µl R100 (100 µg/ml RNase A in TE buffer) for 30 minutes at 37 °C. To remove the RNase A, the samples were mixed again with equal amounts of phenol/chloroform/Isoamyl alcohol (25:24:1) and were centrifuged for 10 minutes at 13500 x g and 4 °C. The supernatants were washed with chloroform three times and were precipitated with 1/10 volume 3 M sodium acetate (pH 5.2) and 2.5 volumes ethanol for 4 hours at -80 °C. After centrifugation for 30 min at 13500 x g and 4 °C the pellet was washed with 1 ml 80% ethanol twice. The genomic DNA was resuspended in 50-100 µl ddH_2O. Library preparation, HiSeq Illumina sequencing and the bioinformatic analysis were carried out by Eurofins Genomics (Ebersberg, Germany).

3.5.5 Infection assays

For oomycete infection, two-week-old soil-grown seedlings were sprayed with a *H.a.* Noco2 conidiospore suspension at a concentration of 50,000 or 100,000 spores/ml. The infected plants were then domed and maintained at 18°C under 80% humidity in a long-day growth chamber. After 7 days, oomycete growth was quantified following a protocol described in (Zhang and Li, 2005).

For bacterial infection, leaves of 4-week-old plants were infiltrated with a suspension of *P.s.m.* ES4326, *P.s.t.* DC3000, *P.s.t.* DC3000 (AvrRpt2) or *P.s.t.* DC3000 (AvrRps4) at the dosage indicated in the figure legend respectively. Bacterial growth was assayed by quantification of colony-forming-units (cfu) at 0 dpi and 3 dpi, respectively, as described previously in (Li et al., 2001a).

3.5.6 Gene Expression Analysis

Total RNA was extracted from four-week-old soil-grown plants using the EZ-10 Spin Column Plant RNA Mini-Preps Kit (Bio Basic, Canada). The extracted RNA was then

reverse transcribed to cDNA with Easy Script^{TM} reverse transcriptase (ABM, Canada). RT-PCR was conducted using the total cDNA as template to determine the expression of the tested genes.

3.5.7 ROS Assay

The Arabidopsis leaf discs from four-week-old soil-grown plants were sliced by six cuts with a razor blade to increase surface area, and were placed into a distilled H_20 containing 96-well plate for overnight incubation under dim light condition. After incubation, the water was removed, the elicitation buffer containing 20 mM luminol, 10 mg mL^{-1} horseradish peroxidase with 100 nM flg22 was added into the plate. Quantification of luminescence was determined by a 96 microplate luminometer.

3.5.8 Construction of plasmids

For the construction of *pCam1300 SAUL1,* the *SAUL1* cDNA was amplified from the wild-type cDNA using primers 5'-CGCGCTCTAGAATGGTTGGAAGCTCGGATG-3' and 5'-CGCCGGGATCCTGCGATGTTTGGGAATATACTTG-3'. The amplified fragment was then digested with XbaI and BamHI and ligated into *pCam1300* vector. For the construction of *pCam1300 SAUL1*Δ*U-box,* the *SAUL1* cDNA was amplified from the wild-type cDNA using primers 5'-CGCGCTCTAGAATGAGATCCAGGAATGATGCTGC-3' and 5'-CGCCGGGATCCTGCGATGTTTGGGAATATACTTG-3'. The amplified fragment was then digested with XbaI and BamHI and ligated into *pCam1300* vector. The *HA-SAUL1* construct was described previously (Drechsel et al., 2011) For cloning *GFP-SUSA1*, *SUSA1* (*At1g17600*) was amplified from genomic DNA using primers 5'-CACCATGGTGTCCTCCTCTGCAC-3' and 5'-GGATCMCTTGAAAACACGCAGGAG-3'. The PCR fragment was cloned into the

pENTR/D-TOPO vector (Thermo Fisher Scientific, Waltham, USA) and the construct was confirmed by sequencing. Using the gateway cloning technology (Thermo Fisher Scientific), the genomic *SUSA1* fragment was recombined into the destination vector pMDC43 for N-terminal fusion (Curtis and Grossniklaus, 2003). The *GFP-PUB43* construct was described previously (Drechsel et al., 2011). The constructs: *pCam1300 SAUL1, pCam1300 SAUL1ΔU-box* and *GFP-PUB43* were electroporated in *Agrobacterium tumefaciens* GV3101 and transformed into Arabidopsis by a floral dipping method (Clough and Bent, 1998). For cloning SAUL1-RFP, *SAUL1* cDNA was amplified as previously described [51]. Using the gateway technology (Thermo Fisher Scientific, Waltham, USA) *SAUL1* was recombined from the pENTR^{TM}/D-TOPO® vector into the destination vector pH7RWG2.0 for N-terminal fusion with RFP (Karimi et al., 2007). The binding domain vector for the yeast two-hybrid experiments was cloned from the previously described pENTR_SAUL1ΔNΔC vector (Drechsel et al., 2011). The *SAUL1ΔNΔC* fragment was cloned into the pGBT9 vector (provided by Frederik Börnke, Leibniz-Insitut für Gemüse- und Zoerpflanzenbau Großbeeren, Germany) by using the gateway cloning technology (Thermo Fisher Scientific, Waltham, USA). The coding sequence of *SUSA1* was amplified using primers 5´-CACCATGGTGTCCTCCTCTGCAC-3´ and 5`-GGATCMCTTGAAAACACGCAGGAG -3´. For cloning the TIR domain, *SUSA1-TIR* was amplified from cDNA using the primers 5´-CACCATGGTGTCCTCCTCTGCAC-3´ and 5`-GTGGCTTGAAACCACGCC-3`. *SUSA1* and the TIR domain of *SUSA1* (*SUSA1-TIR*, CDS 1-462 (exon 1)) were recombined from the entry vector into the destination vector pGAD-CF with a C-terminally fused activation domain (provided by Frederik Börnke, Leibniz-Insitut für Gemüse- und Zierpflanzenbau Großbeeren, Germany) by using the gateway cloning technology (Thermo Fisher Scientific, Waltham, USA).

3.5.9 Transformation of yeast cells

Transformation of the yeast strain AH109 was carried out according to Gietz et al. (1997) (Gietz et al., 1997). In brief, the binding and activation domain vectors were transformed simultaneously and the cells were spread on yeast minimal medium (SD medium: 0,66% Yeast Nitrogen Base without amino acids, 0,066% amino acid mix, 2% glucose) lacking leucine and tryptophan (SD -L-W). After three days of incubation at 29°C, overnight cultures of single colonies were grown in double dropout medium (SD -L-W) under continuous shaking for 24 hours at 29°C. The optical density was set to OD_{600}=4 and a dilution series from 10^{-1} to 10^{-3} was dripped on selection agar plates lacking histidine (SD -L-W-H) and containing 0.5 mM 3-Amino-1,2,4-triazole (3-AT) as well as on SD -L-W as a control. As a positive control for transformation pGAD-424_KNU 3´UTR and pGBKT7_TPL were transformed, as a negative control pGAD-424_KNUΔEAR and pGBKT7_TPL (Causier et al., 2012).

3.5.10 Split-luciferase assay

The split-luciferase assay system has been previously described (Chen et al., 2008). Briefly, the constructs were transformed into *Agrobacterium tumefaciens* GV3101 cells. The cells were collected and resuspended in an infiltration medium (10 mM MES, pH 5.6, 150 µM acetosyringone) to a final concentration of OD_{600} = 0.6. Four-week-old *N. benthamiana* leaves were infiltrated using 1 ml syringes with different combinations of bacterial suspensions. The plants were incubated at room temperature in the dim light for 48 h. 1 mM of D-Luciferin (Sigma-Aldrich) dissolved in DMSO, 10 mM MgCl2 and 10 mM MES, pH 5.6, were infiltrated into the Agrobacteria-infiltrated leaves before cutting the leaves for luminescence imaging. Luminescence was visualized after a 20-30 min exposure using a CCD camera with a low-light imaging system (ChemiDocTM XRS+; Bio-Rad, http://www.bio-rad.com/) using a 3x3 binning

settings for all images.

3.5.11 Protoplasts isolation

Protoplast isolation was carried out as previous protocols with minor changes (Drechsel et al., 2011). Mesophyll protoplasts were isolated from leaves of 6 weeks-old plants in protoplasting buffer (500 mM sorbitol, 1 mM $CaCl_2$, 0.25% Macerozym R10, 1% cellulase R10, 10 mM MES-KOH, pH 5.7). The protoplast transformation was performed with 150 µl of protoplasts, 20 µg plasmid DNA and 165 µl PEG-Ca buffer (40 % PEG 4000, 200 mM sorbitol, 100 mM $CaCl_2$). The transformation sample was mixed completely by gently rotating the tube and was incubated for 30 minutes at room temperature in the dark. To stop this process, the sample was diluted with W5 buffer (154 mM NaCl, 125 mM $CaCl_2$, 5 mM KCl, 5 mM glucose, 2 mM MES, pH 5.7) in three steps of 500 µl, 1 ml and 1.5 ml. The sample was centrifuged at 60 x g for 3 minutes (without brake) and was washed with 3 ml W5 buffer twice. The protoplasts were incubated for 24 hours at room temperature in the dark and GFP signals were analysed by confocal laser scanning microscopy.

3.5.12 Confocal laser scanning microscopy

To detect fluorescence of GFP-fusion proteins in living cells, confocal laser scanning microscopy was applied by using the Leica TCS SP8 Confocal Platform (Leica Microsystems, Wetzlar, Germany). The cytosol/nucleus marker Wave1R*mCherry*pNIGEL (Geldner et al., 2009) and the ER marker ER-rk CD3-959 (Nelson et al., 2007) were used for co-localization experiments. For excitation of GFP and *mCherry/RFP* laser light of 488 nm and 561 nm was used, respectively. The detection windows ranged from 496 nm to 511 nm (GFP), 569 nm to 591 nm (*mCherry/RFP*) and from 690 nm to 708 nm for detection of chlorophyll auto-fluorescence.

3.5.13 Transient protein expression and co-immunoprecipitation in *N. benthamiana*

The transient protein expression in *N. benthamiana* leaves was carried out as previously described (Drechsel et al., 2011). The infiltration buffer was adjusted to 0.1 M Na-phosphate buffer (pH 6.0), with 10 mM $MgCl_2$ and 0.01 mM acetosyringone. GFP-SUSA1 and pBIN19-35S::GFP (Tan, 2012) were co-infiltrated with vector P19 (Lakatos et al., 2004), respectively. The Co-IP protocol was followed as previously described (Moffett et al., 2002; Xu et al., 2014b).

3.5.14 Isolation of total protein from *N. benthamiana* leaves

For total protein isolation infiltrated *N. benthamiana* leaves were grounded in liquid nitrogen. To each sample 700 µl phenol and 700 µl crude extract buffer (30% sucrose, 2% SDS, 5% DTT, 0.1M Tris-HCl pH 8.0) were added. The samples were centrifuged for 5 minutes at 10000 x g at room temperature. The supernatant was precipitated with 1.5 ml 0.1M ammonium acetate (in methanol) for 45 minutes at -20°C. After centrifugation for 8 minutes at 10000 x g the pellet was washed with 800 µl 0.1M ammonium acetate (in methanol) and 800 µl 80% acetone two times, respectively. The pellet was resuspended in 100 µl Laemmli buffer.

3.5.15 SDS-PAGE and immunoblotting

For SDS-PAGE, the *TruPAGE™ Precast Gels* (gradient: 4-20%) (Sigma-Aldrich Chemie GmbH, Taufkirchen, Deutschland) were used and the proteins were transferred to nitrocellulose membrane. For immunodetection the anti-GFP antibody (dilution: 1:3500;

rabbit IgG; Sigma-Aldrich Chemie GmbH, Taufkirchen, Germany) and Goat Anti-Rabbit IgG Antibody with HRP (dilution: 1:5000; peroxidase conjugated; Merck Millipore, Merck Chemicals GmbH, Darmstadt, Germany) were used.

3.5.16 Accession numbers

The T-DNA alleles of *saul1-1*, *susa1-14, susa1-15*, *pub43-1* and *tn2* are SALK_063974, SALK_200339, SALK_069931, SALK_112870 and SALK_204239, respectively.

4. The ADR1 family is required for the signalling of typical TNL-mediated immunity in *Arabidopsis*[1]

4.1 Summary

Nucleotide-binding leucine-rich repeat proteins (NLRs; or Nod-like receptors) serve as intracellular immune receptors in animals and plants. Sensor NLRs recognize pathogen-derived effector molecules and trigger robust host defense responses. Recent studies revealed the role of the three CC-type NLRs (CNLs) of the ADR1 family, ADR1, ADR1-L1 and ADR1-L2, as redundant helper NLRs, whose function is required for defense mediated by multiple sensor NLRs. Here we showed that the autoimmunity of *snc1* and *chs2*, which encodes typical TIR-type NLRs (TLRs) is fully suppressed by *adr1 adr1-L1 adr1-L2* triple mutant, suggesting that the *ADR1* triple function downstream of TLR signalling. Using the *snc1*-suppressing phenotype as criteria, we found that among the three *ADR1* genes, *ADR1* is the leading contributor while *ADR1-L1* is the least contributor. Interestingly, we found the unexpected enhancement of *snc1*-related phenotypes in *adr1-l1 snc1* double mutants, possibly because of the over compensation from the transcripts of *ADR1* and *ADR1-L2*. Collectively, we showed a complex genetic interplay among *ADR1* genes, which are required for typical TNL-mediated immune signalling in *Arabidopsis.*

[1]A portion of this chapter has been published. Dong, O. *; Tong, M. *; Bonardi, V.; Kasmi, F.; Woloshen, V.; Wünsch, L.; Dangl, J.; Li, X. (* Co-first authors) (2016) New Phytologist. doi: 10.1111/nph.13821

4.2 Introduction

Plants are equipped with two layers of innate immunity to combat with pathogens. The first layer is dependent on membrane localized pattern recognition receptors (PRRs), which recognize conserved pathogen-associated molecular patterns (PAMPs) to turn on the immune responses termed as PAMP-triggered immunity (PTI) (Boller and Felix, 2009). Adaptive pathogens have evolved to deliver effector molecules to dampen PTI and favor their own growth. To overcome the interference of pathogens, plants have evolved a second layer of immunity that is initiated by intracellular nucleotide-binding/leucine-rich repeats (NLR) immune receptors. The NLR proteins are able to recognize the presence of effectors and trigger effector-triggered immunity (ETI) (Jones and Dangl, 2006). The NLR proteins further fall into two different classes depending on their different N-termini. The first class has a N-terminal coiled-coil (CC) domain, termed as CNL protein, whereas the second class contains a N-terminal Toll/Interleukin-1-receptor-like (TIR) domain, termed as TNL protein (Meyers, 2003). The presence of either a CC or TIR domain typically determines whether the NLR mediated defense response requires either NDR1 (Non-race-specific Disease Resistance) or the EDS1 (Enhanced Disease Susceptibility 1) / PAD4 (Phytoalexin Deficient 4) / SAG101 (Senescence Associated Gene 101) complex, respectively (Aarts et al., 1998). However, the detailed molecular linkages between these pathways remain elusive.

SNC1 encodes a canonical TNL that was identified through a suppressor screen of *npr1 (nonexpresser of PR gene 1)* (Zhang et al., 2003b; Xu et al., 2014a). The mutant *snc1* carries a glutamic acid to lysine gain-of-function mutation in the linker region between the NB and LRR domains (Zhang et al., 2003b). This mutation consequently results in constitutive activation of defense responses with increased levels of SA, constitutive expression of *PR* genes, and increased resistance against virulent pathogens such as the bacteria *Pseudomonas syringae* pv. *maculicola* (*P.s.m*) ES4326 and the oomycete *Hyaloperonospora arabidopsidis* (*H.a.*) Noco2 (Zhang et al., 2003b).

ACTIVATED DISEASE RESISTANCE 1 (*ADR1*), *ADR1-LIKE 1* (*ADR1-L1*) and *ADR1-LIKE2* (*ADR1-L2*) are three homologous genes that are redundantly required for basal resistance and ETI responses mediated by the CNL protein RESISTANT TO PSEUDOMONAS SYRINGAE 2 (RPS2) and TNLs RECOGNITION OF PERONOSPERA PARASITICA 2 (RPP2) and RECOGNITION OF PERONOSPERA PARASITICA 4 (RPP4) (Bonardi et al., 2011). *ADR1s* encode CNLs with a non-canonical N-terminal CC domain, which shares closest sequence homology with *RESISTANCE TO POWDERY MILDEW8* (*RPW8*), a resistance (R) gene that confers a broad range of powdery mildew resistance in *Arabidopsis* (Xiao et al., 2001; Grant et al., 2003; Collier et al., 2011). Beyond the typical effector recognition function of NLRs, the ADR1 family may work as helper NLRs required for typical NLRs (Bonardi et al., 2011).

In this study, we further investigated the specificity of *ADR1*'s requirement for a variety of different NLRs and found that *ADR1*s are fully required for the functionality of typical TNLs including *SNC1* and *CHS2*, but not that of *CHS3, SLH1* and *UNI* encoding atypical TNLs and CNLs. Moreover, we also found that among the three *ADR1* genes, *ADR1* is the biggest contributor whereas *ADR1-L1* negatively regulates *snc1*-mediated immunity. Collectively, these data indicate the complex genetic interplay of *ADR1s* downstream of typical *TNL*s.

4.3 Results

4.3.1 The ADR1 gene family is fully required for SNC1-mediated immunity

In order to test whether the *ADR1* family is required for *SNC1*-mediated immunity, we introduced the T-DNA knockout mutations in an *adr1 adr1-L1 adr1-L2* triple mutant (hereafter, *adr triple*) (Bonardi et al., 2011) into the autoimmune mutant *snc1*. Intriguingly, the dwarfism of *snc1* was completely suppressed in the presence of *adr1 adr1-L1 adr1-L2* triple mutations (Figure 4.1A). In addition, consistent with the suppression of morphology, the resistance against virulent bacteria pathogen *Pseudomonas syringae* pv. *maculicola* (*P.s.m*) ES4326 (Figure 4.1B) and the levels of salicylic acid (Figure 4.1C) of *snc1* mutants were largely suppressed in *snc1 adr triple* mutants, suggesting that the *ADR1* family is fully required for *snc1* downstream signalling.

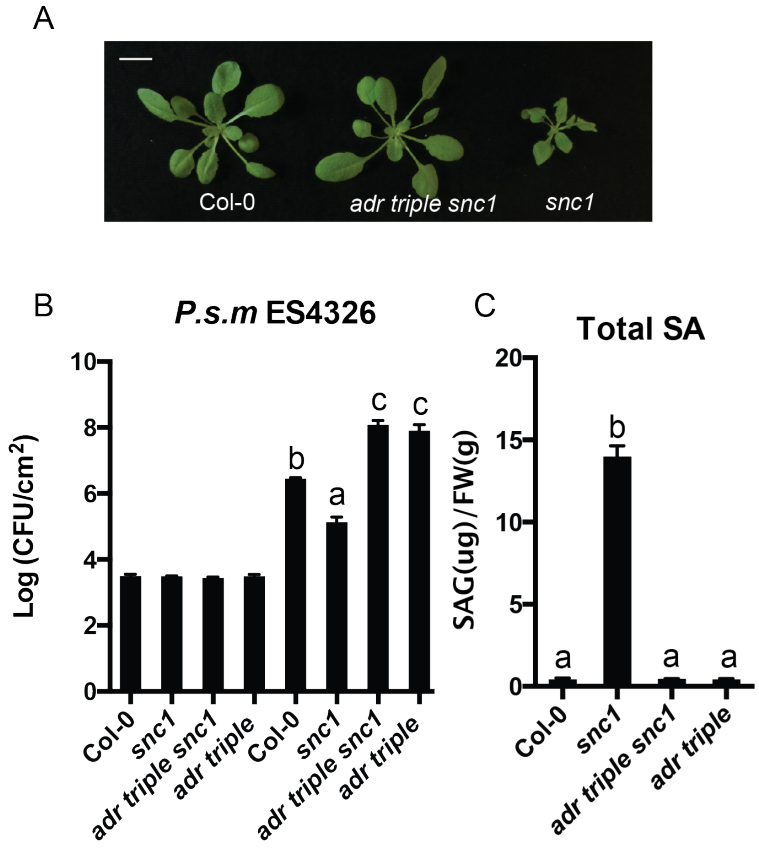

Figure 4.1 The *ADR1* family is required for *snc1*-mediated immunity

(A) Morphology of four-week-old soil-grown Col-0, *adr triple snc1* and *snc1* plants.

(B) Bacterial growth of *P.s.m.* ES4326 in the indicated genotypes. Leaves of four-week-old plants were infiltrated with *P.s.m.* ES4326 at OD_{600}=0.001. Quantification of colony-forming-units (cfu) was examined at 0 and 3 dpi, respectively. Data represent means of five replicates. Error bars are standard deviations. Different superscripts indicate significant differences between groups, whereas identical superscripts denote no significant differences (One-way ANOVA, GraphPad Prism 6).

(C) Total SA levels in four-week-old soil grown Col-0, *snc1, adr triple snc1* and *adr triple* plants. Four replicates were included for each genotype. Data represent means of four

replicates. Error bars are standard deviations. Different superscripts indicate significant differences between groups, whereas identical superscripts denote no significant differences (One-way ANOVA, GraphPad Prism 6).

4.3.2 Genetic interplay among the three redundant *ADR1* genes

To further elucidate the detailed contribution of each *ADR1* gene in the requirement for *snc1* downstream signalling, we generated a collection of double mutants: *snc1 adr1*, *snc1 adr1-L1*, *snc1 adr1-L2*, and triple mutants: *snc1 adr1 adr1-L1*, *snc1 adr1 adr1-L2, snc1 adr1-L1 adr1-L2*. The collection of mutants was then assayed for morphology, fresh weight and *PR* gene expressions (Figure 4.2A-C). The results showed that, among the three *adr1* single knockout genes, *adr1* suppressed *snc1*-related phenotypes the most, whereas *adr1-l2* did not show significant suppression or the suppression was too small to be detected. Interestingly, we observed *snc1*-enhancing phenotypes in *snc1 adr1-L1* double mutant (Figure 4.2). In addition, the *snc1*-enhancing phenotypes in *snc1 adr1-L1* double mutant were largely suppressed by *adr1* and fully suppressed by *adr1 adr1-L2* as observed in morphology, fresh weight and the expression levels of *PR1* and *PR2* (Figure 4.2), suggesting that the *snc1*-enhancing phenotypes in *snc1 adr1-L1* are dependent on *ADR1* and *ADR1-L2*.

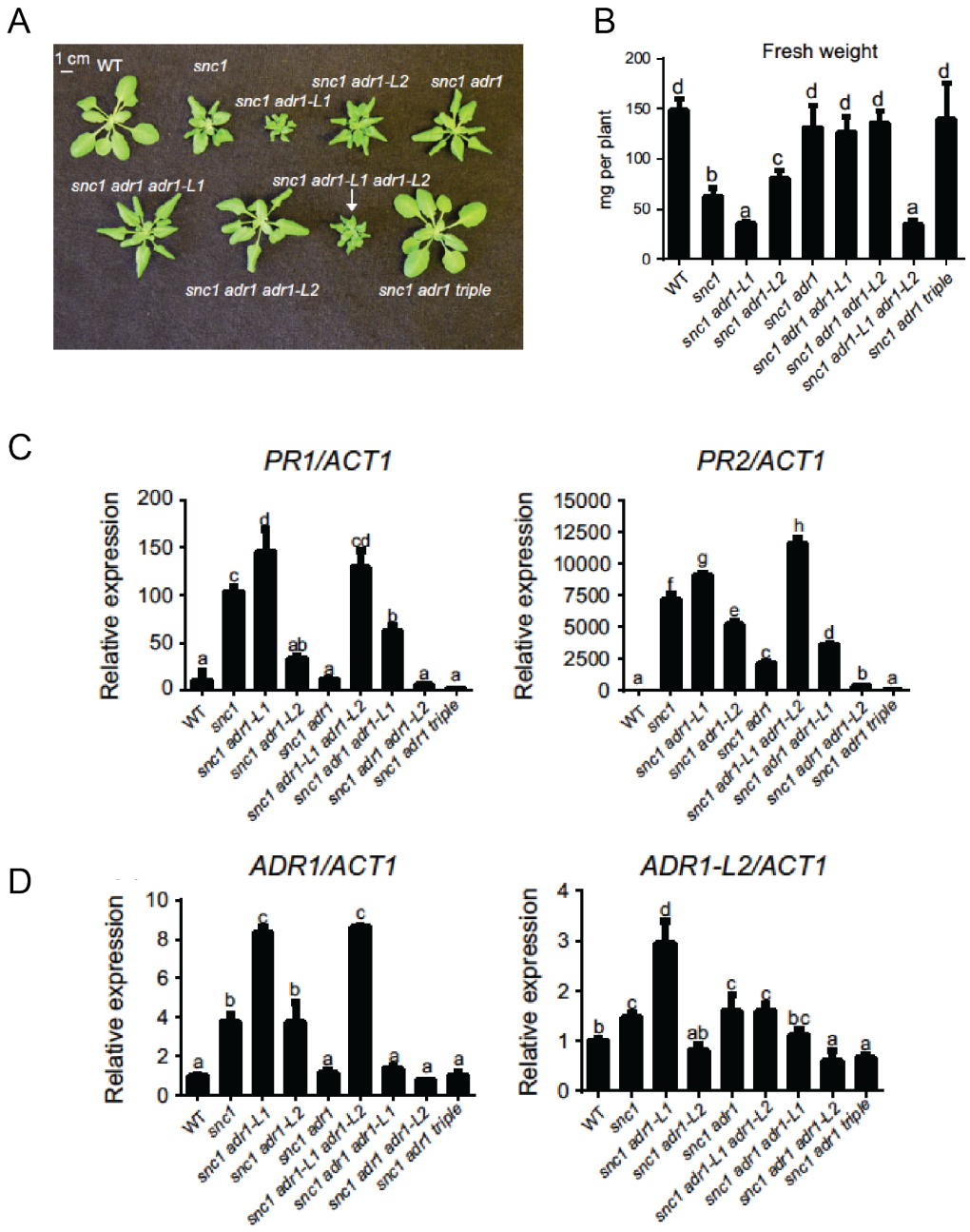

Figure 4.2 Characterization of combinatory mutants between *snc1* and *adr1*s.

(A) Morphological phenotypes of four-week-old WT, *snc1*, *snc1 adr1-L1*, *snc1 adr1-L2*, *snc1 adr1*, *snc1 adr1-L1 adr1-L2*, *snc1 adr1 adr1-L1*, *snc1 adr1 adr1-L2* and *snc1 adr1 adr1-L1 adr1-L2* plants grown at 22°C under long day conditions (16 hr light/8hr dark).

(B) Fresh weights of four-week-old plants of the indicated genotypes grown at 22°C under

long day conditions (16hr light/8hr dark). Six replicates were included for each genotype. Error bars are standard deviations. One-way ANOVA was used to calculate the statistical significance between genotypes, as indicated by different letters ($P < 0.05$).

(C, D) Relative transcript levels of *PR1* and *PR2* (C); *ADR1* and *ADR1-L2* (D) in the indicated genotypes as determined by RT-PCR. Total RNA was extracted from four-week-old plants grown at 22°C under long day conditions (16hr light/8hr dark). *ACT1* was used to normalize the transcript levels. Data represent means of three replicates. Error bars are standard deviations. One-way ANOVA was used to calculate the statistical significance between genotypes, as indicated by different letters ($P < 0.05$).

4.3.3 Loss of all three ADR members completely suppresses the phenotypes of the typical *TNL CHS2*, but not that of atypical *NLR*s: *CHS3, SLH1* and *UNI*

When the *adr1 triple* (*adr1-1 adr1-L1-2 adr1-L2-4*) *snc1* quadruple mutant was generated, a complete *snc1*-suppressing phenotype was observed (Figure 4.1A under UBC and 4.3A under UNC growth conditions), suggesting that ADRs are fully required for *snc1* signalling.

We then tested whether the autoimmune phenotypes caused by additional NLR gain-of-function mutants also require the combined action of the ADR helpers. We crossed the *adr1 triple* mutant into *chs2-1*, *chs3-1*, *slh1-9* and *uni-1D*, each of which causes autoimmune phenotypes under particular growth conditions. The *uni-1D* mutant carries a missense mutation in a CNL (*At1g61180*) gene in Ws-0 (Wassilewskija), causing severe dwarfism and seedling-lethality under certain conditions (Igari et al., 2008). *uni-1D* was introgressed to Col-0 and *uni-1D/+* plants were used for our cross with the *adr1 triple* mutant. The Arabidopsis *slh1* (*sensitive to low humidity 1*) mutant has a mutation in the WRKY domain of the atypical TNL RRS1 that causes activation of defense responses and hypersensitive cell death (Noutoshi et al., 2005).

As shown in Figure 4.3B, the *adr1 triple* mutant completely suppressed *chs2-1* under *chs2-1*-phenotype-inducing growth conditions, although leaves from the suppressed, wild-type sized plants were often curled. We observed weak or partial suppression of the autoimmune phenotypes of *chs3* encoding an atypical TNL with TNL-LIM fusion (Yang et al., 2010), *uni-1D* (Igari et al., 2008) and *slh1-9* (Noutoshi et al., 2005), in each of the respective phenotype-inducing growth conditions (Figure 4.3C-E, Figure 4.4C). We also observed weak suppression of the seedling lethal phenotype for *uni-1D adr1 triple* plants under our short day conditions on plates and on soil (Figure 4.4). Together, these results are consistent with a general helper function for the ADR family for NLR signalling (Bonardi et al., 2011). More specifically, the ADRs seem to be fully required for typical TNL signalling. We collected all known epistasis data to address what possible common signalling pathway might function downstream of the ADR helper NLRs and found that loss of SA biosynthesis was the only function that also suppressed all of the tested gain-of-function NLR mutations. This is consistent with the loss of pathogen-induced SA accumulation in the triple *adr* mutant (Bonardi et al., 2011).

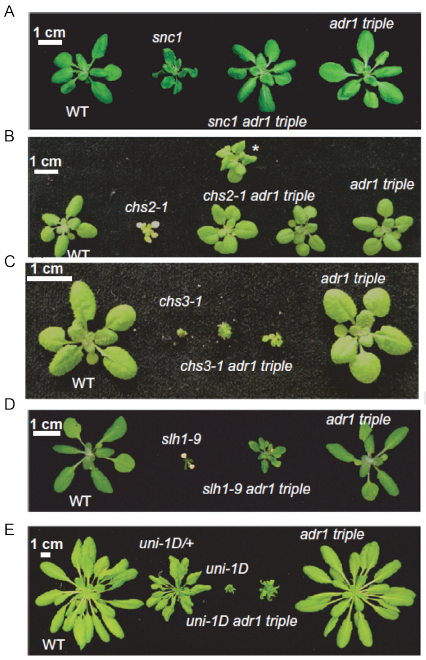

Figure 4.3 *adr1 triple* mutant suppresses the autoimmune phenotypes of gain-of-function typical *TNL* mutants, but not others[1].

(A) Morphological phenotypes of four-week-old WT, *snc1*, *snc1 adr1* triple and *adr1* triple mutant plants grown at 22°C under long day conditions (16hr light/8hr dark).

(B) Morphological phenotypes of three-week-old WT, *chs2-1*, *chs2-1 adr1* triple and *adr1* triple mutant plants grown at 16°C under long day conditions (16hr light/8hr dark). Asterisk denotes the curled leaf suppression phenotype of some *chs2-1 adr1* triple mutant plants.

(C) Morphological phenotypes of three-week-old WT, *chs3-1*, *chs3-1 adr1* triple and *adr1* triple mutant plants grown at 16°C under long day conditions (16hr light/8hr dark).

(D) Morphological phenotypes of three-week-old WT, *slh1-9*, *slh1-9 adr1* triple and *adr1* triple mutant plants grown at 22°C under long day conditions (16hr light/8hr dark).

(E) Morphological phenotypes of six-week-old WT, *uni-1D/+*, *uni-1D, uni-1D adr1* triple and *adr1* triple mutant plants grown at 21°C/18°C under short day conditions (9hr light/15hr dark).

[1]This figure was generated by Bonardi V., Kasmi F. and Wünsch L. from UNC

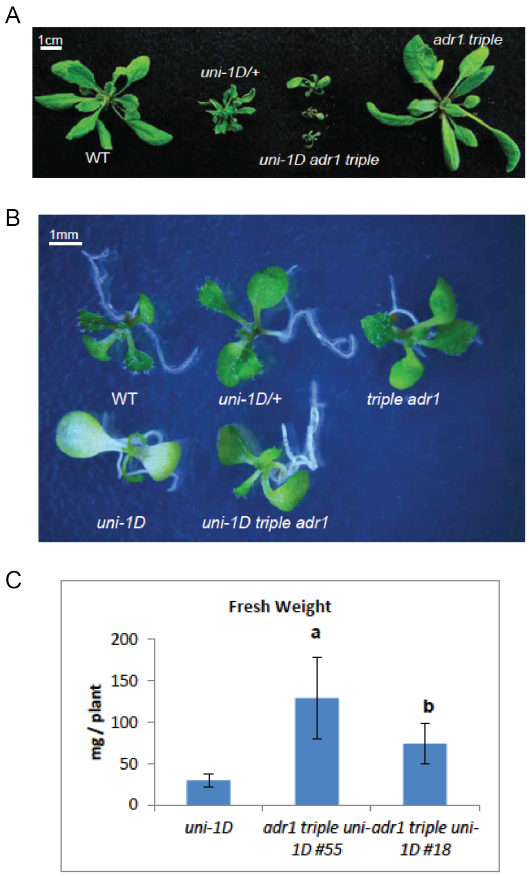

Figure 4.4 Partial suppression of the *uni-1D* autoimmune pheonotypes by *adr1* triple mutant[1].

(A) Morphological phenotypes of four-week-old WT, *uni-1D/+*, *uni-1D adr1* triple and *adr1* triple mutant plants grown at 22°C under long day conditions (16hr light/8hr dark).

(B) Morphological phenotypes of 14-day-old WT, *uni-1D/+*, *adr1* triple, *uni-1D* and *uni-1D adr1* triple seedlings grown at 22°C in continuous light on 1/2 MS agar.

(C) Fresh weights of eight week old *uni-1D* and *adr1 triple uni-1D* plants grown at 21°C/18°C under short day conditions (9hr light/15hr dark). One-way ANOVA was used to calculate the statistical significance between genotypes, as indicated by different letters ($P < 0.002$).

[1]This figure was generated by Bonardi V., Kasmi F. and Wünsch L. from UNC

4.4 Discussion

Here we reported that the triple mutant of *adr1 adr1-L1 adr1-L2* is able to completely suppress the autoimmunity mediated by the typical TNL proteins SNC1 and CHS2 but not that of the atypical TNLs or CNLs CHS3, SLH1 and UNI. Using the *snc1*-suppressing phenotype as criteria, these three *ADR1* genes of *ADR1* family seem to exhibit unequal redundancy, where *ADR1* seems to be the major contributor while *ADR1-L1* is the minor contributor. The unexpected *snc1*-enhancing phenotypes of *adr1-L1* loss-of-function alleles reveal an apparent negative role in plant defense. The *snc1*-enhancing phenotypes in *snc1 adr1-L1* mutants are fully dependent on *ADR1* and *ADR1-L2*. It is possible that loss of *ADR1-L1* results in the over compensation in the synthesis of transcripts for *ADR1* and *ADR1-L2*, as revealed by the up-regulated expression of *ADR1* and *ADR1-L2* in the RT-PCR assays.

The non-canonical function of the ADR1 family as helper NLRs is reminiscent of NLRC4 (Nod-like receptor 4) (Kofoed and Vance, 2011). NLRC4 associates with two independent immune receptors NAIP2 (neuronal apotopsis inhibitory protein 2) and NAIP5 upon PAMP perception. In this scenario, NLRC4 works as a signalling convergent module to transduce signals from the sensor NLRs to activate downstream defense responses (Kofoed and Vance, 2011). Similarly, the ADR1 family could play a general role to mediate signal transduction from different NLRs, especially from typical TNLs.

The function of the ADR1 family resembles those of PAD4 and EDS1, which are signalling intermediates of many typical TNLs upstream of SA synthesis (Wiermer et al., 2005). These observations beg many questions to be addressed in the future. These questions include: What is the relationship between EDS1/PAD4 and ADRs? Where and how do these CNLs transduce signal downstream of TNLs? What protein partners are working together with these helper ADRs and how do the ADR protein dynamics change during defense? Answers to these questions will be key to understanding the involvement of ADRs in the

activation of sensor TNLs.

4.5 Materials and methods

4.5.1 Plant materials used

Arabidopsis mutants used in this thesis include *snc1* (Li et al., 2001), *adr1-1* (Bonardi et al., 2011), *adr1-L1-2* (Bonardi et al., 2011), *adr1-L2-4* (Bonardi et al., 2011), *lsd1-2* (Jabs et al., 1996), *chs1-2* (Wang et al., 2013), *chs2-1* (Huang et al., 2010), *chs3-1* (Yang et al., 2010), *uni-1D* (Igari et al., 2008), and *slh1-9* (Noutoshi et al., 2005).

4.5.2 Growth conditions

For soil grown plants, seeds were vernalized at 4°C for two days, sown onto sterile soil and transferred to plant growth rooms for either long day (22°C/18°C, 16h light/8h dark; ~50% relative humidity) or short day (21°C/18°C, 9h light/15h dark; ~50% relative humidity) or continuous light (22°C) conditions as specified in figure legends. Phenotypes were scored at indicated time points. For all agar plate-grown seedlings, seeds where surface sterilized and sown on 1/2 MS agar plates, vernalized for two days and grown under long day at 22°C.

4.5.3 Plant genotyping

Mutant genotyping primers used are as follows: *adr1* (SAIL_842_B05) ADR1-1_s-Gen: CAA AGG ACG ATG ATG TTC GAG, ADR1-1_as: CGG ATT GTT CAC TAT AGT AAG G, LB_SAIL: TTT CAT AAC CAA TCT CGA TAC AC; *adr1-L1-1* (SAIL_302_C06) L1_1-s: ATG GCC ATC ACC GAT TTT TTC, adr1-L1_as: GTC AGG AAC AGG ATT TCC AG, LB_SAIL; *adr1-L2-4* (Salk_126422) PHX21_1_s: ATG GCA GAT ATA ATC

GGC GG, PHX_ReT4_as: TGG GAG ATT GTG ACA CAG TC, LB1.3: ATT TTG CCG ATT TCG GAA C; *uni-1D* (Col-0, introgressed Ws line): VB14: GTT ATT TCT CGG AGA TAC CAT GC, VB15: GGA CAG TTT GAA ACA TCC ATG, *Col-0* amplicon is ~300bp and *uni-1D* amplicon is ~260bp; *chs2* (*RPP4*) VB12: GAT TGA CCT TGT ATA TGA GGT GG, VB13: CAC TCA TCT TTG TCC CTT CCT TTT GAA, cut amplicon with MboII at 37°C o/n, *Col-0* 138bp and 35bp, *chs2* 138bp and 60bp; *chs3* VB10: TCC TCC TTA CTC CTT GTG AGA C, VB11: TCT CTC TCT CAC TCT CTT CGT AGT TCC CA, cut amplicon with Bci130I at 37°C or 8hr, *Col-0* 170bp and 25bp, *chs3* 194bp; *slh1-9* LW1: GTT ATA TCG ACG TTG GAT GCA G, LW2: CCA GCA AGT TTA GGA TGA TTA CG, cut amplicon with DdeI at 37°C o/n, *Col-0* 260bp and 120bp, *slh1-9* 380bp. *cpr1* (SALK_045148) LP: TTT CGT AAA TTT TTA CAC AAA ATC G, RP: TGT GAG TAG CCT TGT CTT GGG. To genotype homozygous *eds5-3*, SNP primers F: ACT TCA GAG CGG TGA TCA GA and R: CAT CAA CGG TCC ACA AGT C were used. All mutant combinations were confirmed by genotyping.

4.5.4 Infection assay

Ten-day-old soil-grown *Arabidopsis* seedlings were spray-inoculated with freshly harvested *H.a.*Noco2 spores re-suspended in water. Infected plants were kept at 18ºC with 80% humidity for seven days before data collection. Growth of the pathogen was measured by totaling the number of spores per gram of fresh weight.

4.5.5 Total SA measurement

Leaf tissue was harvested from four-week-old *Arabidopsis* plants and homogenized and mixed with 0.2 mL 90% methanol. Samples were sonicated using a water bath sonicator for 20 minutes and centrifuged at 15000 g for 20 minutes. 0.3 mL 100% methanol was added to

the debris for a second extraction. Samples were thoroughly votexed, spun down again and the supernatant from the two extractions were combined and left to dry overnight at room temperature. The next day, 0.1 mL β-glucosidase solution (80unit/mL β-glucosidase (Sigma G0395), in 0.1M NaAc, pH5.2) was added to each sample. Samples were vortexed and sonicated for 5 minutes and incubated at 37°C for 90 minutes. 0.5mL 0.5% TCA (Sigma T6399) was added to the samples. Samples were spun down at 15000g for 15 minutes and the supernatant was transferred to a new set of tubes and was extracted 3 times using extraction medium (ethylacetate:cyclopentant:isopropanol=100:99:1). The combined extraction product was left to dry overnight at room temperature. SA samples were dissolved in mobile phase (0.2M KAc, 0.5mM EDTA, pH5.0) and the quantity of SA was measured using HPLC. The abundance of SA was presented as μg SA per gram fresh weight of plant tissue.

4.5.6 RNA extraction and gene expression analyses

Total RNA was extracted from two-week-old seedlings grown on 1/2 MS medium or four-week-old soil grown plants using Totally RNA kit (Ambion). Reverse transcription was performed using Easyscript Reverse Transcription Kit (ABM). Semi-quantitative PCR was performed as described before (Zhang et al., 2003). Real-time PCR was performed using Perfect Realtime Kit (TAKARA). Sequences of the primers used are *ACT7* F: GGTGTCATGGTTGGTATGGGTC, R: CCTCTGTGAGTAGAACTGGGTGC; *PR1* F: GTAGGTGCTCTTGTTCTTCCC, R: CACATAATTCCCACGAGGATC; *PR2* F: GCTTCCTTCTTCAACCACACAGC, R: CGTTGATGTACCGGAATCTGAC; *ADR1* F: ATAGTGAACAATCCGAGGTT, R: TTTCATCCATTTCCCCTGT; *ADR1-L2* F: CTTGTGAAAGATCCAAGGTT, R: TGAGTCATTTCTCCTGTGT.

4.5.7 Protein extraction and western blot analysis

Total protein was extracted from two-week-old *Arabidopsis* seedlings grown on 1/2 MS medium. The whole extraction was performed either on ice or in a 4°C cold room. Tissues were homogenized and mixed with extraction buffer (100 mM Tris-HCl pH 8.0, 0.1% SDS and 2% β-mercaptoethanol). Samples were vortexed and centrifuged at 15000 g for 10 minutes. SDS loading buffer was added to supernatants and samples were boiled for 5 minutes before loading onto a SDS-PAGE gel. After electrophoresis, separated protein samples were transferred to a membrane and subjected to western blot analyses.

4.5.8 Transient protein expression and co-immunoprecipitation in *N. benthamiana*

The transient protein expression in *N. benthamiana* leaves was carried out as previously described (Drechsel et al., 2011). The infiltration buffer was adapted to 0.1 M Na-phosphate buffer (pH 6.0), with 10 mM $MgCl_2$ and 0.01 mM acetosyringone. The Co-IP protocol was followed as previously described (Moffett et al., 2002; Xu et al., 2014b).

5. Discussion

SNC1 encodes a typical TNL that has been extensively studied in our lab over the last 15 years. The mutant *snc1* harbors a gain-of-function mutation that renders *snc1* with constitutively activated defense responses including enhanced *PR* gene expression, elevated levels of salicylic acid and reduced pathogen growth (Li et al., 2001a; Zhang et al., 2003b). Additionally, the constitutive defense responses in *snc1* lead a dwarf morphology with dark green and curly leaves. Forward genetic screens including MOS (Modifier of *snc1*) *snc1* suppressor and MUSE (Mutant, *snc1*-enhancing) *snc1* enhancer screens in the *snc1* background have resulted in successful identification of many important regulators of NLR-mediated immunity (Johnson et al., 2012; Huang et al., 2013).

Studies on individuals in the collection of identified genes from the genetic screens, including *CPR1*, *MUSE3*, *MUSE10* and *MUSE12*, have highlighted the significant role of ubiquitination in the homeostatic control of the immune receptors (Cheng et al., 2011a; Huang et al., 2014b, 2014a). In order to identify key E3 ubiquitin ligases in plant immunity, we conducted a *snc1*-influencing plant E3 ubiquitin ligase reverse genetic (SNIPER) screen and identified six *SNIPER* candidates: four *snc1*-suppressors and two *snc1*-enhancers. Among the six *SNIPERs, SNIPER 3* was chosen for characterization and described thoroughly in Chapter 3.

The *ADR1* family encodes three homologous non-canonical CNLs with a unique N-terminal CC domain, which shares closest sequence homology with *RESISTANCE TO POWDERY MILDEW8* (*RPW8*), thus termed as CC_R domain (Xiao et al., 2001; Grant et al., 2003; Collier et al., 2011). The three members of *ADR1* family including *ADR1*, *ADR1-LIKE1* (*ADR1-L1*) and *ADR1-L2* were shown to regulate basal defense and some NLR-mediated ETI responses involving RPP2 and RPP4 (Bonardi et al., 2011). Chapter 4 described the specificity of the *ADR1* family's requirement for additional NLRs, both

genetically and biochemically, and also explored the different contributions of *ADR1* family members to NLR-mediated immunity.

5.1 A positive immune regulator SNIPER3/SAUL1 is guarded by a TNL immune receptor SUSA1

SNIPER3/SAUL1 (*AT1G20780*, hereafter, *SAUL1, SENESCENCE-ASSOCIATED UBIQUITIN LIGASE1*) was identified through the SNIPER screen as a *snc1*-enhancer. Overexpression of *SAUL1* leads to the enhancement of *snc1* dwarfism and increased disease resistance in Col-0 background with reduced pathogen growth and heightened expression levels of *PR* genes. SAUL1 protein contains an N-terminal U-box domain, that is involved in E2 binding, and C-terminal armadillo (ARM) repeats, which likely constitute interface for protein-protein interactions (Raab et al., 2009). Loss-of-function mutant of *SAUL1* displays autoimmunity with severe cell death and seedling lethality, which was previously misinterpreted as early senescence phenotypes (Raab et al., 2009). Interestingly, the autoimmunity of *saul1* is fully dependent on *EDS1* and *PAD4*, which are both key downstream components of TNL proteins (Disch et al., 2015). Suppressor screens of *saul1* from two independent groups have identified 11 *saul1* suppressors, all with mutations with the same gene encoding a typical TNL protein SUSA1 (Suppressor of *saul1*).

To test for the role of *SAUL1* in basal resistance, *saul1 susa1* double mutants were used to block the interference of the activation of SUSA1-mediated ETI responses. The results showed the increase growth of virulent bacterial pathogens *Pseudomonas syringae* pv. *maculicola* (*P.s.m*) ES4326 and *P.s.* pv tomato (*P.s.t.*) DC3000 in *saul1 susa1* double mutants. However, the bacterial growth of *P.s.t.* DC3000 carrying the effectors AvrRps4 and AvrRpt2 was not affected in *saul1 susa1* double mutants. *SAUL1* shares the closest sequence similarities with *PUB43*, and therefore studies were done to confirm its homology. A reduction of flg22-induced MPKs activation and an enhanced susceptibility to a type III secretion system (T3SS) deficient bacteria mutant *P.s.t.* DC3000 hrcC- were shown in *saul1*

pub43 susa1 triple mutants, suggesting that SAUL1 and PUB43 may redundantly and positively regulate PTI responses.

Collectively, these data suggest that SAUL1 plays a dual role in plant immunity. On one hand, SAUL1 positively regulates basal resistance. On the other hand, SAUL1 suppresses a typical TNL immune receptor SUSA1 to prevent its autoimmunity. As SAUL1 is an E3 ligase, it is plausible to suspect that SUSA1 could be SAUL1's ubiquitination target. However, this is probably not true, since if SAUL1 targets SUSA1 for degradation, overexpression of *SAUL1* would yield plants with a wild-type like morphology similar to *susa1* mutant plants. Contrary to this theory, *SAUL1* overexpression lines are dwarfed with autoimmunity, arguing against it being the substrate of SAUL1. Based on the phenotypes of *SAUL1* overexpression lines and *saul1 susa1* double mutant plants, SAUL1 likely regulates PTI through ubiquitinating one or more PTI negative regulator(s), leading to their further degradation by the proteasome. Hence, future identification of the ubiquitination substrate(s) of SAUL1 is a critical step to understand how exactly SAUL1 regulates PTI and basal resistance.

SAUL1 was previously shown to associate with the plasma membrane with its extended C-terminal ARM repeats (Vogelmann et al., 2014), whereas SUSA1 mainly localizes in the cytosol. We did not observe any change of SAUL1's membrane localization upon pathogen treatment (Stefan Hoth, personal communication). Considering their different localizations, it remains obscure how SUSA1 guards SAUL1. Does the association of SUSA1 and SAUL1 require additional components and/or pathogen elicitation? Is there any pathogen effector targeting SAUL1 that can be recognized by SUSA1? Answers to these questions would help us to better understand the relationship between SAUL1 and SUSA1.

Identified from the CCSB interactome database (Dreze et al., 2011), one of SAUL1's alleged interactors is LORE1/SD1.29. *LORE1* encodes a bulb-type lectin S-domain-1 receptor-like kinase, which was shown to confer the recognition of lipopolysaccharide (LPS) from Gram-negative bacteria (Ranf et al., 2015). It is speculated that SAUL1 could act

downstream of LORE1 upon LPS elicitation. To test whether SAUL1 is required for LORE1-mediated immunity, *saul1 susa1* or *saul1 pub43 susa1* mutants can be assayed for impaired PTI responses upon LPS treatment. Moreover, it is also worthwhile to test whether SAUL1 can be phosphorylated by LORE1 after LPS elicitation, and if it can, the following up would be to test whether this phosphorylation is critical for SAUL1's function.

SUSA1 encodes a typical TIR-type NLR protein. The two motifs essential for proper NLR activity are the P-loop (phosphate-binding loop) motif and MHD motif. The P-loop motif coordinates with ATP binding and works as a molecular switch to turn on (ATP-bound) and off (ADP-bound) the NLR protein (Hanson and Whiteheart, 2005). Mutations in the P-loop often result in the loss-of-function of NLR proteins (Tameling et al., 2006; Williams et al., 2011; Zhang et al., 2012). Two P-loop mutants, *susa1-7* and *susa1-8*, have been identified through the *saul1* suppressor screens, suggesting that SUSA1 is a typical TNL protein that requires an intact P-loop motif.

MHD motif is a conserved plant-specific motif that locates in the ARC2 sub-domain of the extended NB-ARC domain. In contrast with the effects of P-loop motif mutations, mutation of the Aspartic acid (D) in the MHD motif often results in auto activating NLR proteins that induce pathogen-independent, constitutively activated defense responses in plants (Williams et al., 2011; Zhang et al., 2012). Interestingly, SUSA1 protein contains a MHV motif instead of MHD motif, presumably conferring autoactivation. Thus, it is highly possible that SUSA1 is an autoactive NLR in *Arabidopsi*s, whose activity must be repressed by one or more negative regulator(s), such as SAUL1.

SUSA1 gene forms a head-to-head triplet cluster with two *TIR-NB* (*TN*) genes: *CHS1* (*CHILING SENSITIVE 1*, *AT1G17610*) and *TN2* (*AT1G17615*). The head-to-head arrangement indicates a possible co-regulation between these genes as suggested in recent studies (Deslandes et al., 2003; Gassmann et al., 1999; Narusaka et al., 2009; Williams et al., 2014; Sarris et al., 2015; Jander et al., 2002; van der Biezen et al., 2002; Le Roux et al., 2015; Xu et al., 2015b; Bi et al., 2011). It is possible that the two neighbour TNs of SUSA1 may

work to fine-tune the activation of SUSA1. CHS1 has been shown to weakly interact with SAUL1 in protoplasts (Stefan Hoth, personal communication). It is possible that CHS1 could work together with SAUL1 to suppress the activation of SUSA1. In this scenario, it is expected that overexpression of *CHS1* could rescue *saul1*'s autoimmunity, and knocking out of *CHS1* in *saul1* mutant could yield a similar phenotype as *saul1*. Future experimental evidence can help us better understand the CHS1-SAUL1-SUSA1 relationship.

5.2 The ADR1 family acts downstream of typical TNLs

The *ACTIVATED DISEASE RESISTANCE 1* (*ADR1*) gene family (*ADR1*, *ADR1-L1* and *ADR1-L2*) has been previously shown to play positive roles in basal resistance and ETI responses (Bonardi et al., 2011). The *adr1 adr1-L1 adr1-L2* triple mutant (hereafter "*adr1 triple*") displayed significantly compromised disease resistance against various pathogens including the bacterial pathogen *Pseudomonas syringae* pv. *tomato* (*P.s.t*) DC3000 expressing either the AvrRpm1 or AvrRpt2 effectors, and two isolates of the biotrophic oomycete pathogen *Hyaloperonospora arabidopsidis* (*H.a.* isolates Emwa1 and Cala2); these pathogens contain effectors that can be recognized by NLR receptors RPM1, RPS2, RPP4 and RPP2, respectively (Bonardi et al., 2011). It was suggested that the *ADR1* family works as helper NLRs to transduce signals downstream of specific NLR receptors after effector recognition and activation.

Results described in chapter 4 revealed that *adr1 triple* is able to suppress the autoimmunity of NLR mutants including *snc1* (Li et al., 2001a), *chs2-1* (Huang et al., 2010), but not that of *chs3-1* (Yang et al., 2010), *uni-1D* (Igari et al., 2008) and *slh1-9* (Noutoshi et al., 2005). *SNC1* and *CHS2* both encode typical TNL proteins, whereas *CHS3*, *UNI* and *SLH* encode a TIR-NB, a CNL and a TNL-WRKY, respectively, suggesting that *ADR1* family is required for typical TNL-mediated signalling. It also supports the notion that there are different signalling mechanisms downstream of different types of NLRs.

Using the *snc1*-suppressing phenotype as criterion, we found that among the three *ADR1* genes, *ADR1* is the leading contributor while *ADR1-L1* makes the least contribution in suppressing *snc1* phenotypes. Interestingly, we also identified unexpected *snc1*-enhancing phenotypes in *adr1-L1 snc1* double mutants: the transcripts of *ADR1* and *ADR1-L2* were up-regulated compared with *snc1* in *adr1-L1 snc1* mutants; and the loss of *ADR1* and *ADR1-L2* can fully suppress the *snc1*-enhancing phenotypes in *snc1 adr1-L1* mutant. Thus it is possible that the *snc1*-enhancing phenotypes caused by loss of *ADR1-L1* are contributed by the over compensation of the expression of *ADR1* and *ADR1-L2* transcripts.

The ADR1 family contains a unique CC domain, which has high homology with *RPW8*, a resistance (R) gene that confers a broad range of powdery mildew resistance in *Arabidopsis* (Xiao et al., 2001; Grant et al., 2003; Collier et al., 2011). Thus, the RPW8-like CC domain is termed as CC_R domain (Xiao et al., 2001; Grant et al., 2003; Collier et al., 2011). The second CC_R-NB-LRR encoding gene group is typified by the *Nicotiana benthamiana N-required gene 1* (*NRG1*) (Collier et al., 2011; Peart et al., 2005), which is required for TNL protein N mediated-resistance against tobacco mosaic virus (TMV) (Whitham et al., 1994; Peart et al., 2005). There are two *NRG1*-like genes (*At5g66900*/*NRG1.1*and *At5g66910*/*NRG1.2*) that lie in tandem repeats in the *Arabidopsis* genome (Collier et al., 2011). The expression of CC_R domain of *NRG1.2* is able to trigger severe cell death in *N. benthimiana* (Collier et al., 2011), suggesting that the gene product of *NRG1.2* is functional. However, so far, there is no genetic evidence in *Arabidopsis* suggesting *NRG1s'* role in plant immunity, possibly because of the difficulty of generating an *nrg1.1nrg1.2* double mutant given their tandem repeated organization. The availability of new tools like CRISPR and TALENs will allow us to knock out adjacent *NRG1* gene and study the *nrg1* mutants to investigate their potentially significant roles in NLR-mediated immunity.

Here we provide additional evidence suggesting that, in contrast to the classical role of effector recognition, the NLR ADR1s have acquired expanded functions to transduce signals downstream of effector-recognizing NLRs. But where and how do ADR1s function

downstream of NLRs? It has been previously shown that nuclear translocation is required for the proper function of some NLRs (Shen et al., 2007; Tasset et al., 2010; Xu et al., 2014a). It is speculated that the nuclear entry of ADR1s is required to activate defense. Future examination of the subcellular localization of ADR1s upon elicitation would help to answer this question. The phenotypes of *adr triple* are reminiscent of the phenotypes of loss-of-function of *EDS1 or PAD4,* which are the signalling intermediates of many typical *TNL*s. It would be interesting to examine the genetic and biochemical relationships between *EDS1/PAD4* and *ADR1*s.

Overall, the report of two stories in my Ph.D. thesis: 1) A positive regulator SAUL1 is guarded by a NLR immune receptor SUSA1; 2) *ADR1* family is required for downstream signalling of typical NLRs, emphasizes the importance of the guarding model and the roles of ADR1 family as NLR helpers in defense response. The findings in my Ph.D. thesis therefore push the boundaries of our knowledge on the sophisticated regulatory mechanisms behind plant innate immunity.

References

Aarts, N., Metz, M., Holub, E., Staskawicz, B.J., Daniels, M.J., and Parker, J.E. (1998). Different requirements for EDS1 and NDR1 by disease resistance genes define at least two R gene-mediated signaling pathways in Arabidopsis. Proc. Natl. Acad. Sci. U. S. A. **95**: 10306–11.

Andreasson, E. et al. (2005). The MAP kinase substrate MKS1 is a regulator of plant defense responses. EMBO J. **24**: 2579–2589.

Axtell, M.J. and Staskawicz, B.J. (2003). Initiation of RPS2-specified disease resistance in Arabidopsis is coupled to the AvrRpt2-directed elimination of RIN4. Cell **112**: 369–77.

Azevedo, C., Sadanandom, A., Kitagawa, K., Freialdenhoven, A., Shirasu, K., and Schulze-Lefert, P. (2002). The RAR1 interactor SGT1, an essential component of R gene-triggered disease resistance. Science **295**: 2073–6.

Bednarek, P., Pislewska-Bednarek, M., Svatos, A., Schneider, B., Doubsky, J., Mansurova, M., Humphry, M., Consonni, C., Panstruga, R., Sanchez-Vallet, A., Molina, A., and Schulze-Lefert, P. (2009). A glucosinolate metabolism pathway in living plant cells mediates broad-spectrum antifungal defense. Science **323**: 101–106.

Bi, D., Johnson, K.C.M., Zhu, Z., Huang, Y., Chen, F., Zhang, Y., and Li, X. (2011). Mutations in an Atypical TIR-NB-LRR-LIM Resistance Protein Confer Autoimmunity. Front. Plant Sci. **2**: 1–10.

van der Biezen, E. a, Freddie, C.T., Kahn, K., Parker, J.E., and Jones, J.D.G. (2002). Arabidopsis RPP4 is a member of the RPP5 multigene family of TIR-NB-LRR genes and confers downy mildew resistance through multiple signalling components. Plant J. **29**: 439–51.

Blume, B., Nürnberger, T., Nass, N., and Scheel, D. (2000). Receptor-mediated increase in cytoplasmic free calcium required for activation of pathogen defense in parsley. Plant Cell **12**: 1425–1440.

Boller, T. and Felix, G. (2009). A renaissance of elicitors: perception of microbe-associated molecular patterns and danger signals by pattern-recognition receptors. Annu. Rev. Plant Biol. **60**: 379–406.

Bonardi, V., Tang, S., Stallmann, A., Roberts, M., Cherkis, K., and Dangl, J.L. (2011). Expanded functions for a family of plant intracellular immune receptors beyond specific recognition of pathogen effectors. Proc. Natl. Acad. Sci. U. S. A. **108**: 16463–8.

Bos, J.I.B. et al. (2010). Phytophthora infestans effector AVR3a is essential for virulence and manipulates plant immunity by stabilizing host E3 ligase CMPG1. Proc. Natl. Acad. Sci. U. S. A. **107**: 9909–9914.

Broekaert, W.F., Terras, F.R., Cammue, B.P., and Osborn, R.W. (1995). Plant defensins: novel antimicrobial peptides as components of the host defense system. Plant Physiol. **108**: 1353–1358.

Cardinale, F., Jonak, C., Ligterink, W., Niehaus, K., Boller, T., and Hirt, H. (2000). Differential activation of four specific MAPK pathways by distinct elicitors. J. Biol. Chem. **275**: 36734–36740.

Causier, B., Ashworth, M., Guo, W., and Davies, B. (2012). The TOPLESS Interactome: A Framework for Gene Repression in Arabidopsis. Plant Physiol. **158**: 423–438.

Chang, C., Yu, D., Jiao, J., Jing, S., Schulze-Lefert, P., and Shen, Q.-H. (2013). Barley MLA immune receptors directly interfere with antagonistically acting transcription factors to initiate disease resistance signaling. Plant Cell **25**: 1158–73.

Chen, H., Zou, Y., Shang, Y., Lin, H., Wang, Y., and Cai, R. (2008). Firefly Luciferase Complementation Imaging Assay for Protein-Protein Interactions in Plants. Plant Physiol. **146**: 368–376.

Cheng, Y.T., Germain, H., Wiermer, M., Bi, D., Xu, F., García, A. V, Wirthmueller, L., Després, C., Parker, J.E., Zhang, Y., and Li, X. (2009). Nuclear pore complex component MOS7/Nup88 is required for innate immunity and nuclear accumulation of defense regulators in Arabidopsis. Plant Cell **21**: 2503–2516.

Cheng, Y.T. and Li, X. (2012). Ubiquitination in NB-LRR-mediated immunity. Curr. Opin. Plant Biol. **15**: 392–399.

Cheng, Y.T., Li, Y., Huang, S., Huang, Y., Dong, X., Zhang, Y., and Li, X. (2011a). Stability of plant immune-receptor resistance proteins is controlled by SKP1-CULLIN1-F-box (SCF)-mediated protein degradation. Proc. Natl. Acad. Sci. U. S. A. **108**: 14694–14699.

Cheng, Y.Y.T., Li, Y., Huang, S., Huang, Y., Dong, X., Zhang, Y., and Li, X. (2011b). Stability of plant immune-receptor resistance proteins is controlled by SKP1-CULLIN1-F-box (SCF)-mediated protein degradation. Proc. Natl. Acad. Sci. **108**: 14694–14699.

Chini, A., Fonseca, S., Fernández, G., Adie, B., Chico, J.M., Lorenzo, O., García-Casado, G., López-Vidriero, I., Lozano, F.M., Ponce, M.R., Micol, J.L., and Solano, R. (2007). The JAZ family of repressors is the missing link in jasmonate signalling. Nature **448**: 666–671.

Chini, A., Grant, J.J., Seki, M., Shinozaki, K., and Loake, G.J. (2004). Drought tolerance established by enhanced expression of the CC-NBS-LRR gene, ADR1, requires salicylic acid, EDS1 and ABI1. Plant J. **38**: 810–822.

Chini, A. and Loake, G.J. (2005). Motifs specific for the ADR1 NBS-LRR protein family in Arabidopsis are conserved among NBS-LRR sequences from both dicotyledonous and monocotyledonous plants. Planta **221**: 597–601.

Chung, E.H., Da Cunha, L., Wu, A.J., Gao, Z., Cherkis, K., Afzal, A.J., MacKey, D., and Dangl, J.L. (2011). Specific threonine phosphorylation of a host target by two unrelated type III effectors activates a host innate immune receptor in plants. Cell Host Microbe **9**: 125–136.

Clay, N.K., Adio, A.M., Denoux, C., Jander, G., and Ausubel, F.M. (2009). Glucosinolate metabolites required for an Arabidopsis innate immune response. Science **323**: 95–101.

Clough, S.J. and Bent, A.F. (1998). Floral dip: A simplified method for Agrobacterium-mediated transformation of Arabidopsis thaliana. Plant J. **16**: 735–743.

Collier, S.M., Hamel, L.-P., and Moffett, P. (2011). Cell death mediated by the N-terminal domains of a unique and highly conserved class of NB-LRR protein. Mol. Plant. Microbe. Interact. **24**: 918–931.

Collins, N.C., Thordal-Christensen, H., Lipka, V., Bau, S., Kombrink, E., Qiu, J.-L., Hückelhoven, R., Stein, M., Freialdenhoven, A., Somerville, S.C., and Schulze-Lefert, P. (2003). SNARE-protein-mediated disease resistance at the plant cell wall. Nature **425**: 973–977.

Curtis, M.D. and Grossniklaus, U. (2003). A Gateway cloning vector set for high-hhroughput hunctional hnalysis of henes in planta. Plant Physiol. **133**: 462–469.

Deshaies, R.J. and Joazeiro, C. a P. (2009). RING domain E3 ubiquitin ligases. Annu. Rev. Biochem. **78**: 399–434.

Deslandes, L., Olivier, J., Peeters, N., Feng, D.X., Khounlotham, M., Boucher, C., Somssich, I., Genin, S., and Marco, Y. (2003). Physical interaction between RRS1-R, a protein conferring resistance to bacterial wilt, and PopP2, a type III effector targeted to the plant nucleus. Proc. Natl. Acad. Sci. U. S. A. **100**: 8024–8029.

Dharmasiri, N., Dharmasiri, S., and Estelle, M. (2005). The F-box protein TIR1 is an auxin receptor. Nature **435**: 441–445.

Disch, E.-M., Tong, M., Kotur, T., Koch, G., Wolf, C.-A., Li, X., and Hoth, S. (2015). Membrane-Associated Ubiquitin Ligase SAUL1 Suppresses Temperature- and Humidity-Dependent Autoimmunity in Arabidopsis. Mol. Plant. Microbe. Interact. **in press**.

Dodds, P.N., Lawrence, G.J., Catanzariti, A.-M., Teh, T., Wang, C.-I.A., Ayliffe, M.A., Kobe, B., and Ellis, J.G. (2006). Direct protein interaction underlies gene-for-gene specificity and coevolution of the flax resistance genes and flax rust avirulence genes. Proc. Natl. Acad. Sci. U. S. A. **103**: 8888–8893.

Dodds, P.N. and Rathjen, J.P. (2010). Plant immunity: towards an integrated view of plant-pathogen interactions. Nat. Rev. Genet. **11**: 539–548.

Downes, B.P., Stupar, R.M., Gingerich, D.J., and Vierstra, R.D. (2003). The HECT ubiquitin-protein ligase (UPL) family in Arabidopsis: UPL3 has a specific role in trichome development. Plant J. **35**: 729–742.

Drechsel, G., Bergler, J., Wippel, K., Sauer, N., Vogelmann, K., and Hoth, S. (2011). C-terminal armadillo repeats are essential and sufficient for association of the plant U-box armadillo E3 ubiquitin ligase SAUL1 with the plasma membrane. J. Exp. Bot. **62**: 775–785.

Dreher, K. and Callis, J. (2007). Ubiquitin, Hormones and Biotic Stress in Plants. Ann. Bot. **99**: 787–822.

Dreze, M. et al. (2011). Evidence for Network Evolution in an Arabidopsis Interactome Map. Science (80-.). **333**: 601–607.

Dubiella, U., Seybold, H., Durian, G., Komander, E., Lassig, R., Witte, C.-P., Schulze,

W.X., and Romeis, T. (2013). Calcium-dependent protein kinase/NADPH oxidase activation circuit is required for rapid defense signal propagation. Proc. Natl. Acad. Sci. U. S. A. **110**: 8744–8749.

Flor, H.H. (1971). Current status of the gene-for-gene concept. Annu. Rev. Phytopathol. **9**: 275–296.

Gagne, J.M., Downes, B.P., Shiu, S.-H., Durski, A.M., and Vierstra, R.D. (2002). The F-box subunit of the SCF E3 complex is encoded by a diverse superfamily of genes in Arabidopsis. Proc. Natl. Acad. Sci. U. S. A. **99**: 11519–11524.

Gao, M., Liu, J., Bi, D., Zhang, Z., Cheng, F., Chen, S., and Zhang, Y. (2008). MEKK1, MKK1/MKK2 and MPK4 function together in a mitogen-activated protein kinase cascade to regulate innate immunity in plants. Cell Res. **18**: 1190–1198.

Gassmann, W., Hinsch, M.E., and Staskawicz, B.J. (1999). The Arabidopsis RPS4 bacterial-resistance gene is a member of the TIR-NBS-LRR family of disease-resistance genes. Plant J. **20**: 265–277.

Geldner, N., Dénervaud-Tendon, V., Hyman, D.L., Mayer, U., Stierhof, Y.-D., and Chory, J. (2009). Rapid, combinatorial analysis of membrane compartments in intact plants with a multicolor marker set. Plant J. **59**: 169–178.

Germain, H. et al. (2010). MOS11: a new component in the mRNA export pathway. PLoS Genet. **6**: e1001250.

Gietz, R.D., Triggs-Raine, B., Robbins, A., Graham, K.C., and Woods, R. a. (1997). Identification of proteins that interact with a protein of interest: Applications of the yeast two-hybrid system. Mol. Cell. Biochem. **172**: 67–79.

González-Lamothe, R., Tsitsigiannis, D.I., Ludwig, A. a, Panicot, M., Shirasu, K., and Jones, J.D.G. (2006). The U-box protein CMPG1 is required for efficient activation of defense mechanisms triggered by multiple resistance genes in tobacco and tomato. Plant Cell **18**: 1067–1083.

Grant, J.J., Chini, A., Basu, D., and Loake, G.J. (2003). Targeted activation tagging of the Arabidopsis NBS-LRR gene, ADR1, conveys resistance to virulent pathogens. Mol. Plant. Microbe. Interact. **16**: 669–680.

Hanson, P.I. and Whiteheart, S.W. (2005). AAA+ proteins: have engine, will work. Nat.

Rev. Mol. Cell Biol. **6**: 519–529.

Harmon, A.C., Gribskov, M., and Harper, J.F. (2000). CDPKs – a kinase for every Ca2+ signal? Trends Plant Sci. **5**: 154–159.

Heath, M.C. (2000). Nonhost resistance and nonspecific plant defenses. Curr. Opin. Plant Biol. **3**: 315–319.

Hershko, a and Ciechanover, a (1998). The ubiquitin system. Annu. Rev. Biochem. **67**: 425–479.

Holt III, B.F., Belkhadir, Y., Dangl, J.L., Holt, B.F., Belkhadir, Y., and Dangl, J.L. (2005). Antagonistic Control of Disease Resistance Protein Stability in the Plant Immune System. Science (80-.). **309**: 929–932.

Huang, S., Monaghan, J., Zhong, X., Lin, L., Sun, T., Dong, O.X., and Li, X. (2014a). HSP90s are required for NLR immune receptor accumulation in Arabidopsis. Plant J. **79**: 427–439.

Huang, Y., Chen, X., Liu, Y., Roth, C., Copeland, C., McFarlane, H.E., Huang, S., Lipka, V., Wiermer, M., and Li, X. (2013). Mitochondrial AtPAM16 is required for plant survival and the negative regulation of plant immunity. Nat. Commun. **4**: 2558.

Huang, Y., Minaker, S., Roth, C., Huang, S., Hieter, P., Lipka, V., Wiermer, M., and Li, X. (2014b). An E4 ligase facilitates polyubiquitination of plant immune receptor resistance proteins in Arabidopsis. Plant Cell **26**: 485–496.

Ichimura, K. et al. (2002). Mitogen-activated protein kinase cascades in plants: a new nomenclature. Trends Plant Sci. **7**: 301–308.

Ichimura, K., Mizoguchi, T., Irie, K., Morris, P., Giraudat, J., Matsumoto, K., and Shinozaki, K. (1998). Isolation of ATMEKK1 (a MAP kinase kinase kinase)-interacting proteins and analysis of a MAP kinase cascade in Arabidopsis. Biochem Biophys Res Commun **253**: 532–543.

Ishikawa, K., Yamaguchi, K., Sakamoto, K., Yoshimura, S., Inoue, K., Tsuge, S., Kojima, C., and Kawasaki, T. (2014). Bacterial effector modulation of host E3 ligase activity suppresses PAMP-triggered immunity in rice. Nat. Commun. **5**: 5430.

Jander, G., Norris, S.R., Rounsley, S.D., Bush, D.F., Levin, I.M., Last, R.L., Llc, C.G.,

and Street, S. (2002). Arabidopsis Map-Based Cloning in the Post-Genome Era. Plant Physiol. **129**: 440–450.

Jia, Y., McAdams, S.A., Bryan, G.T., Hershey, H.P., and Valent, B. (2000). Direct interaction of resistance gene and avirulence gene products confers rice blast resistance. EMBO J. **19**: 4004–4014.

Johnson, K.C.M., Dong, O.X., Huang, Y., and Li, X. (2012). A rolling stone gathers no moss, but resistant plants must gather their MOSes. Cold Spring Harb. Symp. Quant. Biol. **77**: 259–268.

Jones, J.D.G. and Dangl, J.L. (2006). The plant immune system. Nature **444**: 323–9.

Kadota, Y., Sklenar, J., Derbyshire, P., Stransfeld, L., Asai, S., Ntoukakis, V., Jones, J.D., Shirasu, K., Menke, F., Jones, A., and Zipfel, C. (2014). Direct Regulation of the NADPH Oxidase RBOHD by the PRR-Associated Kinase BIK1 during Plant Immunity. Mol. Cell **54**: 43–55.

Kaku, H., Nishizawa, Y., Ishii-Minami, N., Akimoto-Tomiyama, C., Dohmae, N., Takio, K., Minami, E., and Shibuya, N. (2006). Plant cells recognize chitin fragments for defense signaling through a plasma membrane receptor. Proc. Natl. Acad. Sci. U. S. A. **103**: 11086–11091.

Karimi, M., Depicker, A., and Hilson, P. (2007). Recombinational cloning with plant gateway vectors. Plant Physiol. **145**: 1144–1154.

Karnik, R., Zhang, B., Waghmare, S., Aderhold, C., Grefen, C., and Blatt, M.R. (2015). Binding of SEC11 Indicates Its Role in SNARE Recycling after Vesicle Fusion and Identifies Two Pathways for Vesicular Traffic to the Plasma Membrane. Plant Cell Online **27**: tpc.114.134429.

Katsir, L., Schilmiller, A.L., Staswick, P.E., He, S.Y., and Howe, G. a (2008). COI1 is a critical component of a receptor for jasmonate and the bacterial virulence factor coronatine. Proc. Natl. Acad. Sci. U. S. A. **105**: 7100–7105.

Kiegerl, S. (2000). SIMKK, a Mitogen-Activated Protein Kinase (MAPK) Kinase, Is a Specific Activator of the Salt Stress-Induced MAPK, SIMK. Plant Cell Online **12**: 2247–2258.

Kofoed, E.M. and Vance, R.E. (2011). Innate immune recognition of bacterial ligands by

NAIPs determines inflammasome specificity. Nature **477**: 592–595.

Kong, Q., Qu, N., Gao, M., Zhang, Z., Ding, X., Yang, F., Li, Y., Dong, O.X., Chen, S., Li, X., and Zhang, Y. (2012). The MEKK1-MKK1/MKK2-MPK4 kinase cascade negatively regulates immunity mediated by a mitogen-activated protein kinase kinase kinase in Arabidopsis. Plant Cell **24**: 2225–36.

Krasileva, K. V, Dahlbeck, D., and Staskawicz, B.J. (2010). Activation of an Arabidopsis resistance protein is specified by the in planta association of its leucine-rich repeat domain with the cognate oomycete effector. Plant Cell **22**: 2444–2458.

Kudla, J., Batistic, O., and Hashimoto, K. (2010). Calcium Signals: The Lead Currency of Plant Information Processing. Plant Cell **22**: 541–563.

Lakatos, L., Szittya, G., Silhavy, D., and Burgyán, J. (2004). Molecular mechanism of RNA silencing suppression mediated by p19 protein of tombusviruses. EMBO J. **23**: 876–884.

Lamb, C. and Dixon, R.A. (1997). The oxidative burst in plant disease resistance. Annu. Rev. Plant Biol. **48**: 251–275.

Le Roux, C. et al. (2015). A Receptor Pair with an Integrated Decoy Converts Pathogen Disabling of Transcription Factors to Immunity. Cell **161**: 1074–1088.

Lee, D., Bourdais, G., Yu, G., Robatzek, S., and Coaker, G. (2015). Phosphorylation of the Plant Immune Regulator RPM1-INTERACTING PROTEIN4 Enhances Plant Plasma Membrane H^+-ATPase Activity and Inhibits Flagellin-Triggered Immune Responses in Arabidopsis. Plant Cell: tpc.114.132308.

Lee, S., Han, S., Sririyanum, M., Park, C., Seo, Y., and Ronald, P. (2009). A Type I – Secreted, Sulfated Peptide Triggers XA21-Mediated Innate Immunity. Science: 850–85.

Li, L., Li, M., Yu, L., Zhou, Z., Liang, X., Liu, Z., Cai, G., Gao, L., Zhang, X., Wang, Y., Chen, S., and Zhou, J.-M. (2014). The FLS2-Associated Kinase BIK1 Directly Phosphorylates the NADPH Oxidase RbohD to Control Plant Immunity. Cell Host Microbe **15**: 329–338.

Li, X., Clarke, J.D., Zhang, Y., and Dong, X. (2001a). Activation of an EDS1-mediated R-gene pathway in the snc1 mutant leads to constitutive, NPR1-independent pathogen resistance. Mol. Plant. Microbe. Interact. **14**: 1131–9.

Li, X., Kapos, P., and Zhang, Y. (2015). NLRs in plants. Curr. Opin. Immunol. **32**: 114–121.

Li, X., Song, Y., Century, K., Straight, S., Ronald, P., Dong, X., Lassner, M., and Zhang, Y. (2001b). A fast neutron deletion mutagenesis-based reverse genetics system for plants. Plant J. **27**: 235–242.

Li, Y., Tessaro, M.J., Li, X., and Zhang, Y. (2010). Regulation of the expression of plant resistance gene SNC1 by a protein with a conserved BAT2 domain. Plant Physiol. **153**: 1425–1434.

Lipka, V. et al. (2005). Pre- and postinvasion defenses both contribute to nonhost resistance in Arabidopsis. Science **310**: 1180–1183.

Liu, J., Elmore, J.M., Lin, Z.J.D., and Coaker, G. (2011). A receptor-like cytoplasmic kinase phosphorylates the host target RIN4, leading to the activation of a plant innate immune receptor. Cell Host Microbe **9**: 137–146.

Lu, D., Lin, W., Gao, X., Wu, S., Cheng, C., Avila, J., Heese, A., Devarenne, T.P., He, P., and Shan, L. (2011). Direct ubiquitination of pattern recognition receptor FLS2 attenuates plant innate immunity. Science **332**: 1439–1442.

Lu, D., Wu, S., Gao, X., Zhang, Y., Shan, L., and He, P. (2010). A receptor-like cytoplasmic kinase, BIK1, associates with a flagellin receptor complex to initiate plant innate immunity. Proc. Natl. Acad. Sci. **107**: 496–501.

Lu, X., Dittgen, J., Piślewska-Bednarek, M., Molina, A., Schneider, B., Svatoš, A., Doubský, J., Schneeberger, K., Weigel, D., Bednarek, P., and Schulze-Lefert, P. (2015). Mutant Allele-Specific Uncoupling of PENETRATION3 Functions Reveals Engagement of the ATP-Binding Cassette Transporter in Distinct Tryptophan Metabolic Pathways. Plant Physiol. **168**: 814–827.

Mackey, D., Belkhadir, Y., Alonso, J.M., Ecker, J.R., and Dangl, J.L. (2003). Arabidopsis RIN4 is a target of the type III virulence effector AvrRpt2 and modulates RPS2-mediated resistance. Cell **112**: 379–389.

Maekawa, T. et al. (2011). Coiled-Coil Domain-Dependent Homodimerization of Intracellular Barley Immune Receptors Defines a Minimal Functional Module for Triggering Cell Death. Cell Host Microbe **9**: 187–199.

Mao, G., Meng, X., Liu, Y., Zheng, Z., Chen, Z., and Zhang, S. (2011). Phosphorylation of a WRKY Transcription Factor by Two Pathogen-Responsive MAPKs Drives Phytoalexin Biosynthesis in Arabidopsis. Plant Cell **23**: 1639–1653.

Mauch, S., Shen, Q., Peart, J., Devoto, A., and Casais, C. (2004). RAR1 Positively Controls Steady State Levels of Barley MLA Resistance Proteins and Enables Sufficient MLA6 Accumulation for Effective Resistance. **16**: 3480–3495.

Meyers, B.C. (2003). Genome-Wide Analysis of NBS-LRR-Encoding Genes in Arabidopsis. Plant Cell **15**: 809–834.

Miya, A., Albert, P., Shinya, T., Desaki, Y., Ichimura, K., Shirasu, K., Narusaka, Y., Kawakami, N., Kaku, H., and Shibuya, N. (2007). CERK1, a LysM receptor kinase, is essential for chitin elicitor signaling in Arabidopsis. Proc. Natl. Acad. Sci. U. S. A. **104**: 19613–19618.

Moffett, P., Farnham, G., Peart, J., and Baulcombe, D.C. (2002). Interaction between domains of a plant NBS-LRR protein in disease resistance-related cell death. EMBO J. **21**: 4511–4519.

Monaghan, J., Matschi, S., Shorinola, O., Rovenich, H., Matei, A., Segonzac, C., Malinovsky, F.G., Rathjen, J.P., MacLean, D., Romeis, T., and Zipfel, C. (2014). The Calcium-Dependent Protein Kinase CPK28 Buffers Plant Immunity and Regulates BIK1 Turnover. Cell Host Microbe **16**: 605–615.

Monaghan, J. and Zipfel, C. (2012). Plant pattern recognition receptor complexes at the plasma membrane. Curr. Opin. Plant Biol. **15**: 349–357.

Mudgil, Y., Shiu, S.-H., Stone, S.L., Salt, J.N., and Goring, D.R. (2004). A large complement of the predicted Arabidopsis ARM repeat proteins are members of the U-box E3 ubiquitin ligase family. Plant Physiol. **134**: 59–66.

Narusaka, M., Shirasu, K., Noutoshi, Y., Kubo, Y., Shiraishi, T., Iwabuchi, M., and Narusaka, Y. (2009). RRS1 and RPS4 provide a dual Resistance-gene system against fungal and bacterial pathogens. Plant J. **60**: 218–226.

Nelson, B.K., Cai, X., and Nebenführ, A. (2007). A multicolored set of in vivo organelle markers for co-localization studies in Arabidopsis and other plants. Plant J. **51**: 1126–1136.

Ntoukakis, V., Saur, I.M., Conlan, B., and Rathjen, J.P. (2014). The changing of the guard: the Pto/Prf receptor complex of tomato and pathogen recognition. Curr. Opin. Plant Biol. **20C**: 69–74.

Nühse, T.S., Peck, S.C., Hirt, H., and Boller, T. (2000). Microbial elicitors induce activation and dual phosphorylation of the Arabidopsis thaliana MAPK 6. J. Biol. Chem. **275**: 7521–7526.

Ohi, M.D., Vander Kooi, C.W., Rosenberg, J. a, Chazin, W.J., and Gould, K.L. (2003). Structural insights into the U-box, a domain associated with multi-ubiquitination. Nat. Struct. Biol. **10**: 250–255.

Okushima, Y. et al. (2005). Functional Genomic Analysis of the AUXIN RESPONSE FACTOR Gene Family Members in Arabidopsis thaliOkushima, Y., Overvoorde, P. J., Arima, K., Alonso, J. M., Chan, A., Chang, C., Ecker, J. R., et al. (2005). Functional Genomic Analysis of the AUXIN RESPONSE. Plant Cell **17**: 444–463.

van Ooijen, G., Mayr, G., Kasiem, M.M. a, Albrecht, M., Cornelissen, B.J.C., and Takken, F.L.W. (2008). Structure-function analysis of the NB-ARC domain of plant disease resistance proteins. J. Exp. Bot. **59**: 1383–1397.

Palma, K., Zhang, Y., and Li, X. (2005). An importin alpha homolog, MOS6, plays an important role in plant innate immunity. Curr. Biol. **15**: 1129–1135.

Palma, K., Zhao, Q., Yu, T.C., Bi, D., Monaghan, J., Cheng, W., Zhang, Y., and Li, X. (2007). Regulation of plant innate immunity by three proteins in a complex conserved across the plant and animal kingdoms. Genes Dev. **21**: 1484–1493.

Peart, J.R., Mestre, P., Lu, R., Malcuit, I., and Baulcombe, D.C. (2005). NRG1, a CC-NB-LRR protein, together with N, a TIR-NB-LRR protein, mediates resistance against tobacco mosaic virus. Curr. Biol. **15**: 968–973.

Petersen, M. et al. (2000). Arabidopsis map kinase 4 negatively regulates systemic acquired resistance. Cell **103**: 1111–1120.

Pratt, W.B., Krishna, P., and Olsen, L.J. (2001). Hsp90-binding immunophilins in plants: The protein movers. Trends Plant Sci. **6**: 54–58.

Pruitt, R.N. et al. (2015). The rice immune receptor XA21 recognizes a tyrosine-sulfated protein from a Gram-negative bacterium. Sci. Adv. **1**: e1500245–e1500245.

Qiu, J.-L. et al. (2008). Arabidopsis MAP kinase 4 regulates gene expression through transcription factor release in the nucleus. EMBO J. **27**: 2214–2221.

Raab, S., Drechsel, G., Zarepour, M., Hartung, W., Koshiba, T., Bittner, F., and Hoth, S. (2009). Identification of a novel E3 ubiquitin ligase that is required for suppression of premature senescence in Arabidopsis. Plant J. **59**: 39–51.

Ranf, S., Gisch, N., Schäffer, M., Illig, T., Westphal, L., Knirel, Y.A., Sánchez-Carballo, P.M., Zähringer, U., Hückelhoven, R., Lee, J., and Scheel, D. (2015). A lectin S-domain receptor kinase mediates lipopolysaccharide sensing in Arabidopsis thaliana. Nat. Immunol. **16**: 426–433.

Ravensdale, M., Bernoux, M., Ve, T., Kobe, B., Thrall, P.H., Ellis, J.G., and Dodds, P.N. (2012). Intramolecular Interaction Influences Binding of the Flax L5 and L6 Resistance Proteins to their AvrL567 Ligands. PLoS Pathog. **8**: e1003004.

Roux, M., Schwessinger, B., Albrecht, C., Chinchilla, D., Jones, A., Holton, N., Malinovsky, F.G., Tor, M., de Vries, S., and Zipfel, C. (2011). The Arabidopsis Leucine-Rich Repeat Receptor-Like Kinases BAK1/SERK3 and BKK1/SERK4 Are Required for Innate Immunity to Hemibiotrophic and Biotrophic Pathogens. Plant Cell **23**: 2440–2455.

Sarris, P.F. et al. (2015). A Plant Immune Receptor Detects Pathogen Effectors that Target WRKY Transcription Factors. Cell **161**: 1089–1100.

Schroder, K. and Tschopp, J.J.J. (2010). The inflammasomes. Cell **140**: 821–832.

Shao, F., Golstein, C., Ade, J., and Stoutemyer, M. (2003). Cleavage of Arabidopsis PBS1 by a bacterial type III effector. Science **301**: 1230-1233.

Shen, Q.-H., Saijo, Y., Mauch, S., Biskup, C., Bieri, S., Keller, B., Seki, H., Ulker, B., Somssich, I.E., and Schulze-Lefert, P. (2007). Nuclear activity of MLA immune receptors links isolate-specific and basal disease-resistance responses. Science **315**: 1098–1103.

Smalle, J. and Vierstra, R.D. (2004). the Ubiquitin 26S Proteasome Proteolytic Pathway. Annu. Rev. Plant Biol. **55**: 555–590.

Song, W.Y., Wang, G.L., Chen, L.L., Kim, H.S., Pi, L.Y., Holsten, T., Gardner, J., Wang, B., Zhai, W.X., Zhu, L.H., Fauquet, C., and Ronald, P. (1995). A receptor

kinase-like protein encoded by the rice disease resistance gene, Xa21. Science **270**: 1804–1806.

Stegmann, M., Anderson, R.G., Ichimura, K., Pecenkova, T., Reuter, P., Žárský, V., McDowell, J.M., Shirasu, K., and Trujillo, M. (2012). The ubiquitin ligase PUB22 targets a subunit of the exocyst complex required for PAMP-triggered responses in Arabidopsis. Plant Cell **24**: 4703–4716.

Stein, M., Dittgen, J., Sanchez-Rodrguez, C., Hou, B., Molina, A., Schulze-lefert, P., Lipka, V., and Somerville, S. (2006). Arabidopsis PEN3 / PDR8 , an ATP Binding Cassette Transporter , Contributes to Nonhost Resistance to Inappropriate Pathogens That Enter by Direct Penetration. **18**: 731–746.

Takken, F.L.W. and Goverse, A. (2012). How to build a pathogen detector: Structural basis of NB-LRR function. Curr. Opin. Plant Biol. **15**: 375–384.

Takken, F.L.W. and Tameling, W.I.L. (2009). To nibble at plant resistance proteins. Science **324**: 744–746.

Tameling, W.I.L., Vossen, J.H., Albrecht, M., Lengauer, T., Berden, J. a, Haring, M. a, Cornelissen, B.J.C., and Takken, F.L.W. (2006). Mutations in the NB-ARC domain of I-2 that impair ATP hydrolysis cause autoactivation. Plant Physiol. **140**: 1233–1245.

Tan, X. (2012). A Comparative Testing of Cucumber mosaic virus(CMV)-Based Constructs to Generate Virus Resistant Plants. Am. J. Plant Sci. **03**: 461–472.

Tasset, C., Bernoux, M., Jauneau, A., Pouzet, C., Brière, C., Kieffer-Jacquinod, S., Rivas, S., Marco, Y., and Deslandes, L. (2010). Autoacetylation of the Ralstonia solanacearum effector PopP2 targets a lysine residue essential for RRS1-R-mediated immunity in Arabidopsis. PLoS Pathog. **6**: e1001202.

Thines, B., Katsir, L., Melotto, M., Niu, Y., Mandaokar, A., Liu, G., Nomura, K., He, S.Y., Howe, G.A., and Browse, J. (2007). JAZ repressor proteins are targets of the SCFCOI1 complex during jasmonate signalling. Nature **448**: 661–665.

Thomma, B.P.H.J., Nelissen, I., Eggermont, K., and Broekaert, W.F. (1999). Deficiency in phytoalexin production causes enhanced susceptibility of Arabidopsis thaliana to the fungus Alternaria brassicicola. Plant J. **19**: 163–171.

Torres, M.A., Jones, J.D.G., and Dangl, J.L. (2005). Pathogen-induced, NADPH

oxidase-derived reactive oxygen intermediates suppress spread of cell death in Arabidopsis thaliana. Nat. Genet. **37**: 1130–1134.

Trujillo, M., Ichimura, K., Casais, C., and Shirasu, K. (2008). Negative Regulation of PAMP-Triggered Immunity by an E3 Ubiquitin Ligase Triplet in Arabidopsis. Curr. Biol. **18**: 1396–1401.

Tsuda, K., Mine, A., Bethke, G., Igarashi, D., Botanga, C.J., Tsuda, Y., Glazebrook, J., Sato, M., and Katagiri, F. (2013). Dual regulation of gene expression mediated by extended MAPK activation and salicylic acid contributes to robust innate immunity in Arabidopsis thaliana. PLoS Genet. **9**: e1004015.

Vierstra, R.D. (2009). The ubiquitin-26S proteasome system at the nexus of plant biology. Nat. Rev. Mol. Cell Biol. **10**: 385–397.

Vierstra, R.D. (2003). The ubiquitin/26S proteasome pathway, the complex last chapter in the life of many plant proteins. Trends Plant Sci. **8**: 135–142.

Vogelmann, K., Drechsel, G., Bergler, J., Subert, C., Philippar, K., Soll, J., Engelmann, J.C., Engelsdorf, T., Voll, L.M., and Hoth, S. (2012). Early Senescence and Cell Death in Arabidopsis saul1 Mutants Involves the PAD4-Dependent Salicylic Acid Pathway. Plant Physiol. **159**: 1477–1487.

Vogelmann, K., Subert, C., Danzberger, N., Drechsel, G., Bergler, J., Kotur, T., Burmester, T., and Hoth, S. (2014). Plasma membrane-association of SAUL1-type plant U-box armadillo repeat proteins is conserved in land plants. Front. Plant Sci. **5**: 37.

Wei, F., Gobelman-Werner, K., Morroll, S.M., Kurth, J., Mao, L., Wing, R., Leister, D., Schulze-Lefert, P., and Wise, R.P. (1999). The Mla (powdery mildew) resistance cluster is associated with three NBS-LRR gene families and suppressed recombination within a 240-kb DNA interval on chromosome 5S (1HS) of barley. Genetics **153**: 1929–1948.

Whitham, S., Dinesh-Kumar, S.P., Choi, D., Hehl, R., Corr, C., and Baker, B. (1994). The product of the tobacco mosaic virus resistance gene N: Similarity to toll and the interleukin-1 receptor. Cell **78**: 1101–1115.

Williams, S.J. et al. (2014). Structural basis for assembly and function of a heterodimeric plant immune receptor. Science **344**: 299–303.

Williams, S.J., Sornaraj, P., deCourcy-Ireland, E., Menz, R.I., Kobe, B., Ellis, J.G., Dodds, P.N., and Anderson, P. a (2011). An autoactive mutant of the M flax rust resistance protein has a preference for binding ATP, whereas wild-type M protein binds ADP. Mol. Plant. Microbe. Interact. **24**: 897–906.

Xia, S., Cheng, Y.T., Huang, S., Win, J., Soards, A., Jinn, T.-L., Jones, J.D.G., Kamoun, S., Chen, S., Zhang, Y., and Li, X. (2013). Regulation of transcription of nucleotide-binding leucine-rich repeat-encoding genes SNC1 and RPP4 via H3K4 trimethylation. Plant Physiol. **162**: 1694–1705.

Xiang, T., Zong, N., Zou, Y., Wu, Y., Zhang, J., Xing, W., Li, Y., Tang, X., Zhu, L., Chai, J., and Zhou, J.-M. (2008). Pseudomonas syringae Effector AvrPto Blocks Innate Immunity by Targeting Receptor Kinases. Curr. Biol. **18**: 74–80.

Xiao, S., Ellwood, S., Calis, O., Patrick, E., Li, T., Coleman, M., and Turner, J.G. (2001). Broad-spectrum mildew resistance in Arabidopsis thaliana mediated by RPW8. Science **291**: 118–120.

Xu, F. et al. (2015a). Two N-Terminal Acetyltransferases Antagonistically Regulate the Stability of a Nod-Like Receptor in Arabidopsis. Plant Cell: 1–17.

Xu, F., Cheng, Y.T., Kapos, P., Huang, Y., and Li, X. (2014a). P-Loop-Dependent NLR SNC1 Can Oligomerize and Activate Immunity in the Nucleus. Mol. Plant: 1801–1804.

Xu, F., Kapos, P., Cheng, Y.T., Li, M., Zhang, Y., and Li, X. (2014b). NLR-associating transcription factor bHLH84 and its paralogs function redundantly in plant immunity. PLoS Pathog. **10**: e1004312.

Xu, F., Xu, S., Wiermer, M., Zhang, Y., and Li, X. (2012). The cyclin L homolog MOS12 and the MOS4-associated complex are required for the proper splicing of plant resistance genes. Plant J. **70**: 916–928.

Xu, F., Zhu, C., Cevik, V., Johnson, K., Liu, Y., Sohn, K., Jones, J.D., Holub, E.B., and Li, X. (2015b). Autoimmunity conferred by chs3-2D relies on CSA1, its adjacent TNL-encoding neighbour. Sci. Rep. **5**: 8792.

Xu, S., Zhang, Z., Jing, B., Gannon, P., Ding, J., Xu, F., Li, X., and Zhang, Y. (2011). Transportin-SR Is Required for Proper Splicing of Resistance Genes and Plant Immunity. PLoS Genet. **7**: e1002159.

Yang, K.Y., Liu, Y., and Zhang, S. (2001). Activation of a mitogen-activated protein kinase pathway is involved in disease resistance in tobacco. Proc. Natl. Acad. Sci. U. S. A. **98**: 741–746.

Zhang, J. et al. (2007). A Pseudomonas syringae Effector Inactivates MAPKs to Suppress PAMP-Induced Immunity in Plants. Cell Host Microbe **1**: 175–185.

Zhang, J. et al. (2010). Receptor-like Cytoplasmic Kinases Integrate Signaling from Multiple Plant Immune Receptors and Are Targeted by a Pseudomonas syringae Effector. Cell Host Microbe **7**: 290–301.

Zhang, Y., Cheng, Y.T., Bi, D., Palma, K., and Li, X. (2005). MOS2, a protein containing G-patch and KOW motifs, is essential for innate immunity in Arabidopsis thaliana. Curr. Biol. **15**: 1936–1942.

Zhang, Y., Goritschnig, S., Dong, X., and Li, X. (2003a). A gain-of-gunction mutation in a plant disease resistance gene leads to constitutive activation of downstream signal transduction pathways in suppressor of npr1-1 , constitutive 1. **15**: 2636–2646.

Zhang, Y. and Li, X. (2005). A putative nucleoporin 96 Is required for both basal defense and constitutive resistance responses mediated by suppressor of npr1-1,constitutive 1. Plant Cell **17**: 1306–1316.

Zhang, Y., Zhang, Y., Goritschnig, S., Goritschnig, S., Dong, X., Dong, X., Li, X., and Li, X. (2003b). A Gain-of-Function Mutation in a Plant Disease Resistance Gene Leads to Constitutive Activation of Downstream Signal Transduction Pathways in. Society **15**: 2636–2646.

Zhang, Z., Wu, Y., Gao, M., Zhang, J., Kong, Q., Liu, Y., Ba, H., Zhou, J., and Zhang, Y. (2012). Disruption of PAMP-induced MAP kinase cascade by a Pseudomonas syringae effector activates plant immunity mediated by the NB-LRR protein SUMM2. Cell Host Microbe **11**: 253–263.

Zhou, Z., Wu, Y., Yang, Y., Du, M., Zhang, X., Guo, Y., Li, C., and Zhou, J.-M. (2015). An Arabidopsis Plasma Membrane Proton ATPase Modulates JA Signaling and Is Exploited by the *Pseudomonas syringae* Effector Protein AvrB for Stomatal Invasion. Plant Cell **2**: tpc.15.00466.

Zhu, Z., Xu, F., Zhang, Y., Cheng, Y.T., Wiermer, M., Li, X., and Zhang, Y. (2010). Arabidopsis resistance protein SNC1 activates immune responses through association

with a transcriptional corepressor. Proc. Natl. Acad. Sci. U. S. A. **107**: 13960–13965.

Zipfel, C., Kunze, G., Chinchilla, D., Caniard, A., Jones, J.D.G., Boller, T., and Felix, G. (2006). Perception of the Bacterial PAMP EF-Tu by the Receptor EFR Restricts Agrobacterium-Mediated Transformation. Cell **125**: 749–760.

Zipfel, C., Robatzek, S., Navarro, L., Oakeley, E.J., Jones, J.D.G., Felix, G., and Boller, T. (2004). Bacterial disease resistance in Arabidopsis through flagellin perception. Nature **428**: 764–767.